REPORT

OF THE

TECHNICAL ASSESSMENT PANEL

COLLAPSE OF THE 300 foot RADIO TELESCOPE

For Reference

Not to be taken from this room

PROPERTY OF THE U.S. GOVERNMENT
NATIONAL RADIO ASTRONOMY OBSERVATORY
CHARLOTTESVILLE VA.

SEP 26 2000

Director's Office Copy

TECHNICAL ASSESSMENT PANEL

Mr. Edward Cohen
Professional Engineer and Managing Partner
Ammann & Whitney, Consulting Engineers

Mr. Robert M. Matyas
Private Consultant, Facilities for Advanced Technology
Vice President, Emeritus
Cornell University

Dr. George F. Mechlin
Physicist
Retired Vice President, Research and Development
Westinghouse Electric Corporation

OBSERVERS

Dr. Kenneth J. Johnston
Astrophysicist
Naval Research Laboratory

Dr. Ludwig Oster
Astrophysicist
Division of Astronomical Sciences
National Science Foundation

Mr. Ronald E. Williams
Chief Engineer
Committee on Science, Space & Technology
House of Representatives, U.S.A.

REPORT of the TECHNICAL ASSESSMENT PANEL for the 300 foot RADIO TELESCOPE at GREEN BANK, WV

SUMMARY

The 300 foot Radio Telescope at Green Bank, West Virginia which collapsed under its own weight while transiting on November 15, 1988 appears to have met and exceeded the original expectations of astronomers.

A post collapse finite element space frame stress analysis, under self weight only, indicated that the stresses in a large number of circumferential and radial members were substantially higher than those currently permitted - in some cases by as much as 100% and more. Although only one connection was reviewed, it can be extrapolated that many gusset plates were overstressed by "secondary" forces not considered in the original design.

The fractured gusset plate which was observed during an inspection of the wreckage, was reviewed and found to be a critical connection in the diamond truss.

It was found that the stresses were high and the stress range during telescope transits indicated a limited fatigue life. This was verified by the fractographic examination which indicated that fatigue crack propagation under cyclic loading resulted in eventual fracture of the plate.

The Technical Assessment Panel concludes that the fracture of this gusset plate connection is the most probable cause of the telescope collapse. From a review of Observatory records, the failure of the telescope structure was not a result of inadequate maintenance or inappropriate operation of the telescope.

The analysis methods used in this study were not available at the time the telescope was designed. The understanding of fatigue and crack propagation under cyclic load have greatly advanced since.

This collapse points dramatically to the importance of having an accurate and comprehensive stress analysis for this type of movable structure, which can identify fatigue and crack propagation susceptibility in critical elements in order to establish programs of inspection and subsequent strengthening, repair or replacement.

There are no unfavorable implications about the current ability to engineer future telescopes of this or larger size.

1. BACKGROUND

The 300 foot diameter Radio Telescope at Green Bank was designed and built over a period of two years and put into service in October, 1962. At the time of its construction, this telescope was conceived to be an interim facility which would satisfy certain immediate instrument needs not being satisfied as a result of delays and cancellations of other planned or projected instruments. A high priority was placed on minimum cost and expeditious construction. The minimal environmental requirements imposed on the designer support the conclusion that the telescope was not intended to be a permanent facility. The scientific usefulness extended many years beyond the expectations of the astronomy community as a result of the rapid advancement of detector technology which greatly improved the scientific yield. Since no other comparable United States instrument has been built, the machine never became obsolete.

Another factor which must be understood is a major improvement which has occurred in the design methodologies used by engineers working in the early 1960's as compared to engineers working today. This improvement, called **finite element space-frame stress analysis**, has been made practical by the advent of large capacity digital computers of widespread availability. This analysis method allows the structure being designed to be represented by a large number (e.g., thousands) of mesh points whose stress relationship is determined simultaneously whereas earlier methods required a complex structure to be simplified and typically neglected "secondary" flexural stresses due to frame distortions. Also, this antenna must be considered as a machine and as a dynamic structure, parts of which undergo large stress ranges in each transit of

the structure. In this review, we used these modern methodologies not generally available to designers at that time. Our current understanding of the stresses of the structure thus greatly exceeds that available to the original designer, and our knowledge of fatigue and crack propagation due to cyclic loading is much improved.

2. HISTORY

The operators of the telescope, in routine visual inspection of the radial ribs and circumferential ring structure, observed and repaired occasional failures of smaller structural members from the very beginning of telescope operation. These failures were usually at the connection plates where structural members were joined by bolting. Over the 26 year life of the telescope, a few hundred such repairs were made, some in anticipation of failures in areas with high incidence histories. These repairs were never a detriment to the scientific performance of the instrument.

On a cool, windless night, on November 15, 1988, the telescope collapsed without warning while in transit motion. On November 18, 1988, senior officials of the National Science Foundation (NSF) and Associated Universities, Incorporated (AUI) established a Technical Assessment Panel to determine the cause of the telescope failure. On November 22, 1988, Panel members, E. Cohen and R. M. Matyas joined NSF and AUI officials together with a representative of the House of Representatives, Science, Space & Technology Committee and visited the Observatory at Green Bank. Interviews were conducted along with an examination of the wreckage.

A third Panel member, Dr. G. F. Mechlin, was added on November 28th. The first official meeting of the Technical Assessment Panel was held on December 9, 1988 in Washington, D.C. A key decision at this meeting was to order a finite element analysis of the telescope structure.

Another visit to the Observatory was made on January 4, 1989 by Dr. G. F. Mechlin and R. M. Matyas. During this visit and inspection of the telescope wreckage, there was observed a cracked major gusset plate connecting a lower element of the diamond truss which, at its other end, is connected to the bearing support framework. Based on a visual examination of

the cracked surface, which suggested a significant crack which pre-existed the failure, one half of this cracked gusset was recovered and sent to a qualified metallurgical testing laboratory for examination. This laboratory examination is discussed in section 4 of this report since the gusset plate is believed to have played a significant or causative role in the telescope collapse. There are three other corresponding gusset plates in the structure. Two appear not to have a pre-existing crack. One (not yet recovered) exposed an indication of a pre-existing crack which appears significantly smaller than the crack on the plate already examined.

3. RESULTS OF THE FINITE ELEMENT STRESS ANALYSIS

The full report of this finite element analysis is provided as Appendix A. The salient findings of this analysis are that 1.) certain lower chord gusset plate connections of the diamond truss underwent numerous cycles of severe stress and 2.) the radial rib and circumferential ring structure in the vicinity of the trunion truss bearing support structure operated at stress levels at which buckling and plastic deformation would be expected to take place. Two consequences of resulting deformations are predictable. First, it would cause a redistribution of loads into other adjacent members, which would generally cause loads of these members to increase even beyond the levels calculated by our stress analysis. The second consequence would be the occasional failure of individual structural elements as observed. A design analysis performed four years after completion indicated some such overloaded elements. Some remedial repairs were undertaken accompanied by additional modifications to stiffen the structure and to improve the image stability.

It must be understood that the current analysis was made of the telescope in its idealized dimensional state prior to the collapse. Such a state is never achieved since stresses developed in a partially completed state during erection impose initial deformations and stresses which vary from ideal, which then would be additionally altered by the modifications and repairs mentioned above. As earlier suggested, these effects tend to make actual stresses greater than calculated for the ideal structure.

One concludes from the current analysis that, from the beginning of its life, the structure was marginal with respect to structural failures of a minor or perhaps a major nature. A very significant portion of this marginal status was that the diamond truss structure depended for stability on the interactive support of the radial ribs and circumferential rings which, in turn, contained members required to operate beyond their safe load carrying limit.

Because of complex load redistribution effects, one does not expect a strict correlation between individual members determined to be overloaded and observed individual failures. There is, however, a general correspondence between areas showing calculated overload and observed damage. Early in its life there were several significant modifications made to the telescope. These included the reinforcement and stiffening already alluded to. A new feed structure consisting of a dish-mounted, guyed bipod was added and the original open mesh dish surface was replaced with a finer mesh surface suitable for higher radio frequency operation. The finite element analysis reported herein found that after these modifications, the structural integrity of the directly affected portions of the telescope were somewhat enhanced.

4. SEQUENCE OF FAILURE

The Technical Assessment Panel concludes that the probable cause of telescope collapse was the progressive cracking of the gusset plate at the end of the lower chord of the diamond truss at the northeast corner. This lower chord at its other end intersected with the support bearing structure. The failure of the lower chord of the diamond truss in this location destroys the ability of the truss to carry load as a truss and collapse ensues. The progressive cracking was caused by excessive stress in the gusset. As calculated in the idealized state of the structure, the stress was far beyond limits which would have precluded such progressive cracking. The crack origin was probably associated with two punched bolt holes where the severe working produced by the punch could have left an initiating small crack.

The report on the metallurgical examination is included as Appendix B. Results of the metallurgical investigation of the fractured gusset plate revealed that the plate failed as a result

of progressive cracking in the nature of fatigue. Propagation of these fatigue cracks under cyclic loading from both bolt holes eventually resulted in a fast ductile fracture when the combination of cyclic stress range and crack size exceeded the fracture toughness of the plate material.

The results of the fractographic examination revealed secondary fatigue cracks also had originated at the bolt hole surfaces. The presence of secondary fatigue cracks at the bolt holes indicates the presence of intermediate to high cyclic stresses.

It cannot be unambiguously determined whether the subject progressive crack had simply grown to a point where the remaining material in the gusset could no longer support the load or whether some otherwise minor event or failure immediately preceding the collapse added a new increment of load to the gusset. Two such minor events can be postulated. One event might have arisen from an increased friction force or jamming of a support bearing. The west bearing assembly was recovered for inspection while the east bearing is still inaccessible. During this salvage operation, the unloaded shaft was rotated with ease but when the bearing case was opened, the grease was observed to contain a myriad of metal flakes and the spherical rollers exhibited a peened surface demonstrating progressive damage. The appearance of the bearing rollers suggest only a modest increase in frictional torque, however, the bearing was in the initial stages of failure and probably would have itself prevented use or caused structural failure of the telescope at some future time. Another likely event is one or several failures of already overstressed radial rib or circumferential ring members shifting additional load onto the box frame truss.

The panel sees no merit in terms of lessons for the future in further tedious and perhaps impossible tasks of determining whether the gusset failed first or was driven to failure by such a preceding event. It is very clear that this gusset was rapidly approaching failure prior to the event and that the failure of this plate was the key element in the total collapse of the telescope.

The Panel recommends two additional corroborating investigations be performed by the Observatory as appropriate

prior to or during wrecking. One is the recovery and visual examination (only) of the second gusset believed to be cracked. The second is disassembly and visual examination of the east bearing assembly for signs of distress which might indicate high friction or jamming.

The Panel further recommends caution and extreme care in recovering any artifacts or structural elements from the wreckage. In such activities as well as the subsequent disassembly and removal of the wreckage, it is imperative that the work be supervised and monitored by a competent structural engineer working with an experienced industrial wrecking crew.

5. RESPONSIBILITY

From a review of the records, it is the opinion of the Technical Assessment Panel that the failure of the telescope structure was not a result of inadequate maintenance or inappropriate operation of the telescope.

The contributory roles of the designer, the constructor or of the subsequent reviewer cannot be sensibly commented upon after so long an interval other than to say that the telescope performed longer than the expectations which the observatory and the designers must have shared.

There were no observed structural failures in the history of the telescope which would have suggested a need for a third engineering analysis of the sort performed in this investigation. The gusset plate in question was cracked in a fashion such that most of the crack was concealed beneath the structural elements to which it was connected. There was lacking any signal that the gusset was failing and an examination was not possible without disassembly, which could not be performed.

6. RELATION TO OTHER RADIO TELESCOPES

The Review Panel sees no direct implication from the failure of the 300 foot telescope to other radio telescopes. There were no phenomena observed in the operation of this telescope that could not be dealt with using modern design practice. It does

point very dramatically to the importance of having an accurate stress analysis which would identify critical elements, crack propagation susceptibility, and required frequency of inspection, replacement, strengthening or repair.

The other, relatively minor, structural failures observed in the radial ribs and circumferential rings were detected through periodic inspection and repair. How these repairs contributed over the years to stress increases in the diamond truss gusset plates cannot readily or unambiguously be determined even with today's best state-of-the-art in stress analysis.

It should be understood by all telescope operators that their instruments are more akin to moving machines than to static buildings. Inspection and maintenance plans based on adequate knowledge of structural loads and service environment are a normal requirement of this or any other kind of machinery which the owners wish to keep in service.

It should be a requirement for the designer to identify from his design analysis, places and times where inspection for "fatigue type" progressive cracking should be made. Further, limited life components such as seals, hydraulic components and bearings should be identified and provision made for their inspection and/or replacement.

There are no unfavorable implications about the present ability of engineering science to design and build telescopes of this or larger size.

APPENDIX A

Finite Element Analysis

Volumes 1 and 2

NATIONAL RADIO ASTRONOMY OBSERVATORY
300 FOOT TELESCOPE

FINITE ELEMENT ANALYSIS
VOLUME I

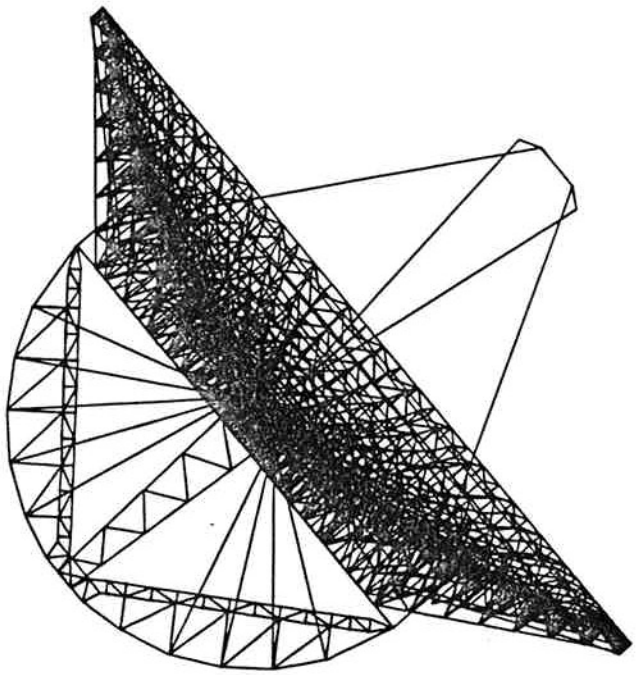

Henry Ayvazyan, M.E.
Joel Stahmer, B.E.
Joseph Vellozzi, Ph.D.

Ammann & Whitney
Consulting Engineers
New York, New York

February 1989

NATIONAL RADIO ASTRONOMY OBSERVATORY
300 FOOT TELESCOPE

FINITE ELEMENT ANALYSIS
VOLUME I

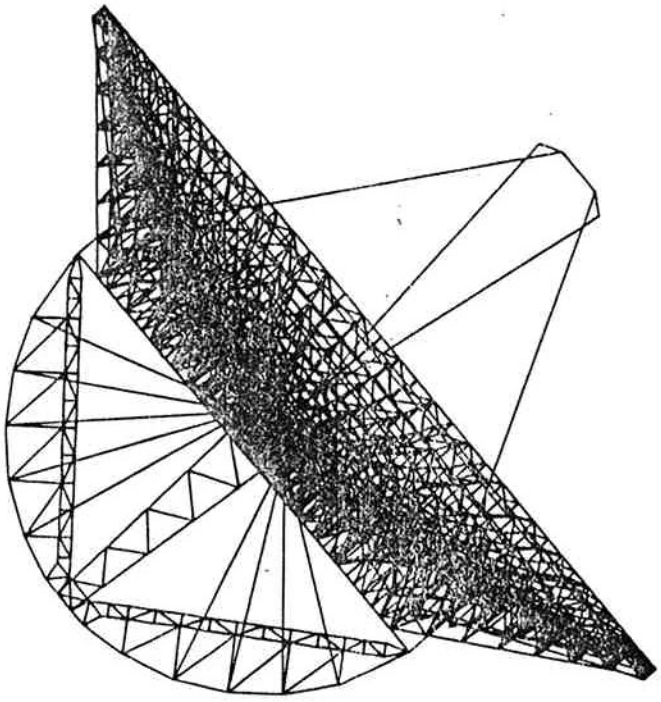

Henry Ayvazyan, M.E.
Joel Stahmer, B.E.
Joseph Vellozzi, Ph.D.

Ammann & Whitney
Consulting Engineers
New York, New York

February 1989

NATIONAL RADIO ASTRONOMY OBSERVATORY
300 FOOT RADIO TELESCOPE
FINITE ELEMENT ANALYSIS
(VOLUME I)

TABLE OF CONTENTS

Section	Description	Page
1.0	PREFACE	1
1.1	Summary Of Conclusions	1
2.0	INTRODUCTION	3
3.0	ANALYSIS	4
4.0	MODELS	5
4.1	General	5
4.2	The Partial Model	6
4.3	The Half Model	8
5.0	RESULTS	10
5.1	The Partial Model	10
5.1.1	General	10
5.1.2	Deflections	11
5.1.3	Ruptured Gusset Plate Forces	11
5.1.4	Ruptured Gusset Plate Stresses	12
5.2	The Half Model	13
5.2.1	General	13
5.2.2	Deflections	13
5.2.3	Member Forces	13
5.2.4	Ruptured Gusset Plate Forces	14
5.2.5	Ruptured Gusset Plate Stresses	14
6.0	CONCLUSIONS	15

FIGURES

Figure	Description	Page
1- 1	Partial Model Plan	17
1- 2	Partial Model Perspective	18
1- 3	Partial Model Viewed Looking South	19
1- 4	Partial Model Viewed Looking North	20
1- 5	Partial Model Viewed Looking East	21
1- 6	Partial Model Deflections, Zenith Position	22
1- 7	Partial Model Deflections, 30 Deg. Inclntn.	23
1- 8	Partial Model Deflections, 45 Deg. Inclntn.	24
1- 9	Partial Model Deflections, 60 Deg. Inclntn.	25
1-10	All Position Deflections Looking East	26
1-11	All Position Deflections Looking South	27
1-12	Zenith Deflections Looking North	28
1-13	30 Degree Inclntn. Defltns. Looking North	29
1-14	45 Degree Inclntn. Defltns. Looking North	30
1-15	60 Degree Inclntn. Defltns. Looking North	31
1-16	Ruptured Gusset Plate Details	32
1-17	Ruptured Gusset Plate Analysis Calculations	33

(Cont'd.)

NATIONAL RADIO ASTRONOMY OBSERVATORY
300 FOOT RADIO TELESCOPE
FINITE ELEMENT ANALYSIS
(VOLUME I)

T A B L E O F C O N T E N T S
(Continued)

VOLUME II	PLOTS: DEFLECTIONS and OVER-STRESSED MEMBERS; Half Model Analysis, Zenith and 45 Degree Inclined Dish Positions.
Figure	D e s c r i p t i o n
	For Half Model Geometry:
2- 1	Plan.
2- 2	Elevation Looking North.
2- 3	Elevation Looking West.
2- 4	Perspective, Inclined Model Looking West.
	For Half Model Deflections:
2- 5	Zenith Position, Plan.
2- 6	Zenith Position, Elevation Looking North.
2- 7	Zenith Position, Elevation Looking West.
2- 8	45 Deg. Inclined Dish Position, Plan.
2- 9	45 Deg. Inclined Dish Position, Elevation.
	For Over-Stresses in Top and Bottom Dish Surface Members in Both the Zenith and 45 Degree Inclined Positions:
2-10	Top Surface Projection Members.
2-11	Bottom Surface Projection Members.
	For Over-Stresses in Main Rib Members:
2-12	Ribs A & D, Zenith Position.
2-13	Ribs B, Zenith Position.
2-14	Ribs C, Zenith & 45 Deg. Inclined Dish Positions.
2-15	Ribs A & D, 45 Degree Inclined Dish Position.
2-16	Ribs B, 45 Degree Inclined Dish Position.
	For Over-Stresses in Auxiliary Rib Members for the Zenith & 45 Degree Inclined Dish Positions:
2-17	Ribs At 0 to 82.5 Degrees (in First Quadrant).
2-18	Ribs At 90 to 172.5 Degrees (in Second Quadrant).
2-19	Ribs At 180 to 262.5 Degrees (in Third Quadrant).
2-20	Ribs At 270 to 352.5 Degrees (in Fourth Quadrant).
	(Cont'd.)

NATIONAL RADIO ASTRONOMY OBSERVATORY
300 FOOT RADIO TELESCOPE
FINITE ELEMENT ANALYSIS
(VOLUME I)

T A B L E O F C O N T E N T S
(Continued)

VOLUME II Cont'd.	PLOTS: DEFLECTIONS and OVER-STRESSED MEMBERS; Half Model Analysis, Zenith and 45 Degree Inclined Dish Positions.
Figure	D e s c r i p t i o n
	For Over-Stresses in the Circumferential Members in the Zenith and 45 Degree Inclined Dish Positions.
2-21	At Circumference 01 (Radius = 150 feet).
2-22	At Circumference 02 (Radius = 140 feet).
2-23	At Circumference 03 (Radius = 130 feet).
2-24	At Circumference 04 (Radius = 120 feet).
2-25	At Circumference 05 (Radius = 110 feet).
2-26	At Circumference 06 (Radius = 100 feet).
2-27	At Circumference 07 (Radius = 90 feet).
2-28	At Circumference 08 (Radius = 80 feet).
2-29	At Circumference 09 (Radius = 70 feet).
2-30	At Circumference 10 (Radius = 60 feet).
2-31	At Circumference 11 (Radius = 50 feet).
2-32	At Circumference 12 (Radius = 40 feet).
2-33	At Circumference 13 (Radius = 30 feet).
2-34	At Circumference 14 (Radius = 20 feet).
2-35	At Circumference 15 (Radius = 10 feet).
VOLUME III	STAAD III OUTPUT: ZENITH DISH POSITION ANALYSIS
VOLUME IV	STAAD III OUTPUT: 45 DEGREE INCLINED DISH POSITION ANALYSIS

NATIONAL RADIO ASTRONOMY OBSERVATORY
300 FOOT RADIO TELESCOPE
FINITE ELEMENT ANALYSIS
(VOLUME I)

1.0 PREFACE

The arrangement of this report is as follows: Section 2.0 is the INTRODUCTION, it contains general information about the structure and the collapse. Section 3.0, titled ANALYSIS, contains general information about the analysis. Section 4.0, titled MODELS, contains general and specific information about the models used in the analysis. Section 5.0, titled RESULTS, contains general information from the partial and half model analysis results. The half model results are summarized graphically in Volume II with Figures 2-1 through 2-35. The CONCLUSIONS are presented in Section 6.0. Conclusions are also summarized below in outline form to permit immediate review of the findings of this analysis.

1.1 Summary Of Conclusions

1) The analysis of the telescope considered only the self-weight of the structure. Under this loading condition many members were found to be overloaded because they did not 'pass' the current AISC code check as implemented in the STAAD program. The maximum over-load determined by STAAD was more than 200 percent, for both the zenith and inclined dish positions. Nominally ninety percent of the overloaded members were in compression, the remainder were in tension. Except for two members in tension, all over-loaded members at 100% or more overload were in compression. These compression members, overloaded at or above twice their allowable capacities, could have theoretically buckled, permitting load redistribution. Such overloads and the attendant load redistributions caused overloading in alternate members over the life of the telescope, and could be considered to have contributed to the collapse.

2) Visual inspection and laboratory tests of the ruptured gusset removed from the telescope wreckage indicated progressive cracking and eventual rupturing of this plate. The analysis showed that the plate stresses were high enough to cause cracking and crack growth under the cyclic loads from the antenna movements. Rupture of the plate would have resulted in the collapse of the telescope. It should be noted that the telescope had a history of several gusset plate replacements throughout its operational life.

3) The reasons for the overstresses were as follows:

a) The original telescope was designed as a pure truss without consideration of any moments induced by the self-weight of members. As a result, when these members were loaded to their axial capacities, even the slightest bending due to self-weight, induced overstress.

b) The circumferential top chord members in the dish structure were designed for tension only. The finite element analysis showed compression in many of these members, and several of these members in compression were overstressed enough to theoretically permit buckling.

c) Even as a pure truss, many members exceeded the allowable slenderness ratio limitations permitted by code.

The following table provides a synopsis of the findings of the half model analysis for the zenith and 45 degree inclined dish positions. The results summarize the percentage of the over-stressed members and the intensity of the over-stress for the two dish positions analyzed. For an in-depth overview of these over-stressed members, the graphic illustrations representing the top, bottom, circumferential, and radial rib framings must be reviewed. These illustrations have been separated from the body of this report (Volume I) and placed in Volume II, as aforementioned. The overstresses are with respect to the current AISC code as implemented by the STAAD program, and the (*) mark members that have theoretically buckled.

Location	Zenith Positn.		45 Deg.Positn.	
	% of membs.	% over-stress	% of membs.	% over-stress
Dish Top Surface Circumferentials	6.4	5- 45	8.9	5- 45
	6.8	45-100	3.1	45-100
	3.5	100-200*	1.0	100-200*
	1.2	>200*	0.3	>200*
Total	17.9		13.3	
Circumferentials Between Top and Bottom Dish Surfaces	0.8	5- 45	0.5	5- 45
	0.3	45-100	0.3	45-100
	0.1	100-200*	0.4	100-200*
	0.1	>200*	0.1	>200*
Total	1.3		1.3	
Dish Bottom Surface Circumferentials	4.7	5- 45	5.8	5- 45
	0.7	45-100	0.7	45-100
	0.4	100-200*	1.1	100-200*
Total	5.8		7.6	
Total of Circmfs.	25.0		22.2	

For the radial ribs, 10 members were overstressed by 68 to 120 percent, and 12 members were overstressed by 10 to 44 percent, respectively for the zenith and 45 degree inclined dish positions. These overstresses were primarily tension.

2.0 INTRODUCTION

On November 15, 1988, the 300 foot diameter National Radio Astronomy Observatory (NRAO) telescope, located in Green Bank, West Virginia, collapsed. The structure collapsed completely on a windless, cool and clear evening. The telescope, built in the early 1960's, was in continuous operation until the time of collapse.

In order to investigate possible reasons for the structure collapse, a dual effort was performed simultaneously consisting of (1) site investigation to evaluate the structure components after the collapse, and (2) an analysis of the most recent structure configuration to determine the possibility of over-stresses. The site investigation was done by the NRAO personnel while Ammann & Whitney, Consulting Engineers of New York City, were retained as structural engineers for the performance of the structural analysis.

The structure consisted of five main components. These components were two support towers, each nominally 87 feet high; a parabolic surface 300 foot diameter three dimensional frame dish with an integral diamond shaped truss in the central region of the dish; a chain-drive circular truss with a centrally located counterweight; and a collector support mast truss.

The towers were located on the East to West cardinal points at approximately half the radius of the dish. They were attached to the underside of the dish structure on the diamond truss. The chain-drive and mast trusses were located along the North-South axis of the dish. The chain-drive truss was suspended from the dish structure at the North and South corners of the integral diamond truss. The mast truss was atop the parabolic surface and was attached to the North and South auxilary ribs and the corners of the diamond truss.

Initially the chain-drive and mast truss structures were laterally supported with guy cables from the dish structure. However, shortly after the telescope became operational, the mast structure was replaced with an improved mast. At a still later date, the 3 inch diameter guy cable support system, which braced the chain-drive truss at counterweight, was replaced with inclined lateral trusses. These new trusses were framed between the dish structure near each support tower and the counterweight of the chain-drive truss.

Additional structural modifications and repairs were made to the radio telescope during erection and over its operational life. All modifications and repairs, however, were not completely and/or specifically documented.

3.0 ANALYSIS

The radio telescope was analyzed with the latest version of the STAAD finite element program. This program was executed on a micro VAX computer. The STAAD program was utilized because it has the best cost/time effective capacity to model the entire telescope structure. Furthermore, the program can determine the AISC allowable capacities of almost all of the specific structural shapes from which the structure was constructed, and compare allowable values to the respective analysis results. This program feature provided analysis output which quickly identified all members which exceeded their AISC allowable capacities.

Finite element analysis is a powerful procedure with which the deflections and member forces of an idealized structure can be determined using digital computers. However, each unique solution is based upon linear principles. Simply put, although the nodal deflections and member forces of a model structure are based upon the stiffness interaction of all members, Hooke's Law is observed at all deflections.

If the analysis equilibrium condition results in forces less than or equal to the maximum capacity of the members, these forces, and the (elastic) deflections required to generate these forces, may be considered to be good approximations of the actual values. On the other hand, if the member forces exceed their capacities, deflections and member forces may no longer be linearly related to each other.

The reason for this conclusion stems from the fact that unique linear solutions do not evaluate the redistribution of applied overloads. In general, a tensile member force can exceed the code specified allowable theoretically with linear increases in deflection until yield stress. At yield stress, a tensile member undergoes plastic straining without increased load until strain hardening. During strain hardening a tensile member undergoes additional straining with increasing and decreasing load, until rupture.

For a compression member, the slenderness of the member interacts with the deflection. An extremely stubby member can undergo additional elastic straining with additional loading, and additional plastic straining without additional loading, both without buckling. A slender member, as did exist in the telescope structure, will undergo additional straining with additional loading, until the buckling load is reached. In a complicated frame structure, additional overloading beyond the incipient buckling load can produce several conditions. If the overload can successfully transfer to an alternate member, the buckled member can continue carrying load. If the overload cannot successfully transfer, increased deflections can be induced, resulting in the ultimate collapse of the member.

This non-linear behavior can be synthesised, however, by using multiple solutions, adjusting the stiffness matrix for each

unique solution. Stiffness matrix adjustments can be manually made, or they can be automated within the computer. The adjustments account for members that in reality can no longer sustain additional loads, although they undergo additional deflections.

Solutions of this nature for the telescope structure would have been very costly, requiring substantially longer computer and engineering time. Whether done manually, with a linear theory program, or with an automated non-linear program, the process would have required slowly loading the structure to determine the sequence in which the members would exceed their capacities. The process would have required the definition of the non-linear tension and compression resistance of each member to permit adjustments to the stiffness matrix as they were required.

The use of such a procedure to evaluate the deflections and member forces in the telescope structure was beyond the scope of work of this analysis. The approximation of member forces and deflections can be assumed to be good since only the identification of overstressed members was sought.

During the investigation of the collapsed structure, a ruptured gusset plate was discovered on the North-East side of the diamond truss. This gusset plate attached the inclined bottom chord member in the first panel of the diamond truss to the adjacent horizontal bottom chord member in the second panel of the diamond truss. In view of this discovery, the scope of work for this analysis was modified to include a preliminary analysis of the stresses in this ruptured gusset plate using the results of the half model analysis for the zenith and 45 degree inclined dish positions.

4.0 MODELS

4.1 General

Two models were employed, a partial substructure model, and a complete half model. The partial model was used to verify the 45 degree inclined dish position for the inclined analysis of the half model. It was also used to quickly determine the approximate order of magnitude of the forces in the diamond truss members adjacent to the trunnion trusses. The half model was used to determine the magnitude of all member forces throughout the structure. Both models considered the structure as a three dimensional frame. The half model analysis was more extensive, and hence, more accurate than the partial model, because it considered the interaction of all main member axial and flexural stiffnesses.

The half model exclusively used the STAAD program SELFWEIGHT nodal load generation feature. The partial model used this feature incombination with applied loads to account for structural components not directly modelled.

Applied and generated loads were specified in the negative vertical direction for the zenith dish position. For the inclined dish positions modelled with the South end of the dish being rotated downward, both models were subjected to loads which synthesized the inclined dish position with applied or generated loads in the appropriate inclination. Specifically, these loads were defined componentially in the negative vertical and southerly directions such that their resultants were all at the appropriate inclinations and equal in magnitude to the zenith position vertical quantities.

The support towers were not modelled in either the partial or half model. In lieu of the support towers, support conditions were defined as translational restraints in the vertical and North-South axis directions at the center of the bottom chords of the trunnion trusses. The partial model contained both the East and West trunnion trusses, the half model only the East trunnion. In addition, the partial model was translationally restrained in the East-West axis direction at one trunnion truss.

Both models were restrained against rotation about the trunnion bearing East-West axis with a translational restraint at the counterweight on the chain-drive truss. In the half model only, this restraint was relocated to the circumferential quarter point on the southern half of the chain drive truss to more accurately model the approximate position of the drive mechanism for the 45 degree inclination.

For both models, member sizes and framing details were determined from the original design drawings, shop drawings, and other available documentation of revisions. Erection drawings were not available for review during formulation of the model inputs.

The plane of the diamond truss required a slight modification to simplify the modelling descretization at the rib intersections for the half model. This modification was utilized in the partial model as well.

4.2 The Partial Model

The partial model depicted the diamond and trunnion trusses. Except for the trunnion truss members, all members in the diamond truss were defined from the AISC table of members. The trunnion truss members were defined as prismatic members. In lieu of the actual radial ribs, stick element links were used to respectively provide the top and bottom chord restraints along the diamond truss at the main rib intersection points. Diamond truss secondary bracing members were not included in the model, but were accounted for by using conservative slenderness factors.

The prismatic links attached to the top and bottom chords of the diamond truss were proportioned with the actual radial rib chord areas and the horizontal stiffness of the radial ribs.

Stick element links were also used in lieu of the actual chain-

drive and (new) lateral trusses. These members provided the (spring) supports at the North and South corners of the diamond truss. They also became the mechanism with which their weight and that of the counterweight were distributed to the diamond truss. The cable guys, however, were not accounted for in the partial model.

These link mechanisms which represented the radial ribs and the chain-drive and lateral trusses were not an attempt to model the actual members. They were approximations utilized to provide the approximate order of magnitude of member forces with fast computer turn around time.

The partial model was loaded with the weights of the ribs, the circumferential bracings, the center hub, the chain-drive and lateral trusses, and the counterweight. The weight of the chain-drive and lateral trusses were applied at the counterweight location. The weights of the ribs, center hub, and circumferential bracings were equally placed on the diamond truss top and bottom chords and at the intersection points of the main radial ribs.

The loading for the partial model was derived from a quantity take off from a typical sector of the dish and from the original calculations on the Faelton drawings. Based on these sources, 1/48 of the total load, not including diamond truss weight, was applied at each top and bottom chord node of the diamond truss, at the attachment point of every main rib. The weight of the diamond truss main members was included using STAAD's SELFWEIGHT specification.

The chain-drive and lateral truss weights were concentrated at the counterweight. This permitted the distribution of these loads to the appropriate connection points along the underside of the diamond truss. Although this distribution was an approximation of the actual condition, because the partial model neglected the guy cables attached to the chain-drive truss, it was utilized to represent the (new) diagonal trusses that replaced the original 3 inch diameter guy cables.

To mimic the support towers in the partial model, support boundary restraints to prevent translations in the vertical and North-South directions were provided at the bottom chord on the centerline of the trunnion truss at the East and West corners of the diamond truss. At one trunnion truss only, the East-West axis translation was also restrained. This permitted the structure to move as a simple span between the trunnions. To mimic the rotational restraint provided by the chain-drive truss, the location of the counterweight was restrained against translation in the North-South axis direction. This permitted the resolution of the North-South axis direction reaction developed in the chain-drive mechanism.

The partial model consisted of 63 nodes and more than 239 members. The analysis CPU time for the zenith and dish positions

of 30, 45, and 60 degree inclination was approximately 3 minutes. The small size of the model permitted the use of the STAADPL plot program to generate the plots of the modelled structure in its unloaded and loaded conditions for the zenith and inclined dish positions of 30, 45, and 60 degrees.

At the 45 degree inclination position, the partial model analysis indicated diamond truss member forces adjacent to the trunnion trusses to be in tension and nearly equal to the compression developed in the zenith position. This verified the use of the 45 degree dish position for the half model as the most suitable.

4.3 The Half Model

The half model contained the actual main members and framing in the diamond truss, the radial ribs, the circumferential bracings, the chain-drive circular truss, and the (new) lateral trusses. All guy cables, laterally supporting the chain-drive and mast structures from the dish, the mast atop the dish, the center hub, and the concrete counterweight, were modelled with prismatic members with the appropriate member properties.

The half model contained 1313 nodes and 3633 members. It modelled the structure in the North-East and South-East quadrants. The required CPU time depended on the core allocation, and was approximately six hours with 4 mega-bytes of RAM.

The half model had 7871 degrees of freedom and a stiffness matrix of nearly 8 million double precision words. It required slightly more than 145 mega-bytes of disk space during execution.

If the full structure were modelled, the number of nodes and members would have nominally doubled, the required RAM, the matrix size, and the disk space would have nominally quadrupled, and the CPU time would have increased well beyond a factor of four.

The half telescope math model was initiated by reviewing the existing structure to determine the most suitable approach for creating the finite element program input. Ultimately, because of the complexity of the three dimensional framing in the structure, the decision was made to input the structure nodes circumferentially. That is, starting from the East axis, a circle of nodes was generated for each unique elevation of nodes at a common radius. This scheme was repeated for circumscribed circles of nodes from the maximum radius of 150 feet inward towards the center hub. The nodal generation utilized the reverse cylindrical coordinate system as defined by STAAD.

Members connected between appropriate nodes were subsequently generated in the same way. Secondary in plane members and their nodes were omitted to simplify and reduce the already large input of the full model . The effects of these secondary members were accounted for by providing appropriate slenderness terms for the main members. Standard members were defined from the built-in

AISC member properties table in the STAAD program. Built-up members, which are not defined in the STAAD program, were defined in a user input member properties table. The STAAD program provided a comparison of analysis member forces and AISC allowable capacities for all standard and user defined members.

The parabolic reflector surface panels and secondary support members were not directly modelled in the half model. Their weights were considered, however, with an increased density in the top surface circumferential members. The magnitude of this increase varied, and was proportional to the tributary area bound by adjacent rib and circumferential top surface members.

Connection weights were considered by increasing the density of all members by five percent. As aforementioned, the counterweight at the center of the chain drive truss and the tubular hub at the dish center were modelled with very rigid prismatic members. Cables were considered as members with the appropriate area, but with little bending capacity. The slenderness ratios of all members defined as structural shapes were evaluated by STAAD based on the idealized lengths of each member. Therefore, the AISC code check provided by STAAD was, in general, conservative.

The half model utilized support restraints similar to the partial model to mimic the East support tower. Specifically, at the center of the bottom chord of the East trunnion truss, restraints were provided to prevent translations in the vertical and North-South axis directions. Because the North-South axis was the axis of symmetry, the structure was bound along this axis with restraints that prevented translations along East-West axis and rotations about the vertical and North-South axis. The directional references are all with respect to the zenith dish position.

The rotation of the dish about the East-West axis (the support bearing axis) was prevented by providing a translational restraint along North-South axis at the point of tangency of the chain-drive truss and the drive mechanism on the ground. This point was at the center of the chain-drive truss for the zenith position, and at the quarter point for the inclined position with 45 degrees rotation.

The nodal loads for all members in the half structure were determined by the STAAD program using the SELFWEIGHT specification. The SELFWEIGHT specification determines nodal loads from member lengths, areas, and densities, and applies them in the defined gravitational axis direction.

The actual material densities were used for all members except the chain-drive and mast structures. The chain-drive and mast structures were on the centerline of symmetry, and were subsequently specified with half the material density, to permit applying half their weights.

For the dish in the zenith position, the nodal loads were

determined by a load factor of negative 1.0 in the Y-axis or vertical direction. For the inclined dish position, the nodal load factors of negative 0.707 were specified in the Y and Z (the Vertical and North-South axis) directions, to mimic a rotation of the dish to the 45 degree inclined position.

The triangular cross sectional chords of the chain-drive truss and the receiver supporting mast were simplified by modelling these structures as equivalent two dimensional or plane trusses. Guy cables laterally bracing these structures were modelled as very flexible rod elements, with cross sectional areas that would result in the appropriate weights and resistances to elongation.

The central hub and the chain drive counterweight were modelled using very stiff members with very low densities. The actual weights were accounted for in the model with one member which was given an appropriate area and density to equal the weight of either the counterweight or the central hub, as appropriate. Secondary bracing members were not included, but were accounted for in the model by adjusting the AISC slenderness factors.

The actual coding of the node coordinates was done using a (reversed) cylindrical coordinate system, specifying radius, elevation and angle. STAAD III converted the cylindrical system to a cartesian system for analysis and final output. For the dish in the initial analysis zenith position, this resulted in a coordinate system that placed the circumferences, or plan of the antenna, in the X-Z plane, with the elevations of the nodes specified by the Y coordinate.

Member properties were specified using STAAD's built-in AISC tables where possible. Many members used in the antenna are no longer included in the current code, and other members were modified to comply with the 1966 Rohr recommendations. The properties of these superceded and built-up or reinforced members were input in user table.

STAAD III does not have the ability to accept the properties of a cruciform shaped member. For members of this configuration which were reinforced by the addition of double angles or T-sections, the properties were specified conservativly as equivalent double angles.

5.0 RESULTS

5.1 The Partial Model

5.1.1 General

The substructure partial model results may be graphically reviewed with Figures 1-1 through 1-15. Figure 1-1 illustrates the diamond truss plan with the radial links. The partial model Y-axis corresponds to the North-South axis. It identifies the locations at which the radial ribs intersect with the diamond and trunnion trusses. Note that in the Half Model, the vertical axis

was the Y-axis and the North-South axis was the Z-axis, because the STAAD 'reversed cylindrical' specification was used to input the nodal coordinates.

Figure 1-2 is a perspective of the partial model. It illustrates the diamond and trunnion trusses, the radial links, and the chain-drive and lateral truss link members. In addition it illustrates the model node numbers in important locations. The perspective is viewed from the West side of the diamond truss, looking East. Figures 1-3 through 1-5 illustrate diamond truss model nodes and elements looking, respectively, South, North, and East. They are perspective views, rotated to permit the bottom or top chord of the diamond truss to appear on the horizon.

Figures 1-6 through 1-9 illustrate the deflected shape of the diamond truss relative to the unloaded geometry, respectively, for the zenith and inclined dish positions of 30, 45, and 60 degrees. The magnitudes of the vertical and horizontal deflections at the North and South end of the diamond truss are respectively provided on each figure. Figures 1-10 and 1-11 simultaneously illustrate all these deflections, respectively looking East and South. Figures 1-12 through 1-15 illustrate these same deflections looking North. These deflections were not displayed simultaneously because the image would be difficult to interpret.

5.1.2 Deflections

The deflections from the partial model indicated the approximate magnitudes of the expected deflected shape of the diamond and trunnion trusses. That is, the diamond truss profiles a simple span between the trunnion trusses, and a two span beam on a pin at its center and on springs at its ends. The magnitude of the diamond truss deflections are indicated on the aforementioned figures.

In the actual structure the dish framing is integrated with the diamond truss. If the diamond truss deflections are simultaneoulsy reviewed in the cardinal directions, the dish structure would have to assume a deflected shape somewhat similar to that of a saddle, to accommodate the diamond truss deflections. The deflected shape of the dish structure, determined with the half model, confirms this.

5.1.3 Ruptured Gusset Plate Forces

Although the partial model results were not expected to be as accurate as those from the half model, they have been summarized below for the diamond truss panel members immediately adjacent to the trunnion trusses. This summary provides preliminary results for the analysis of the ruptured gusset which attached the inclined diamond truss bottom chord to the first horizontal bottom chord in the diamond truss panel just adjacent to the trunnion truss tubular verticals.

For the zenith position, the partial model indicated a 34.5 kip tensile force in the inclined bottom chord members on both the South and North sides of either trunnion truss. The analysis results for rotating the South end of the diamond truss downward, indicated the following forces. For 30, 45, and 60 degree inclinations: the North side chord forces were, respectively, 12.5, 35.4, and 56.0 kips, all in compression; the South side chord forces were, respectively, 72.2, 84.1, and 90.5 kips, also in tension. In addition to these axial forces, for all dish positions, the analysis indicated (very) small shears and moments vectorially parallel and normal to the reported crack in the gusset plate in the North-East side of the diamond truss.

The above information indicates that, for the zenith position, the bottom chord members all carry the same tensile load. It further indicates that, for inclined positions (approximately beyond +/-20 degrees), the lowered side members realize an increase in tension, while the elevated side members realize a reversal into compression.

At the 45 degree inclination, the elevated members realize a reversal into compression nearly equal in magnitude to the zenith position tension, the lowered members realize an increase in tension to nearly the maximum. That is, the North side bottom chords reversed from 34.5 tension to 35.4 compression, the South side bottom chords increased from 34.5 tension to 84.1 tension. These findings and the time history information which indicated that more observations were made at inclinations between, rather than beyond, +/- 45 degrees, justified the use of the 45 degree inclination for the half model.

5.1.4 Ruptured Gusset Plate Stresses

The average axial stress across the crack in the ruptured gusset plate was based on an effective area. This area was determined by evaluating an effective length of plate over which the axial analysis force(s) would act. This effective length was measured along the crack from the bottom of the gusset plate up to a fictitious line intersecting the crack. This line was at 30 degrees from the uppermost bolt line, and originated at the bolt farthest from the crack on this bolt line.

The length of crack determined in this manner was approximately 19.5 inches. Using this length and the half inch plate thickness as indicated on the shop drawings, the effective area was determined as 9.75 square inches. For this area, the axial stresses, in the plane of the gusset plate normal to the crack, were as indicated in the table below.

From the time-history of observations for the telescope, the approximate number of cycles gone through during the 25+ years of service was conservatively determined as one million. The present AISC code allowable reduced stress for this condition is 10 ksi. At first glance, the above summarized stresses do not indicate any overstress, however, the half model results have not yet

been presented.

Dish Position	Gusset Position (elevated=lowered for zenith)			
	elevated		lowered	
	force kips	stress ksi	force kips	stress ksi
Zenith	+34.5	+3.59	+34.5	+3.59
30 Deg. Inclntn.	-12.5	-1.28	+72.2	+7.41
45 Deg. Inclntn.	-35.4	-3.63	+84.1	+8.63
60 Deg. Inclntn.	-56.0	-5.74	+90.5	+9.28

Summary Table of Ruptured Gusset Axial Stresses
From Forces Determined From Partial Model Analysis.
Note: + = Tension, - = Compression

5.2 The Half Model

5.2.1 General

The half model analysis outputs for the zenith and inclined positions were both very extensive. The information contained in the outputs was strictly in relation to the model nodal and elemental numbering scheme, and physically buried in 100's of paper sheets. These findings were made directly visable by graphically relating them to the actual structure with the creation of deflection plots and the color coded identification of all overstressed members marked on appropriate plots. These plots, Figures 2-1 through 2-35, may be found in Volume II of this report.

5.2.2 Deflections

The deflection plots mentioned above were produced with AUTOCAD. They were based on the unloaded and loaded geometry information from the STAAD analysis. They are illustrated on Figures 2-5 through 2-7 for the zenith position analysis, and Figures 2-8 and 2-9 for the 45 degree inclined position analysis.

5.2.3 Member Forces

The color coded overstressed members were manually identified on plots of the framing of the dish top surface, the dish bottom surface, the developed circumferential surfaces, and the layouts for the main and auxiliary radial rib surfaces. They all were plotted with AUTOCAD with the results from both the zenith and inclined position models.

Figures 2-10 and 2-11, respectively, illustrate members on the top and bottom dish surfaces. Figures 2-12 through 2-16 illustrate members on the main radial ribs. Figures 2-17 through

2-20 illustrate members on the auxiliary ribs. The circumferentials are illustrated in Figures 2-21 through 2-35.

The analysis indicated the existence of significant moments and tension overstresses in the top chord members of the trunnion trusses due to frame action. These areas were documented as the location of previous failures and subsequent repairs. The analysis indicated that many of the members in the circumferential surfaces in the dish originally designed for tension only were, in fact, carrying compressive loads; that 25 percent of these members were overstressed in the zenith position; that 22.2 percent were overstressed in the 45 degree inclined position; and that, in general, ninty percent of these overstressed members were in compression. Additionally, the analysis indicated that a significant number of the vertical members in the central hoops exceeded permissible slenderness ratios by up to 60 percent; and that the few members in the overstressed radial ribs were primarily in tension.

5.2.4 Ruptured Gusset Plate Forces

From the half model analysis results, the axial force(s) in the inclined bottom chord member of the diamond truss were as follows: for the zenith position, on both the North and South sides, the forces were 50.0 kips tension; for the inclined position, the elevated (North) side force was 51.0 kips compression, the lowered (South) side force was 120 kips tension.

The above results indicate an increase in the diamond truss bottom chord member forces from those determined with the partial model analysis. Specifically and relative to the partial model for the zenith position the forces increased by 46 percent; for the 45 degree inclined position, the forces increased by 42 percent for the lowered member (at maximum tension) and by 46 percent for elevated member (undergoing reversal).

Like the partial model, the half model analysis indicated small shears on the inclined bottom chord member attached to the gusset plate that had ruptured. Unlike the partial model, however, the in-plane and out-of-plane moments determined by the half model analysis were significantly larger.

5.2.5 Ruptured Gusset Plate Stresses

The evaluation of the ruptured gusset plate stresses from the forces as determined from the half model zenith and 45 degree inclined analysis is summarized in Figures 1-16 and 1-17.

Figure 1-16 illustrates the ruptured gusset plate details as originally specified in the shop drawings. The figure depicts the plate elevation, section, plan, the crack location, and its material call out on the part list. It also includes a reproduction of the photo of the plate.

Figure 1-17 illustrates the elevation view of the ruptured plate

and the inclined bottom chord member bolt holes. It also provides a summary of the analysis forces and the preliminary calculations for the resulting stresses on the plate in the region of the crack.

For these calculations, the vertical direction was taken parallel to the crack and the horizontal direction was taken as normal to the plate surface. Therefore, the out-of-plane bending was due to a moment vector in the vertical (v) direction, while in plane bending was due to a moment vector in the horizontal (h) direction.

The maximum average tensile stress in the rupture gusset was nominally 12.3 ksi. This stress was in the lowered side of the trunnion truss at the 45 degree inclination. The current AISC allowable for 500,000 to 2,000,000 cycles is 10.0 ksi.

The out-of-plane bending stress for this gusset plate for the zenith position was +/- 28.1 ksi at both the North and South gussets. For the 45 degree inclined dish position, it was +/- 117 ksi on the North (elevated) side and +/- 160 ksi on the South (lowered) side.

The average difference between the zenith and the inclined position stresses may be taken as +/- 110 ksi. The magnitude of these out-of-plane bending stresses (well above the yield stress) indicates that plastic straining could have occurred in the gusset due to out-of-plane bending.

6.0 CONCLUSIONS

The NRAO 300 foot diameter dish radio telescope was analyzed with a finite element frame model which represented the ideal configuration of the structure as shown on the plans at the time of collapse. This condition included the various remedial strengthening additions implemented over the life of the telescope.

Although the model did take into account the bending capacity and continuity of members by considering the structure as a three dimensional frame, the analysis was linear, and subsequently, did not permit the consideration of the yield straining of tension members or the buckling distortion of compression members.

The analysis was based on the idealized condition that assumed the model to be simultaneously loaded with its self-weight. The actual deflections and member forces came about from the initial distribution of the dead loads during construction and the redistribution of the dead and the (not considered) live loads during the entire cyclic service life of the dish structure. Therefore, the deflections and member forces determined from the analysis may differ from the actual values in the structure before collapse.

Had the structure not collapsed, the potential to compare the

theoretic and actual deflections for a particular dish position would have existed. This comparison would have been a time consuming and expensive ordeal, and well beyond the scope of work of this analysis. Analysis results must be assumed to be the best approximation of respective actual values presently available, and the following conclusions have been made:

a) The analysis of the telescope only considered the self-weight of the structure. Under this loading condition many members were found to be overloaded in compression. Several of these compression members would have buckled under their overload, thereby redistributing the overloads throughout the life of the structure. Attendant load redistributions may have contributed to the collapse.

b) Visual inspection and laboratory tests of the ruptured gusset removed from the telescope wreckage indicated progressive cracking with eventual rupturing of this plate. The analysis showed that the self-weight plate stresses were high enough to cause cracking and crack growth under the cyclic loads from the antenna movements. These stresses were above their allowable values, and could have initiated and propogated the crack due to years of high (plastic) stress and strain fluctuation. Rupture of the plate could have caused the collapse of the telescope.

c) The structure was highly redundant, however, the capacities of these redundancies were not sufficient to indefinitely permit load redistribution or to halt it. The number of overstressed members distributed throughout the structure was excessive.

d) The number of overstressed members identified was based on the application of only the structure dead load. The inclusion of additional environmental or other short-term loads sustained by the structure over its operational life would have resulted in higher stresses and additional overstressed members.

e) The use of a frame model with moment connections did reflect that the actual members were sustaining additional loads not accounted in the original design of the structure as a truss.

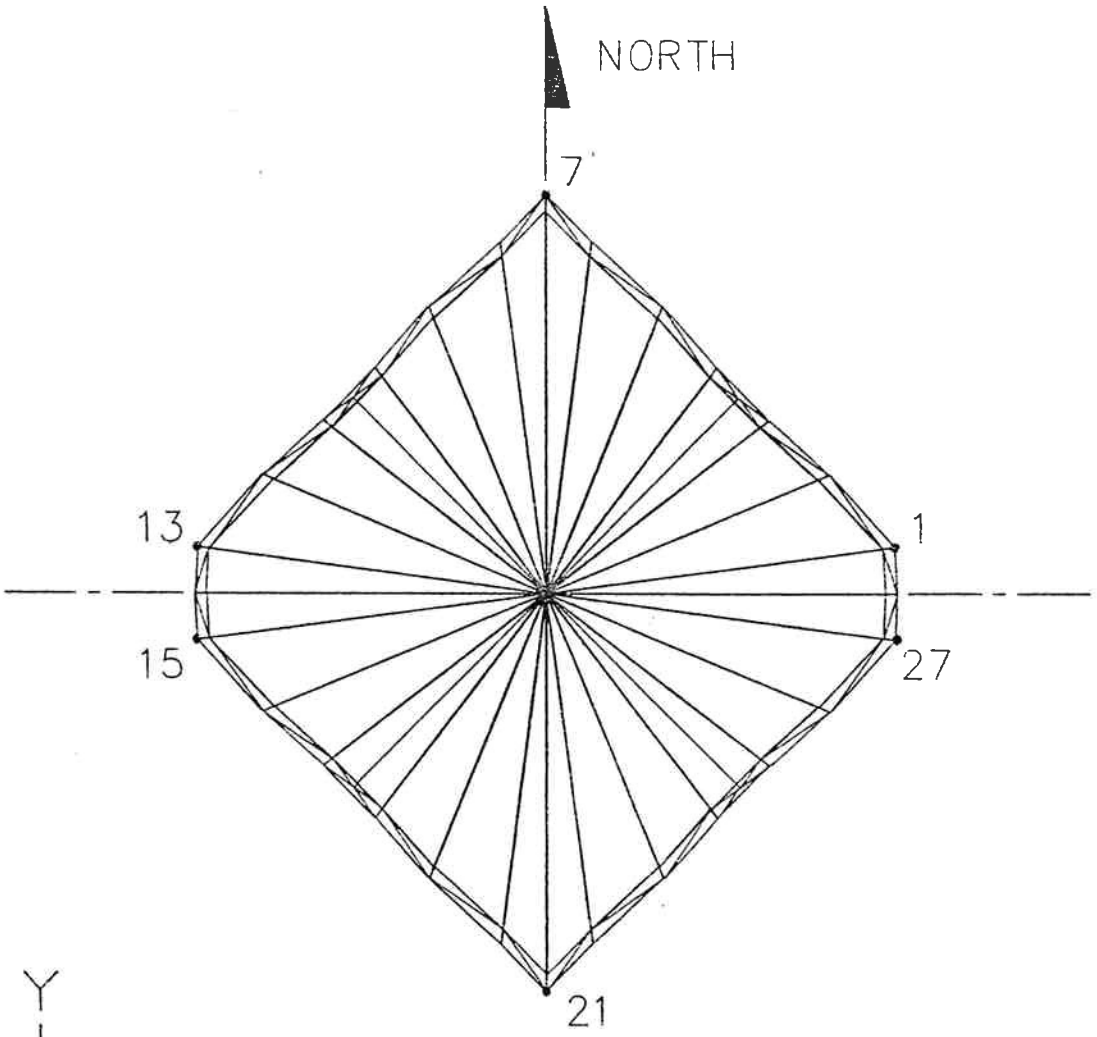

PLAN

STAADPL

(Research Engineers, Inc.)

REVISION 4.2

GRAPHICS DISPLAY

SUBSTR.DAT

TOTAL NO. OF JOINTS = 63
HIGHEST JOINT NUMB = 63
TOTAL NO. OF MEMB = 239
HIGHEST MEMBER NUMB = 247
ORIGIN LOCATED AT:
.0 .0 -27.5
VIEWING DISTANCE = 630.0
DIMENSIONAL RANGE:
-80.00 <X< 80.00
-90.00 <Y< 90.00
-80.00 <Z< 25.00
LENGTH UNIT IS FOOT

FIGURE 1-1

DATE: Feb 8 1989

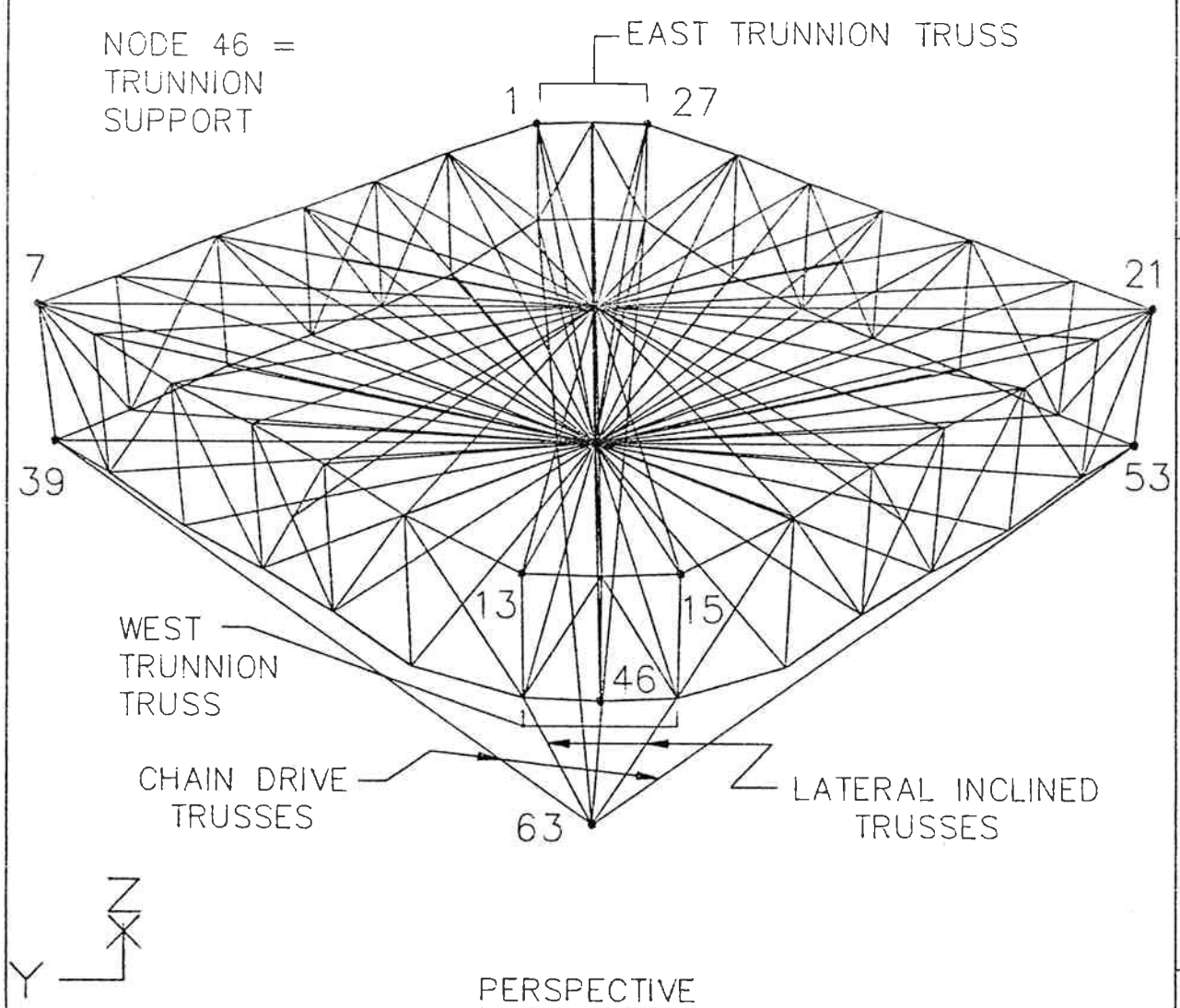

PERSPECTIVE

STAADPL

(Research Engineers, Inc.)

REVISION 4.2

GRAPHICS DISPLAY

SUBSTR.DAT

TOTAL NO. OF JOINTS = 63
HIGHEST JOINT NUMB = 63
TOTAL NO. OF MEMB = 239
HIGHEST MEMBER NUMB = 247
ORIGIN LOCATED AT:
-4.4 19.3 -27.5
VIEWING DISTANCE = 404.6
DIMENSIONAL RANGE.
-80.00 <X< 80.00
-90.00 <Y< 90.00
-60.00 <Z< 25.00
LENGTH UNIT IS FOOT

FIGURE 1-2

DATE: Feb 8 1989

NOTE:

PERSPECTIVE ANGLE SET TO
HORIZONTAL VIEW OF TOP CHORD.

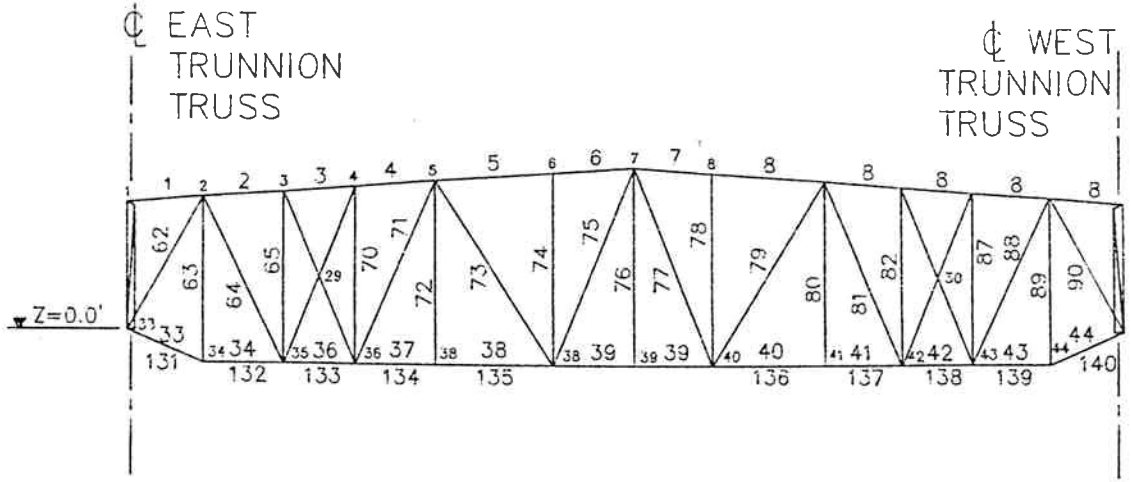

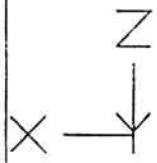

NORTH ELEVATION, MODEL SHOWN w/o
CHAIN DRIVE & INCLINED TRUSSES

STAADPL

(Research Engineers, Inc.)

REVISION 4.2

GRAPHICS DISPLAY

SUBSTR.DAT

TOTAL NO. OF JOINTS = 63
HIGHEST JOINT NUMB = 63
TOTAL NO. OF MEMB = 239
HIGHEST MEMBER NUMB = 247
ORIGIN LOCATED AT.
-5.4 44.5 -27.5
VIEWING DISTANCE = 412.1
DIMENSIONAL RANGE:
-80.00 <X< 80.00
-90.00 <Y< 90.00
-80.00 <Z< 25.00
LENGTH UNIT IS FOOT

o JOINT NUMBERS

FIGURE 1-3

DATE: Feb 8 1989

NOTE:

PERSPECTIVE ANGLE SET TO
HORIZONTAL VIEW OF TOP CHORD.

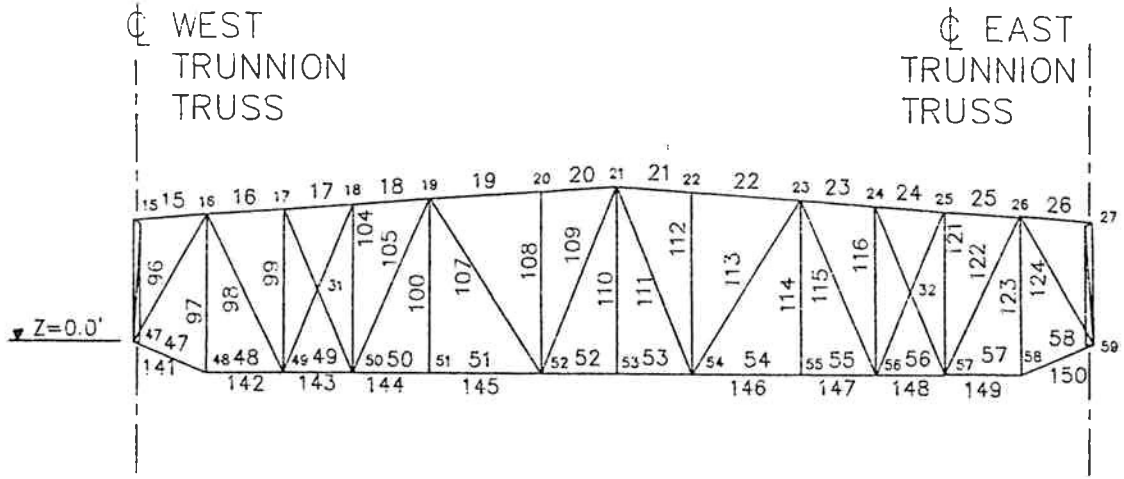

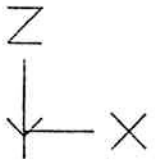

SOUTH ELEVATION, MODEL SHOWN w/o
CHAIN DRIVE & INCLINED TRUSSES

STAADPL

(Research Engineers, Inc.)

REVISION 4.2

GRAPHICS DISPLAY

SUBSTR.DAT

TOTAL NO. OF JOINTS = 63
HIGHEST JOINT NUMB = 63
TOTAL NO. OF MEMB = 239
HIGHEST MEMBER NUMB = 247
ORIGIN LOCATED AT.
-2.7 47.6 -27.5
VIEWING DISTANCE = 429.1
DIMENSIONAL RANGE:
-80.00 <X< 80.00
-90.00 <Y< 90.00
-80.00 <Z< 25.00
LENGTH UNIT IS FOOT

o JOINT NUMBERS

FIGURE 1-4

DATE: Feb 8 1989

NOTE:

PERSPECTIVE ANGLE SET TO
HORIZONTAL VIEW OF TOP CHORD.

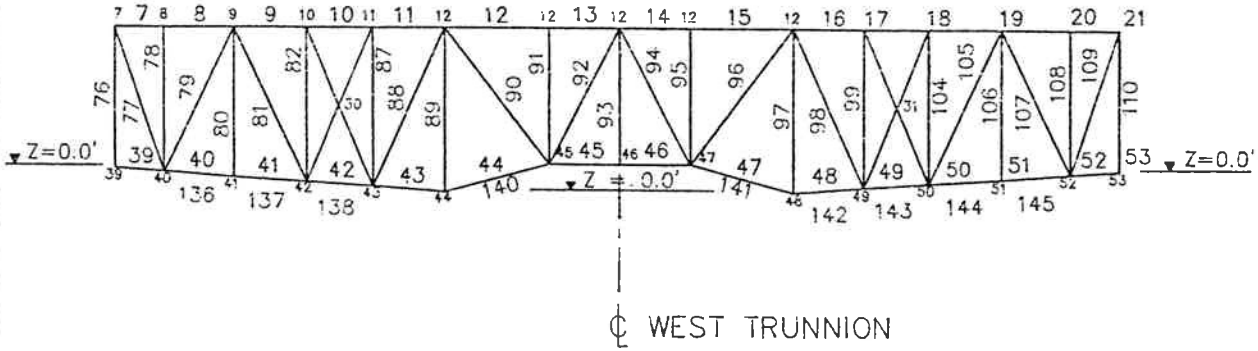

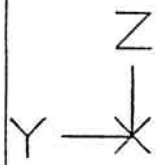

WEST ELEVATION, MODEL SHOWN w/o
CHAIN DRIVE & INCLINED TRUSSES

STAADPL

(Research Engineers, Inc.)

REVISION 4.2

GRAPHICS DISPLAY

SUBSTR.DAT

TOTAL NO. OF JOINTS = 63
HIGHEST JOINT NUMB = 63
TOTAL NO. OF MEMB = 239
HIGHEST MEMBER NUMB = 247
ORIGIN LOCATED AT:
-2.7 45.5 -27.5
VIEWING DISTANCE = 456.3
DIMENSIONAL RANGE:
-80.00 <X< 80.00
-90.00 <Y< 90.00
-80.00 <Z< 25.00
LENGTH UNIT IS FOOT

o JOINT NUMBERS

FIGURE 1-5

DATE: Feb 8 1989

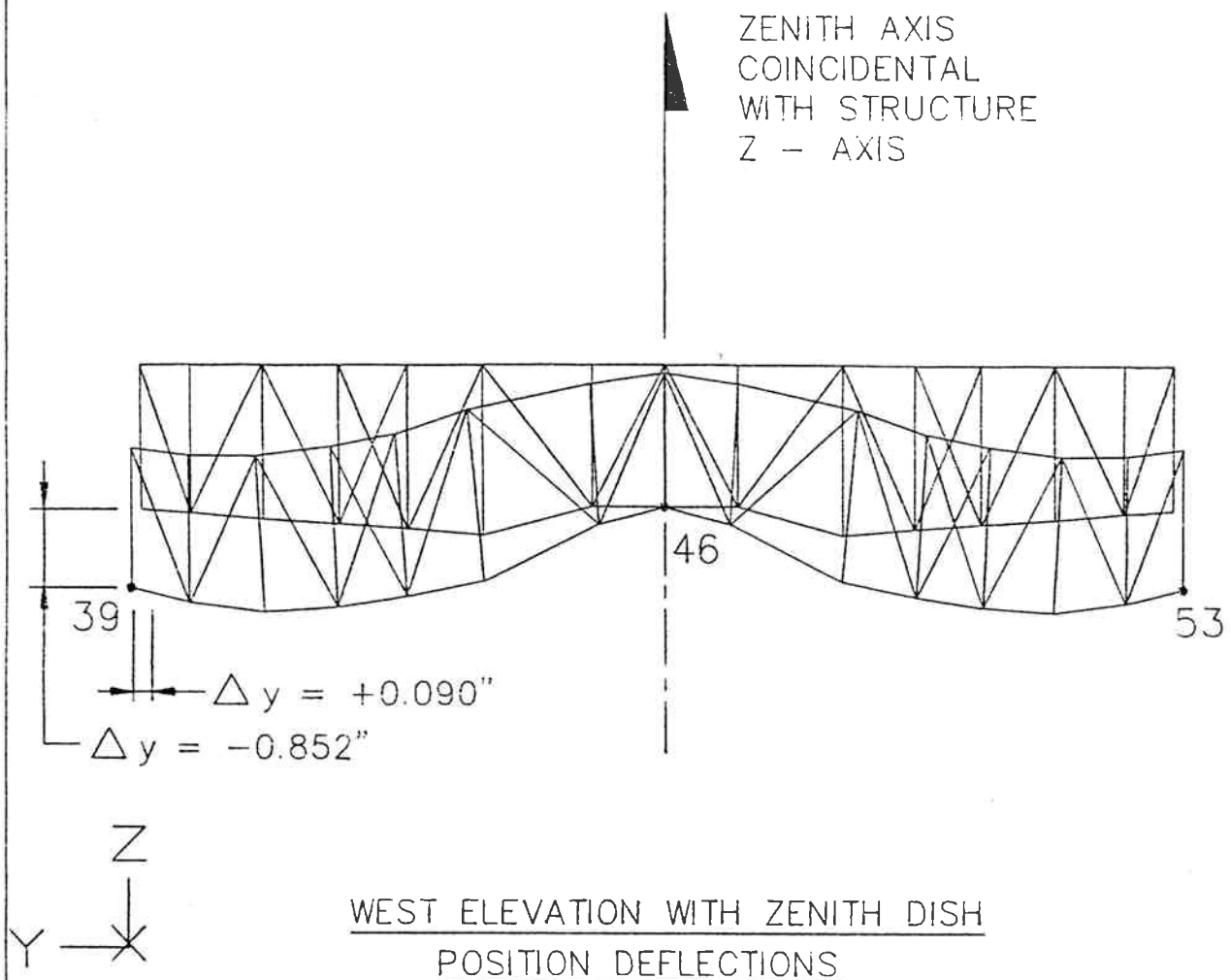

WEST ELEVATION WITH ZENITH DISH
POSITION DEFLECTIONS

STAADPL

(Research Engineers, Inc.)

REVISION 4.2

GRAPHICS DISPLAY

SUBSTR.DAT

STAAD DEFLECTED SHAPE

LOAD CASE NO. 1
0 DEGREE INCLINATION

SCALE FACTOR= 200.0

TOTAL NO. OF JOINTS = 63
HIGHEST JOINT NUMB = 63
TOTAL NO. OF MEMB = 239
HIGHEST MEMBER NUMB = 247
ORIGIN LOCATED AT:
-6.3 36.2 -27.5
VIEWING DISTANCE = 430.8
DIMENSIONAL RANGE:
-80.00 <X< 80.00
-90.00 <Y< 90.00
-80.00 <Z< 25.00
LENGTH UNIT IS FOOT

NOTE: DEFLECTIONS ARE WRT TO MODEL COORDINATE SYSTEM. THIS NOTE APPLIES TO ALL FIGURES.

FIGURE 1-6

DATE: Feb 8 1989

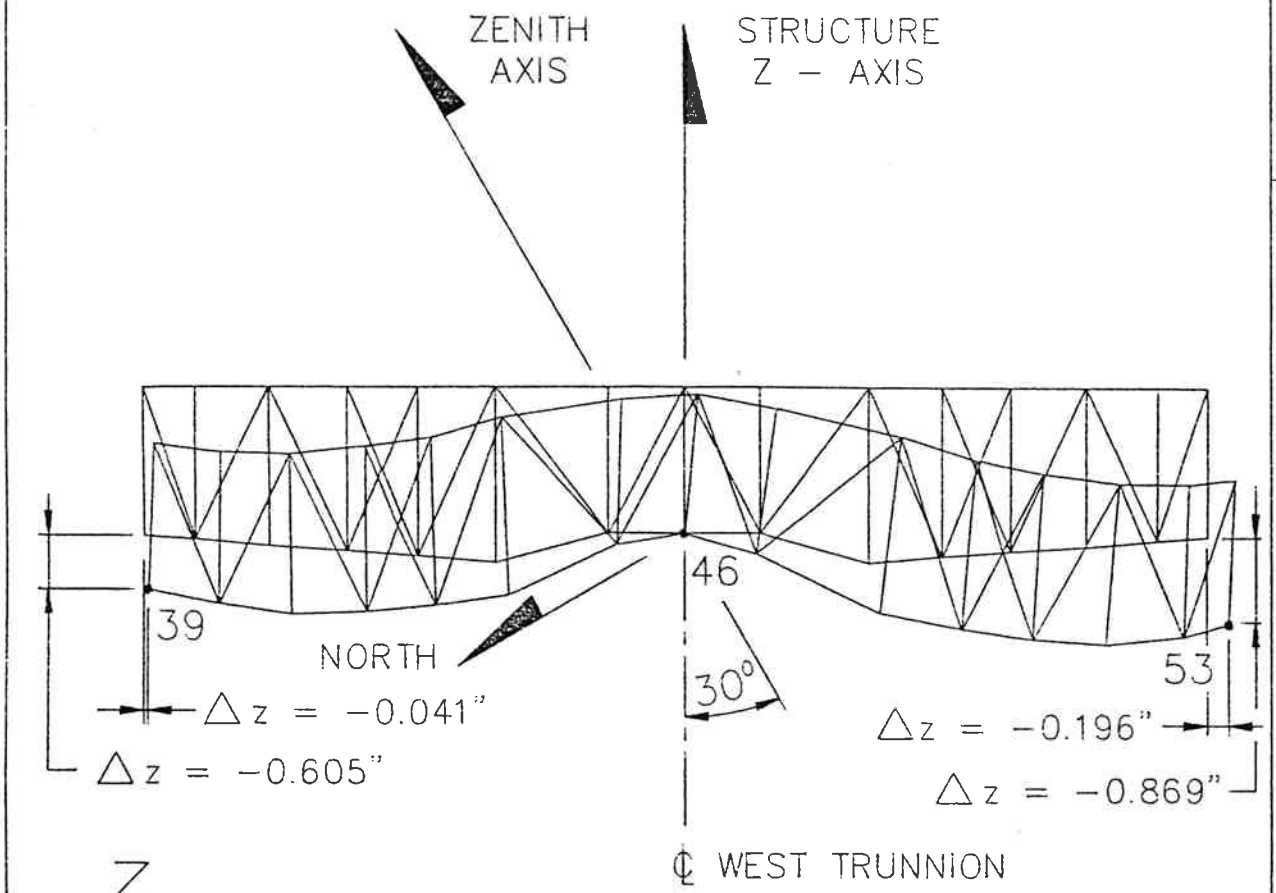

WEST ELEVATION WITH 30° INCLINED
DISH POSITION DEFLECTIONS

STAADPL

(Research Engineers, Inc.)

REVISION 4.2

GRAPHICS DISPLAY

SUBSTR.DAT

STAAD DEFLECTED SHAPE

LOAD CASE NO. 2
30° INCLINATION SOUTHWARD

SCALE FACTOR= 200.0

TOTAL NO. OF JOINTS = 63
HIGHEST JOINT NUMB = 63
TOTAL NO. OF MEMB = 239
HIGHEST MEMBER NUMB = 247
ORIGIN LOCATED AT:
−6.3 36.2 −27.5
VIEWING DISTANCE = 430.8
DIMENSIONAL RANGE:
−80.00 <X< 80.00
−90.00 <Y< 90.00
−80.00 <Z< 25.00
LENGTH UNIT IS FOOT

FIGURE 1-7

DATE: Feb 8 1989

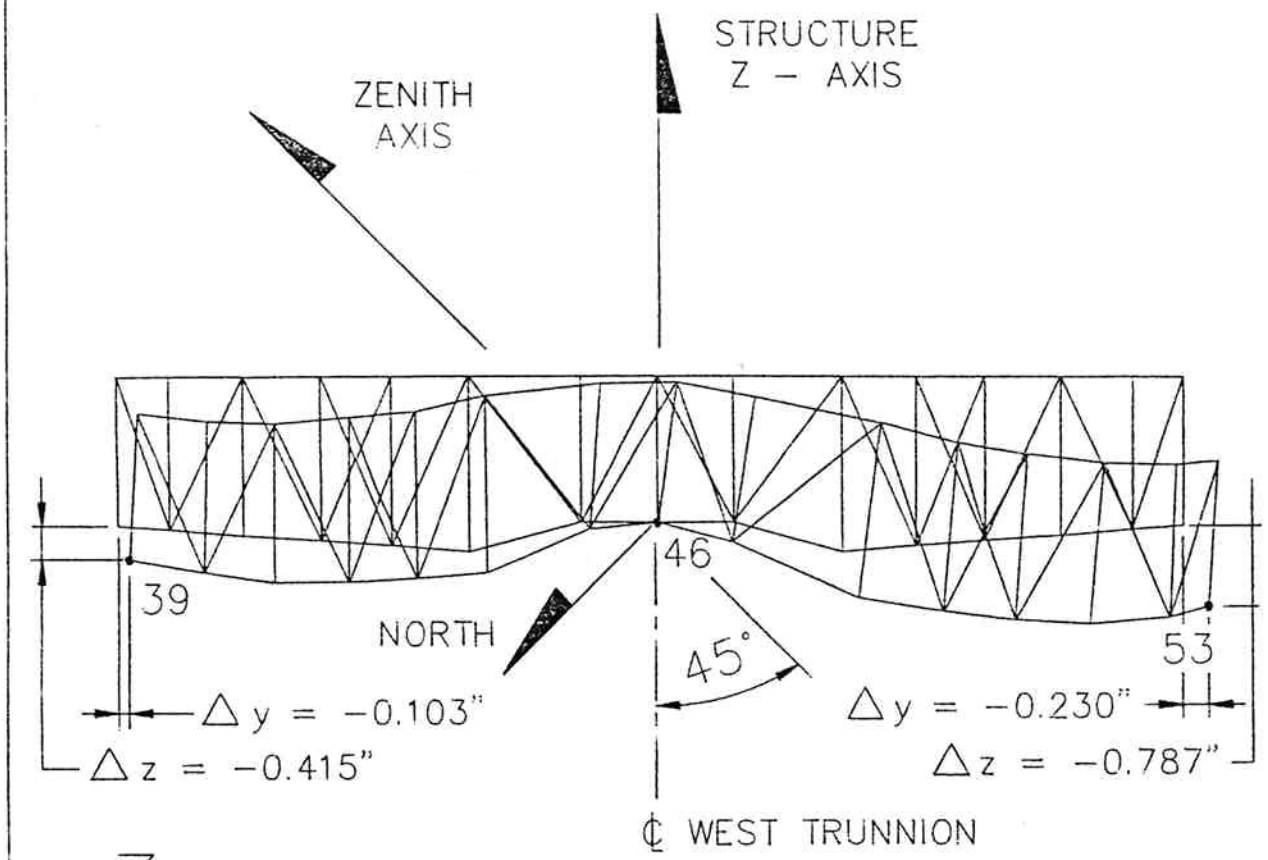

WEST ELEVATION WITH 45° INCLINED
DISH POSITION DEFLECTIONS

STAADPL

(Research Engineers, Inc.)

REVISION 4.2

GRAPHICS DISPLAY

SUBSTR.DAT

STAAD DEFLECTED SHAPE

LOAD CASE NO. 3
45° INCLINATION SOUTHWARD

SCALE FACTOR= 200.0

TOTAL NO. OF JOINTS = 63
HIGHEST JOINT NUMB = 63
TOTAL NO. OF MEMB = 239
HIGHEST MEMBER NUMB = 247
ORIGIN LOCATED AT:
-6.3 36.2 -27.5
VIEWING DISTANCE = 430.8
DIMENSIONAL RANGE:
-80.00 <X< 80.00
-90.00 <Y< 90.00
-80.00 <Z< 25.00
LENGTH UNIT IS FOOT

FIGURE 1-8

DATE: Feb 8 1989

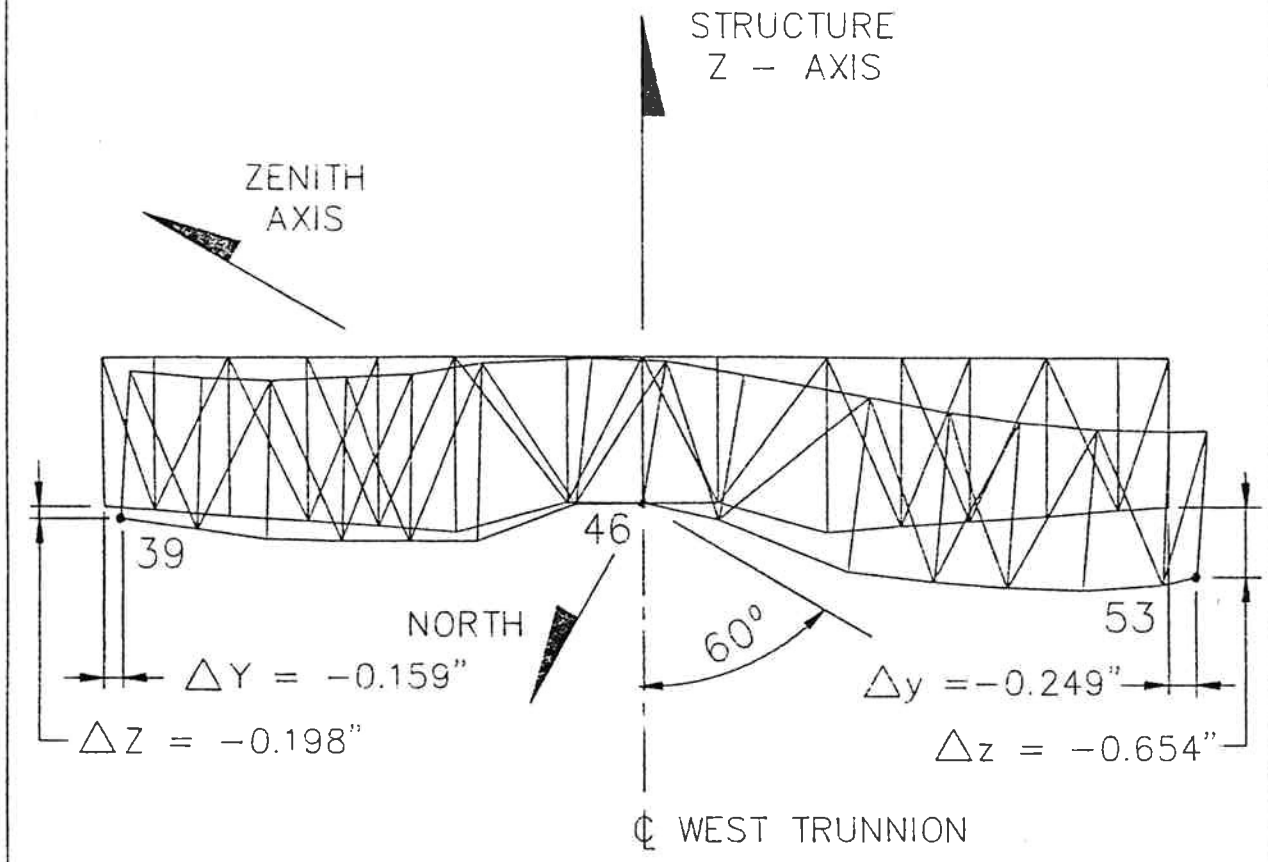

WEST ELEVATION WITH 60° INCLINED
DISH POSITION DEFLECTIONS

STAADPL

(Research Engineers, Inc.)

REVISION 4.2

GRAPHICS DISPLAY

SUBSTR.DAT

STAAD DEFLECTED SHAPE

LOAD CASE NO. 4
60° INCLINATION SOUTHWARD
SCALE FACTOR= 200.0

TOTAL NO. OF JOINTS = 63
HIGHEST JOINT NUMB = 63
TOTAL NO. OF MEMB = 239
HIGHEST MEMBER NUMB = 247
ORIGIN LOCATED AT:
−6.3 36.2 −27.5
VIEWING DISTANCE = 430.8
DIMENSIONAL RANGE:
−80.00 <X< 80.00
−90.00 <Y< 90.00
−80.00 <Z< 25.00
LENGTH UNIT IS FOOT

FIGURE 1-9

DATE: Feb 8 1989

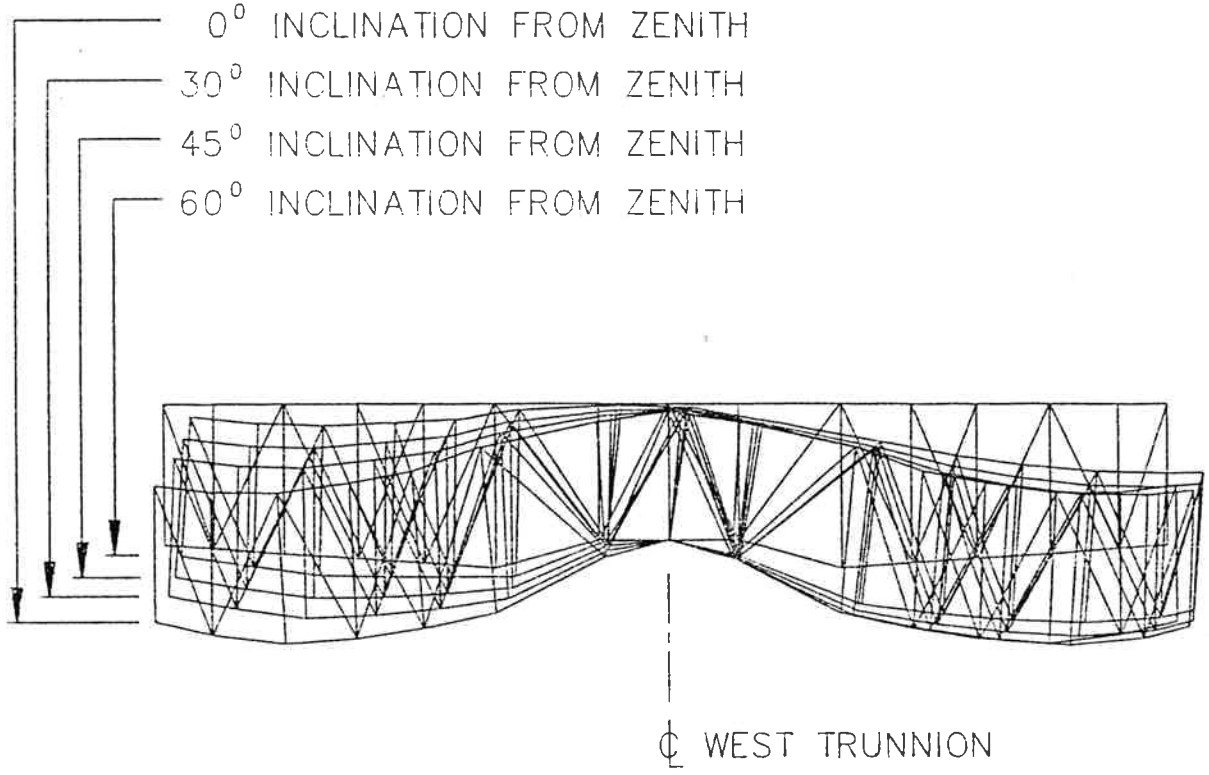

WEST ELEVATION WITH IMPOSED DEFLECTIONS
FOR 0° , 30° , 45°& 60° INCLINATIONS

STAADPL

(Research Engineers, Inc.)

REVISION 4.2

GRAPHICS DISPLAY

SUBSTR.DAT

STAAD DEFLECTED SHAPE

LOAD CASE 1 – 4

SCALE FACTOR= 200.0

TOTAL NO. OF JOINTS = 63
HIGHEST JOINT NUMB = 63
TOTAL NO. OF MEMB = 239
HIGHEST MEMBER NUMB = 247
ORIGIN LOCATED AT:
-2.7 45.5 -27.5
VIEWING DISTANCE = 456.3
DIMENSIONAL RANGE:
-80.00 <X< 80.00
-90.00 <Y< 90.00
-80.00 <Z< 25.00
LENGTH UNIT IS FOOT

FIGURE 1-10

DATE: Feb 8 1989

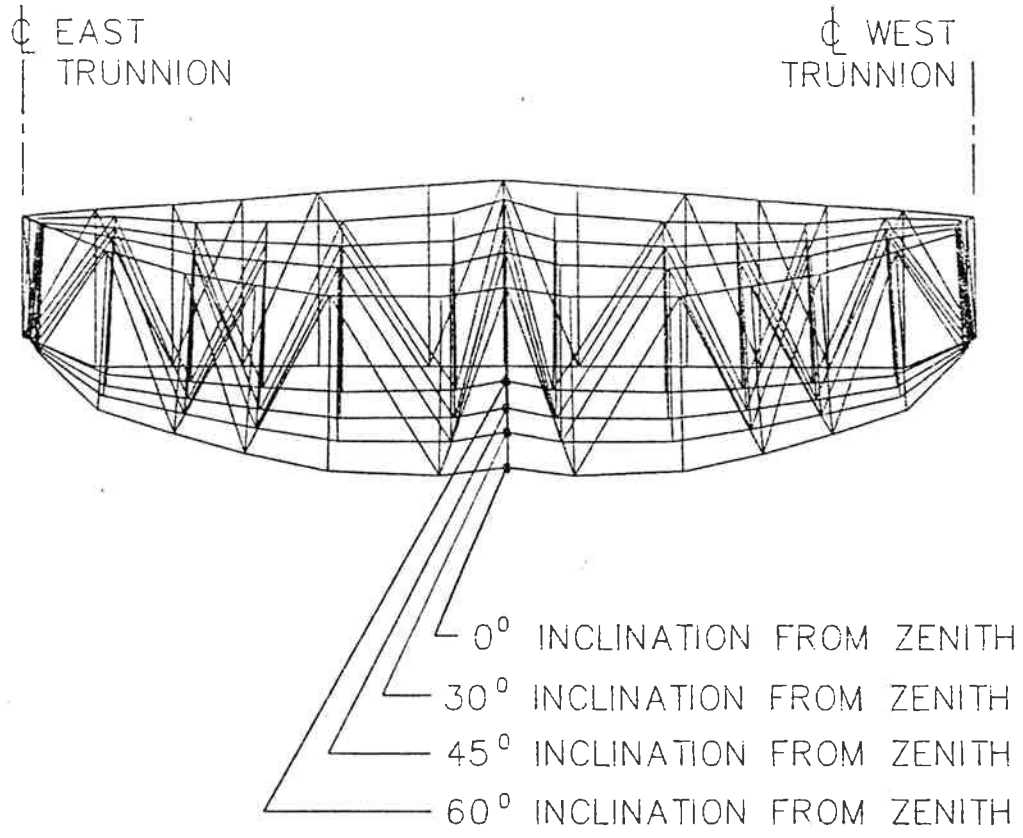

NORTH ELEVATION WITH IMPOSED DEFLECTIONS
FOR 0° , 30° , 45° & 60° INCLINATIONS

STAADPL

(Research Engineers, Inc.)

REVISION 4.2

GRAPHICS DISPLAY

SUBSTR.DAT

STAAD DEFLECTED SHAPE

LOAD CASE NO. 1

SCALE FACTOR= 200.0

TOTAL NO. OF JOINTS = 63
HIGHEST JOINT NUMB = 63
TOTAL NO. OF MEMB = 239
HIGHEST MEMBER NUMB = 247
ORIGIN LOCATED AT.
-2.7 43.5 -27.5
VIEWING DISTANCE = 432.5
DIMENSIONAL RANGE.
-80.00 <X< 80.00
-90.00 <Y< 90.00
-80.00 <Z< 25.00
LENGTH UNIT IS FOOT

FIGURE 1-11

DATE: Feb 9 1989

STAADPL

(Research Engineers, Inc.)

REVISION 4.2

GRAPHICS DISPLAY

SUBSTR.DAT

STAAD DEFLECTED SHAPE

LOAD CASE NO. 1

SCALE FACTOR= 200.0

TOTAL NO. OF JOINTS = 63
HIGHEST JOINT NUMB = 63
TOTAL NO. OF MEMB = 239
HIGHEST MEMBER NUMB = 247
ORIGIN LOCATED AT:
-2.7 43.5 -27.5
VIEWING DISTANCE = 432.5
DIMENSIONAL RANGE:
-80.00 <X< 80.00
-90.00 <Y< 90.00
-80.00 <Z< 25.00
LENGTH UNIT IS FOOT

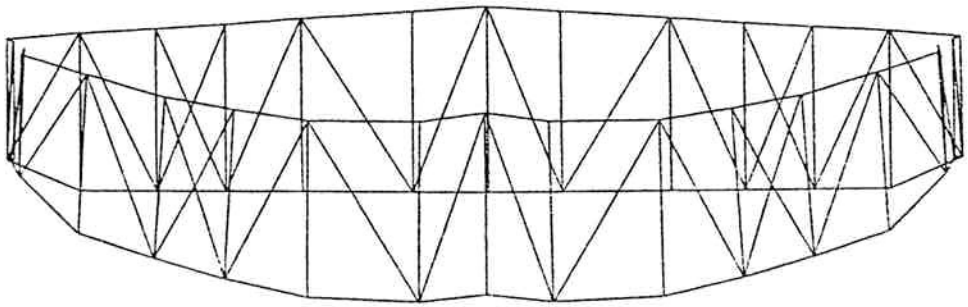

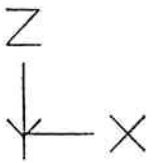

SOUTH ELEVATION WITH 0°
INCLINATION DEFLECTIONS

FIGURE 1-12

DATE: Feb 9 1989

STAADPL

(Research Engineers, Inc.)

REVISION 4.2

GRAPHICS DISPLAY

SUBSTR.DAT

STAAD DEFLECTED SHAPE

LOAD CASE NO. 2

SCALE FACTOR= 200.0

TOTAL NO. OF JOINTS = 63
HIGHEST JOINT NUMB = 63
TOTAL NO. OF MEMB = 239
HIGHEST MEMBER NUMB = 247
ORIGIN LOCATED AT:
-2.7 43.5 -27.5
VIEWING DISTANCE = 432.5
DIMENSIONAL RANGE:
-80.00 <X< 80.00
-90.00 <Y< 90.00
-80.00 <Z< 25.00
LENGTH UNIT IS FOOT

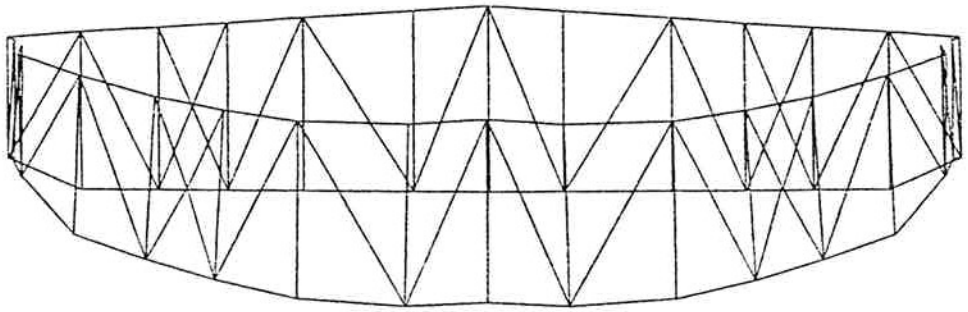

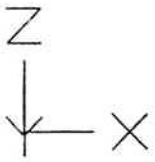

SOUTH ELEVATION WITH 30°
INCLINATION DEFLECTIONS

FIGURE 1-13

DATE: Feb 9 1989

STAADPL

(Research Engineers, Inc.)

REVISION 4.2

GRAPHICS DISPLAY

SUBSTR.DAT

STAAD DEFLECTED SHAPE

LOAD CASE NO. 3

SCALE FACTOR= 200.0

TOTAL NO. OF JOINTS = 63
HIGHEST JOINT NUMB = 63
TOTAL NO. OF MEMB = 239
HIGHEST MEMBER NUMB = 247
ORIGIN LOCATED AT:
-2.7 43.5 -27.5
VIEWING DISTANCE = 432.5
DIMENSIONAL RANGE.
-80.00 <X< 80.00
-90.00 <Y< 90.00
-80.00 <Z< 25.00
LENGTH UNIT IS FOOT

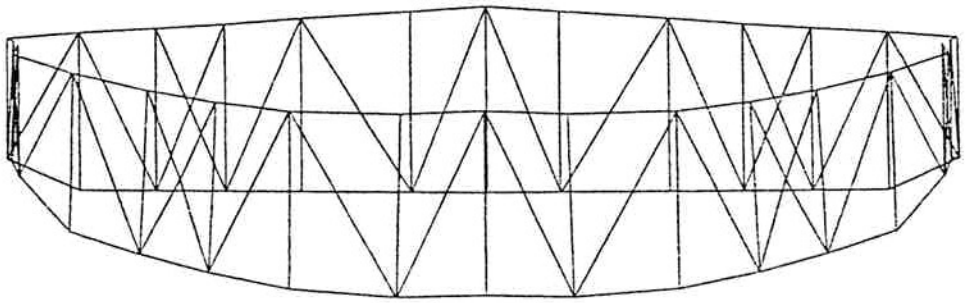

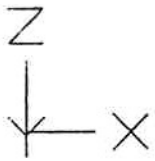

SOUTH ELEVATION WITH 45° INCLINATION DEFLECTIONS

FIGURE 1-14

DATE: Feb 9 1989

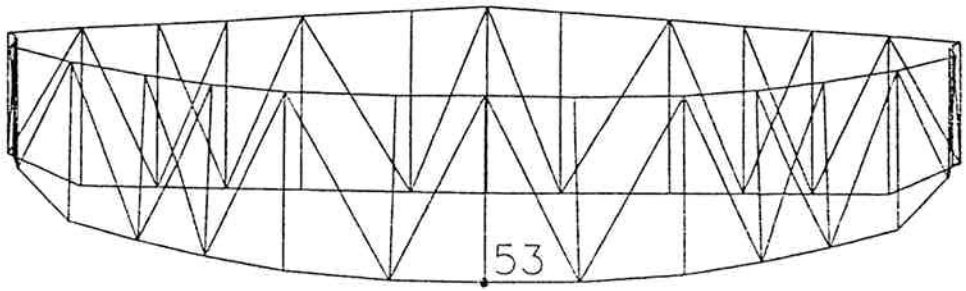

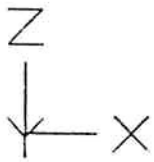

SOUTH ELEVATION WITH 60° INCLINATION REFLECTIONS

STAADPL

(Research Engineers, Inc.)

REVISION 4.2

GRAPHICS DISPLAY

SUBSTR.DAT

STAAD DEFLECTED SHAPE

LOAD CASE NO. 4

SCALE FACTOR= 200.0

TOTAL NO. OF JOINTS = 63
HIGHEST JOINT NUMB = 63
TOTAL NO. OF MEMB = 239
HIGHEST MEMBER NUMB = 247
ORIGIN LOCATED AT:
-2.7 43.5 -27.5
VIEWING DISTANCE = 432.5
DIMENSIONAL RANGE:
-80.00 <X< 80.00
-90.00 <Y< 90.00
-80.00 <Z< 25.00
LENGTH UNIT IS FOOT

FIGURE 1-15

DATE: Feb 9 1989

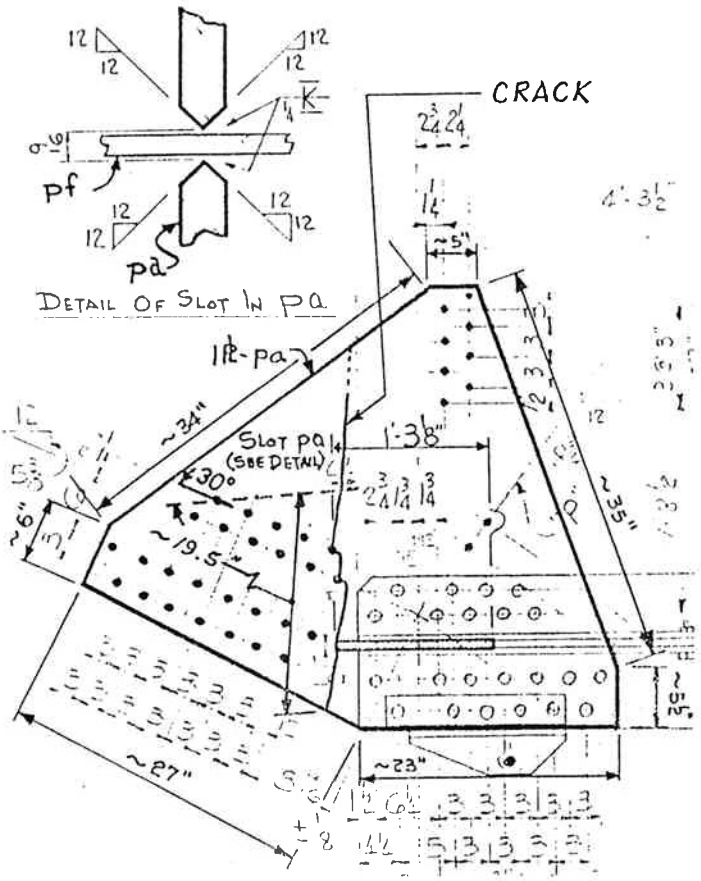

ELEVATION

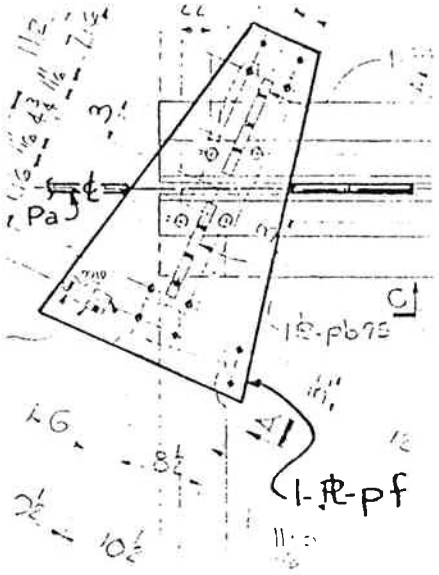

PLAN

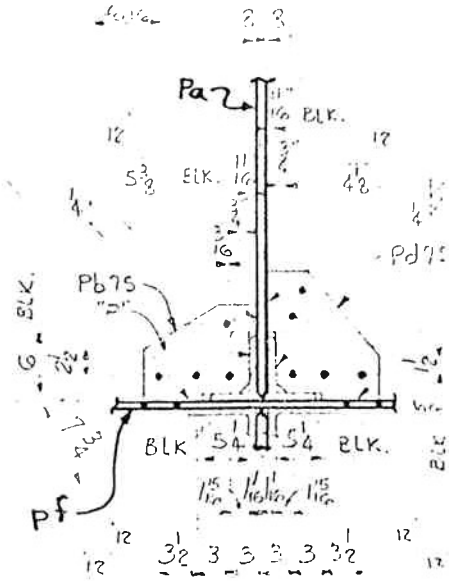

SECTION

GROUP	SHIP MARK	ASS'M MARK	NO PCS.	SECTION	LENGTH FT.	LENGTH IN.	CUT FROM
E1	76BC1	A	1	BOTT. CHORD			
	76BC1	B	1				
	76BC1	D	1				
6	76BC1	C	1	do do			
			8	L 6×4×⅝	37	7¼	
			4	L 8×8×⅝	37	7¼	
			4	L 2×3×⅝	37	7¼	
		Pa	4	PL-43×½	4	1½	
		Pb	4	PL-21¼×½	2	5½	
		Pd	4	PL-13½×½	1	7¾	
		Pc	8	PL-7×½	2	5½	
		Pe	4	PL-8¼×½	-	10⅜	
		Pg	4	PL-10⅝×½	1	0	
		Pf	4	PL-21×½	2	9½	

RUPTURED GUSSET PL (Pa)

PL IN SLOT (Pf)

PART LIST

NOTE: DRAWINGS FROM BRISTOL STEEL & IRON WORKS, INC. SHOP DRAWINGS, SHEET 76

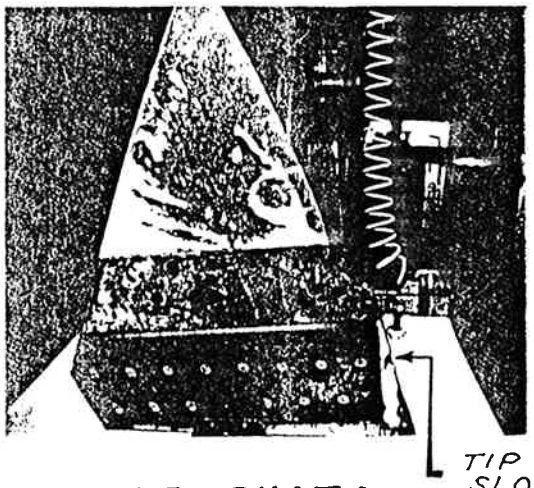

LAB PHOTO

FIGURE 1-16 : RUPTURED GUSSET PLATE DETAILS

RUPTURED GUSSET PLATE STRESSES DUE TO FORCES DETERMINED WITH HALF MODEL ANALYSIS

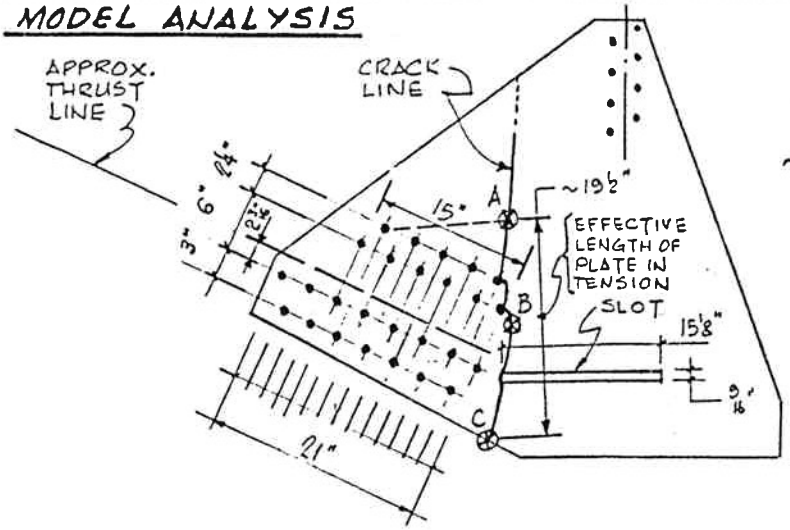

RUPTURED GUSSET PLATE ELEVATION

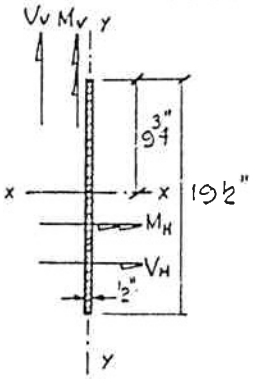

$L_e = 19.5"$, $t = 0.5"$

$A_T = A_v = tL_e = 9.75 in^2$

$S_{xx} = bt^2/6 = 0.5 \times 19.5^2/6$

$= 31.69 in^3$

$S_{yy} = 19.5 \times 0.5^2/6$

$= 0.81 in^3$

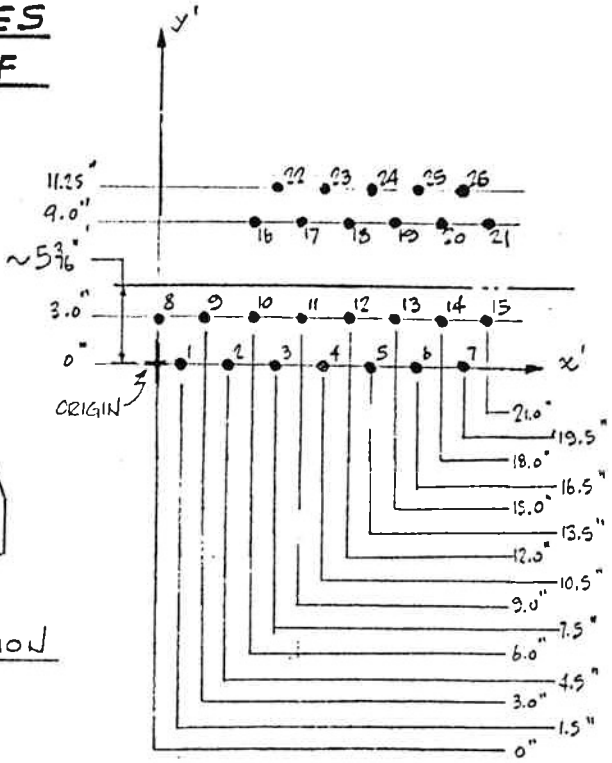

BOTTOM CHORD BOLT SPACING

n	w IN.	H IN.	$\bar{y}$ IN.	$\bar{x}$ IN.	
01	1.0	1.0	0	1.5	✓
2				4.5	✓
3				7.5	✓
4				10.5	✓
5				13.5	✓
6				16.5	✓
7			0	19.5	✓
8			3.0	0.0	✓
9				3.0	✓
10				6.0	✓
11				9.0	✓
12				12.0	✓
13				15.0	✓
14				18.0	✓
15			3.0	21.0	✓
16			9.0	6.0	✓
17				9.0	✓
18				12.0	✓
19				15.0	✓
20				18.0	✓
21			9.0	21.0	✓
22			11.25	7.5	✓
23				10.5	✓
24				13.5	✓
25				16.5	✓
26	1.0	1.0	11.25	19.5	✓

UNIT AREA USED TO DETERMINE $\bar{y}$

($\bar{y} = 5\frac{3}{16}"$ ABOVE x'-AXIS)

DISH POSITN.	SIDE	P / σ_p K/KSI	V_v / σ_{vv} K/KSI	V_H / σ_{vH} K/KSI	M_v / σ_{bv} K"/KSI	M_H / σ_{bH} K"/KSI
ZENITH	N&S	+50 / 5.13	1.3 / 0.13	1.9 / 0.19	22.8 / 28.1	73.2 / 2.31
45°	NORTH	-51 / 5.23	1.0 / 0.10	0.7 / 0.07	91.8 / 117.0	4.8 / 0.15
45°	SOUTH	+120 / 12.3	0.8 / 0.08	1.3 / 0.13	130 / 160	55.2 / 1.74

NOTE: σ_{bv} IS A BENDING STRESS DUE TO OUT OF PLANE BENDING

MAX. STRESSES

AT POINTS A, B & C; $\sigma_t = 12.3$ KSI, $\sigma_{vv} = 0.08$ KSI, $\sigma_{vH} = 0.13$ KSI AND $\sigma_{bv} = \pm 160$ KSI (This indicates yielding takes place)

AT POINTS A & C; $\sigma_{bH} = \pm 1.74$ KSI

AVG. BENDING STRESS FLUCTUATION = $[(117 - 28.1) + (160 - 28.1)]/2 = 110$ KSI ABOVE 28.1 KSI (N&S)

(Therefore, since only the yield stress can be developed, the ℄ will yield)

FIGURE 1-17: RUPTURED GUSSET PLATE ANALYSIS

NATIONAL RADIO ASTRONOMY OBSERVATORY
300 FOOT TELESCOPE

FINITE ELEMENT ANALYSIS
VOLUME II

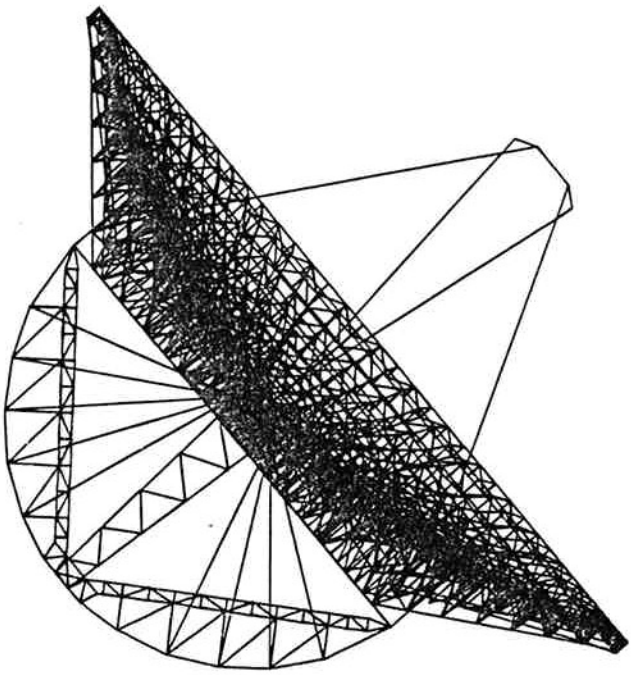

Henry Ayvazyan, M.E.
Joel Stahmer, B.E.
Joseph Vellozzi, Ph.D.

Ammann & Whitney
Consulting Engineers
New York, New York

February 1989

NATIONAL RADIO ASTRONOMY OBSERVATORY
300 FOOT TELESCOPE

FINITE ELEMENT ANALYSIS
VOLUME II

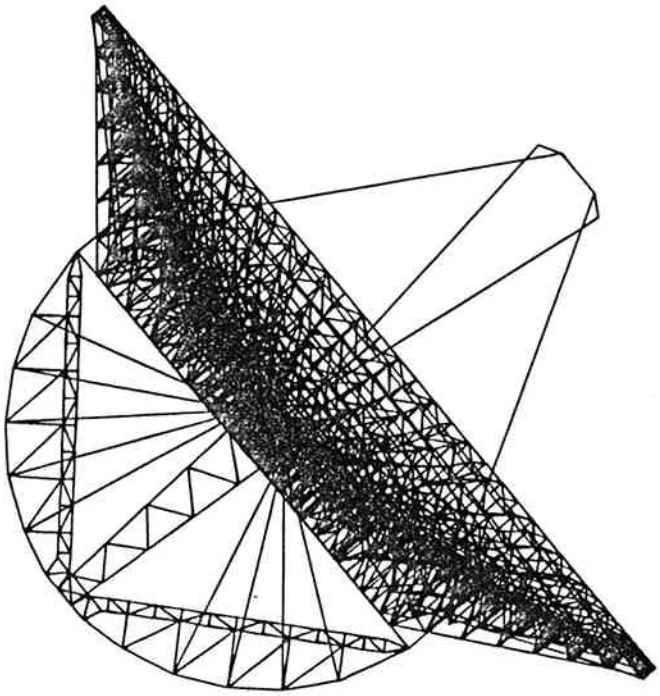

Henry Ayvazyan, M.E.
Joel Stahmer, B.E.
Joseph Vellozzi, Ph.D.

Ammann & Whitney
Consulting Engineers
New York, New York

February 1989

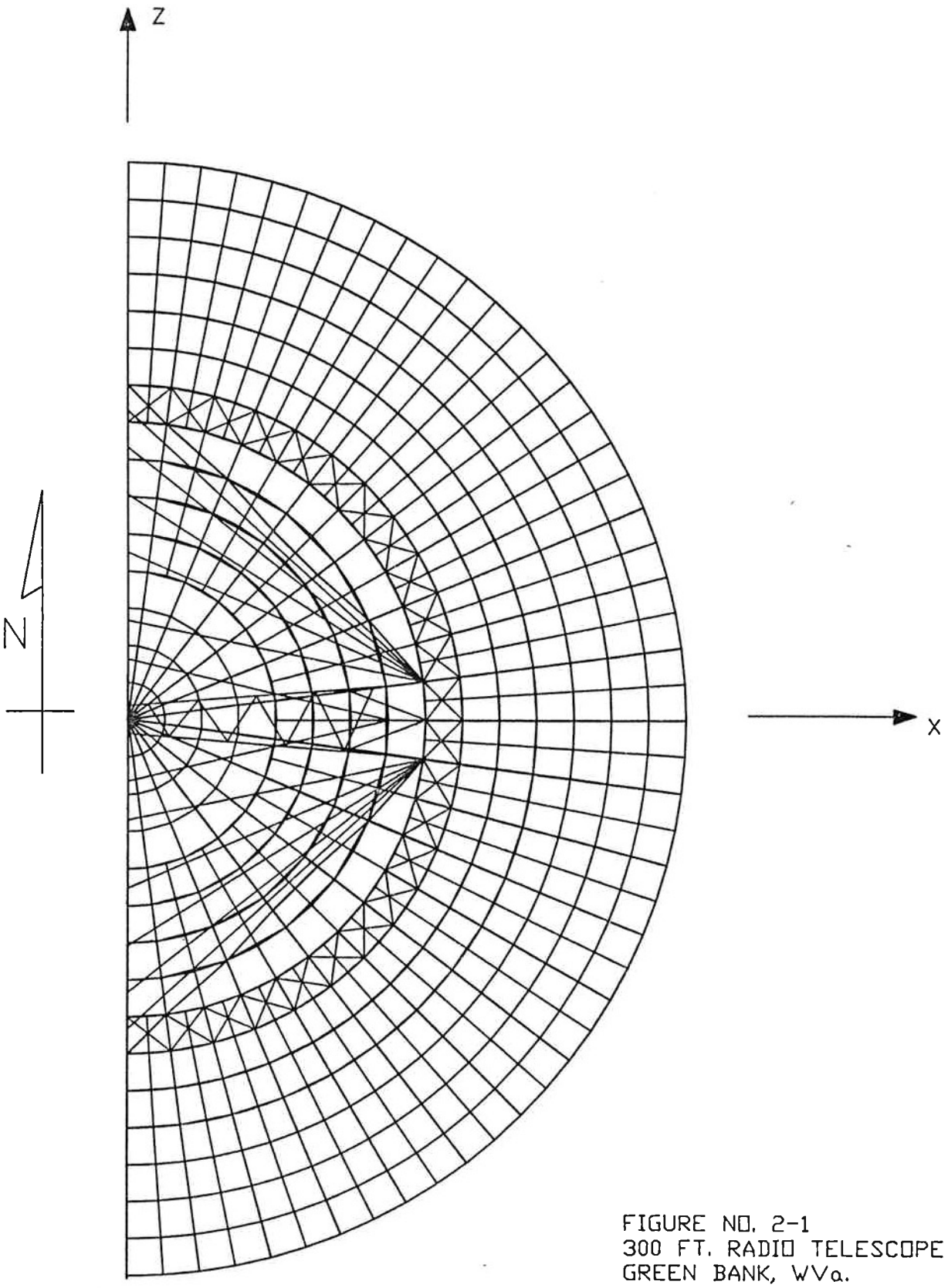

FIGURE NO. 2-1
300 FT. RADIO TELESCOPE
GREEN BANK, WVa.
HALF MODEL PLAN

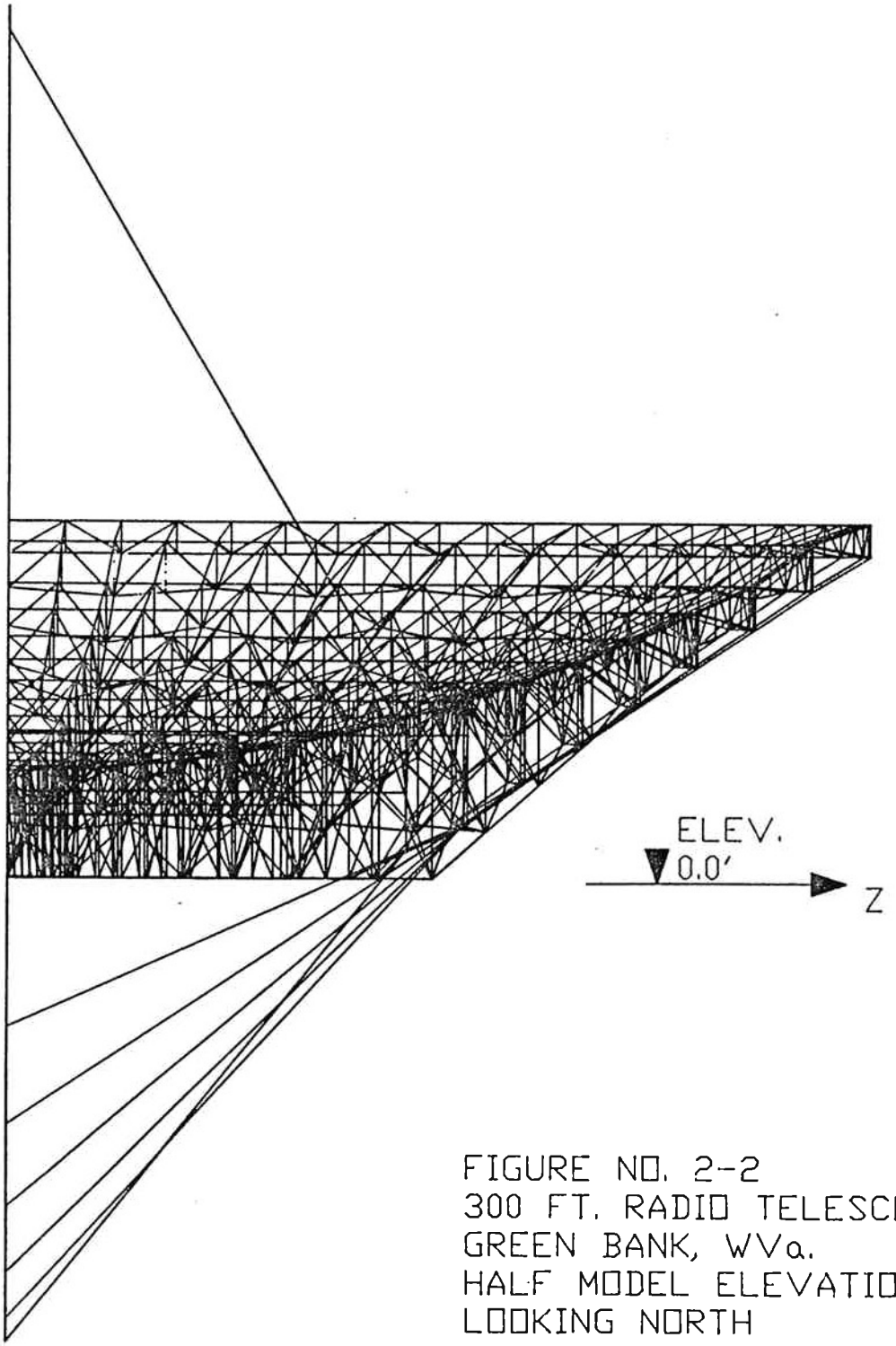

FIGURE NO. 2-2
300 FT. RADIO TELESCOPE
GREEN BANK, WVa.
HALF MODEL ELEVATION
LOOKING NORTH

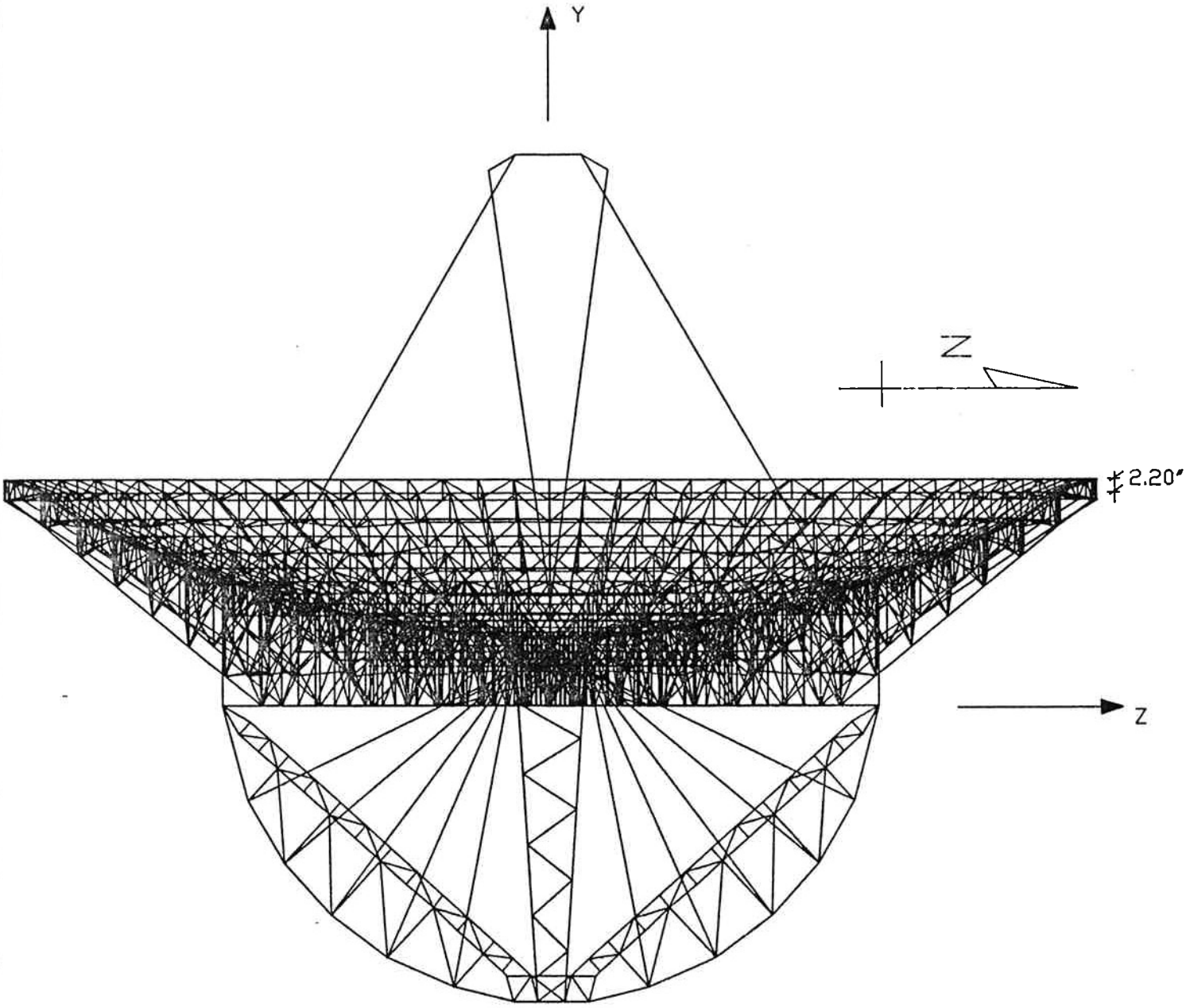

FIGURE NO. 2-3
300 FT. RADIO TELESCOPE
GREEN BANK, WVa.
HALF MODEL
ELEVATION LOOKING WEST

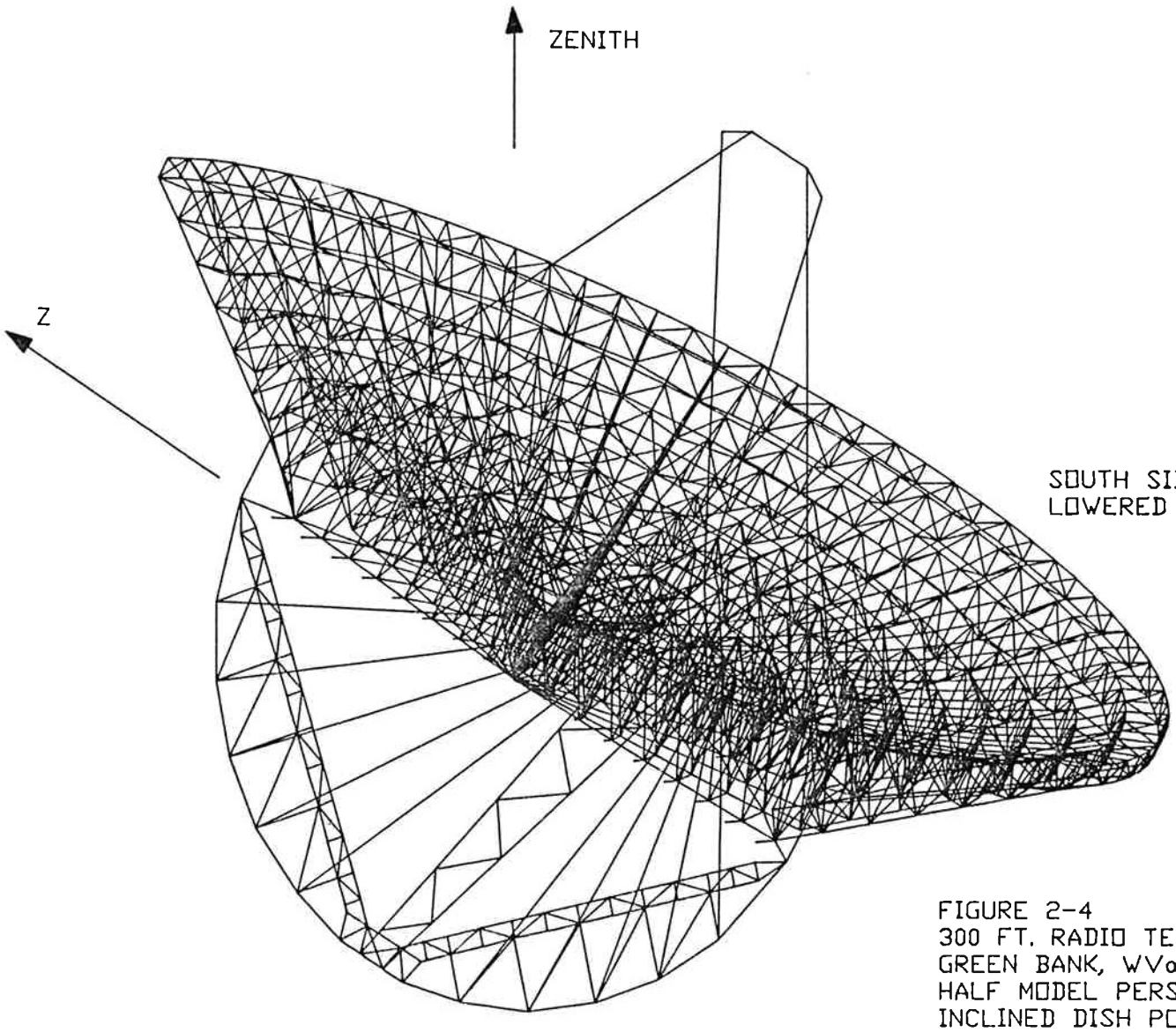

FIGURE 2-4
300 FT. RADIO TELESCOPE
GREEN BANK, WVa.
HALF MODEL PERSPECTIVE
INCLINED DISH POSITION
LOOKING EAST

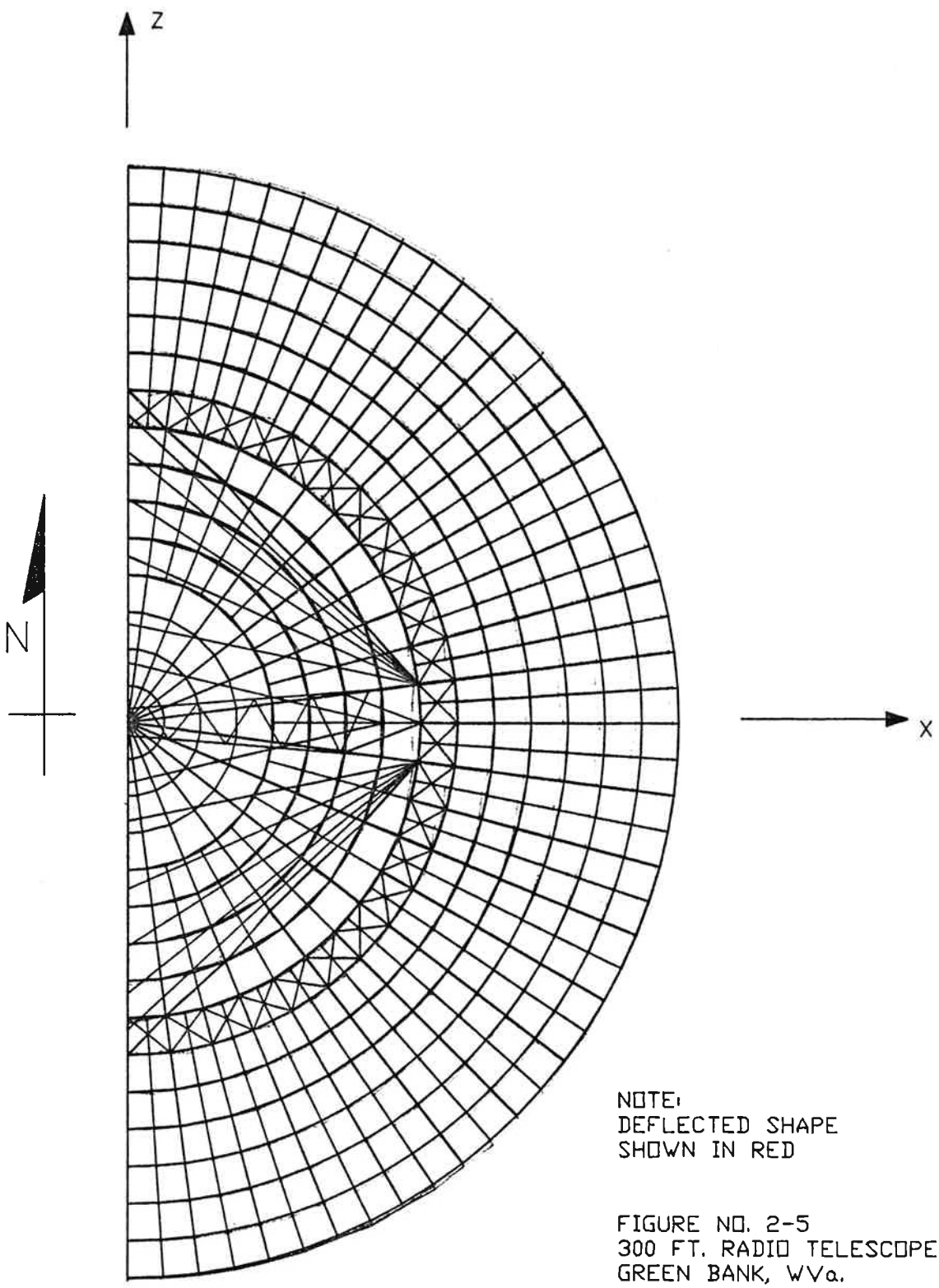

NOTE:
DEFLECTED SHAPE
SHOWN IN RED

FIGURE NO. 2-5
300 FT. RADIO TELESCOPE
GREEN BANK, WVa.
HALF MODEL ZENITH POSITION DEFLECTIC
PLAN

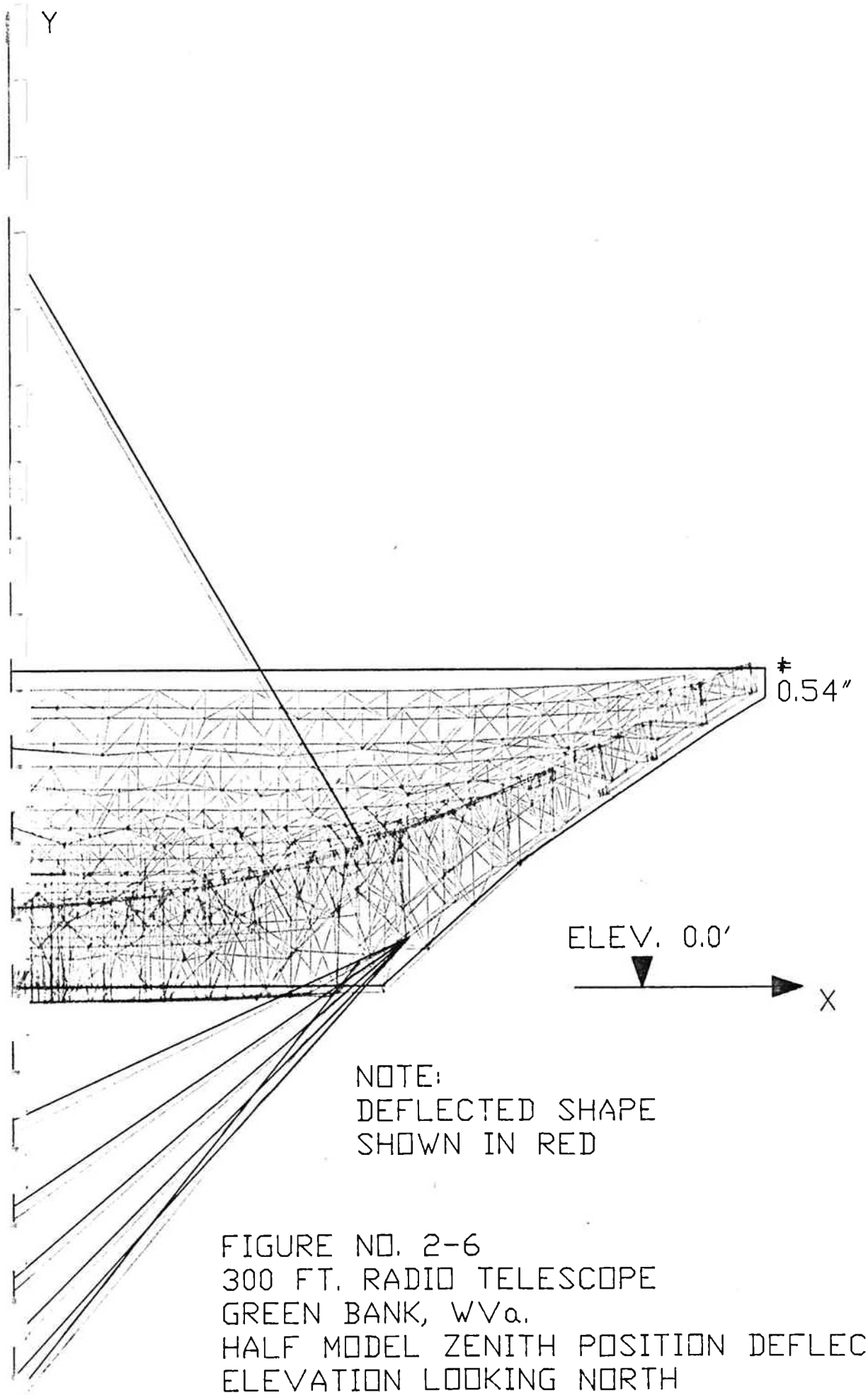

FIGURE NO. 2-6
300 FT. RADIO TELESCOPE
GREEN BANK, WVa.
HALF MODEL ZENITH POSITION DEFLECTIONS,
ELEVATION LOOKING NORTH

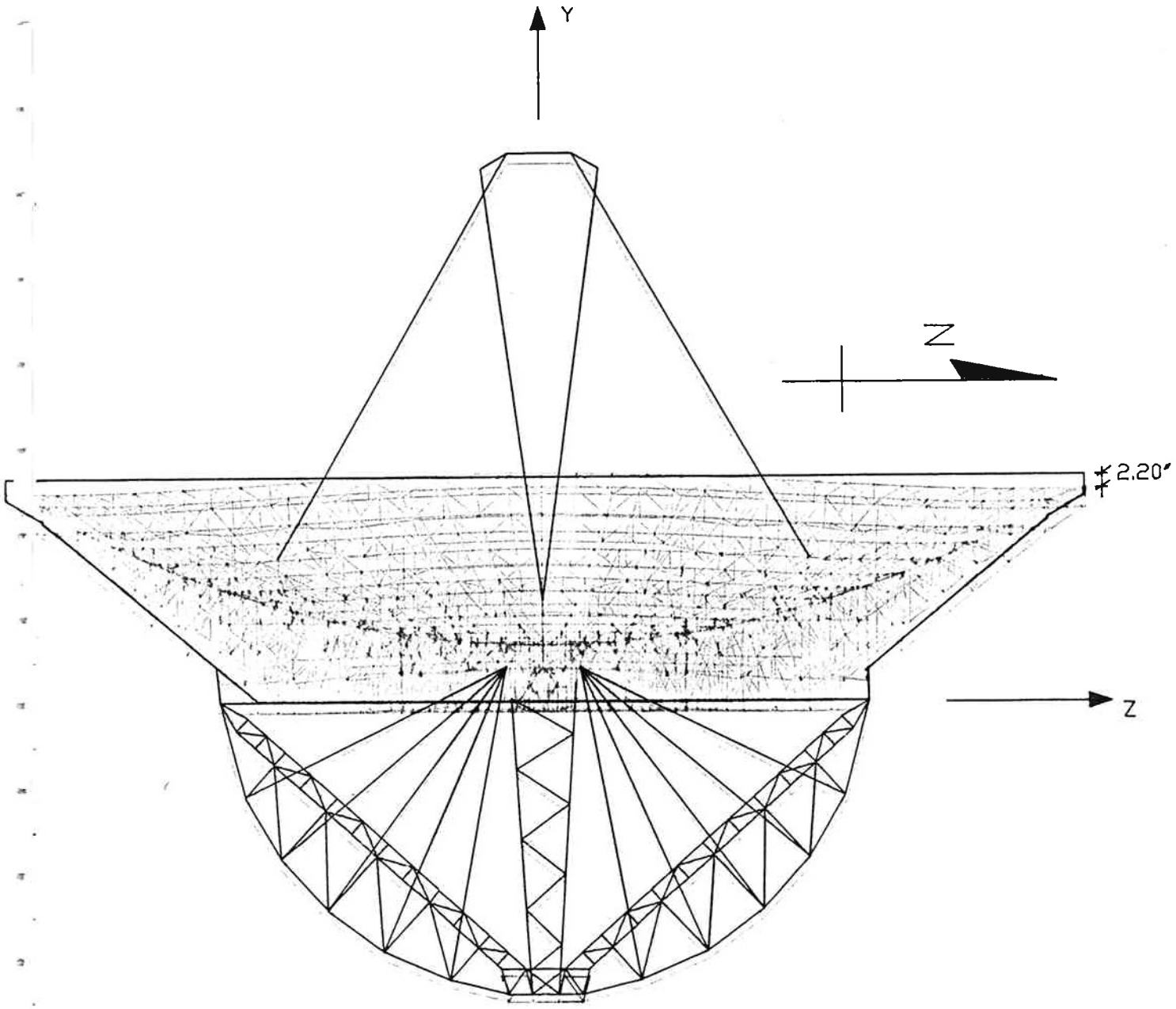

NOTE:
DEFLECTED SHAPE
SHOWN IN RED

FIGURE NO. 2-7
300 FT. RADIO TELESCOPE
GREEN BANK, WVa.
HALF MODEL ZENITH POSITION DEFLECTIONS,
ELEVATION LOOKING WEST

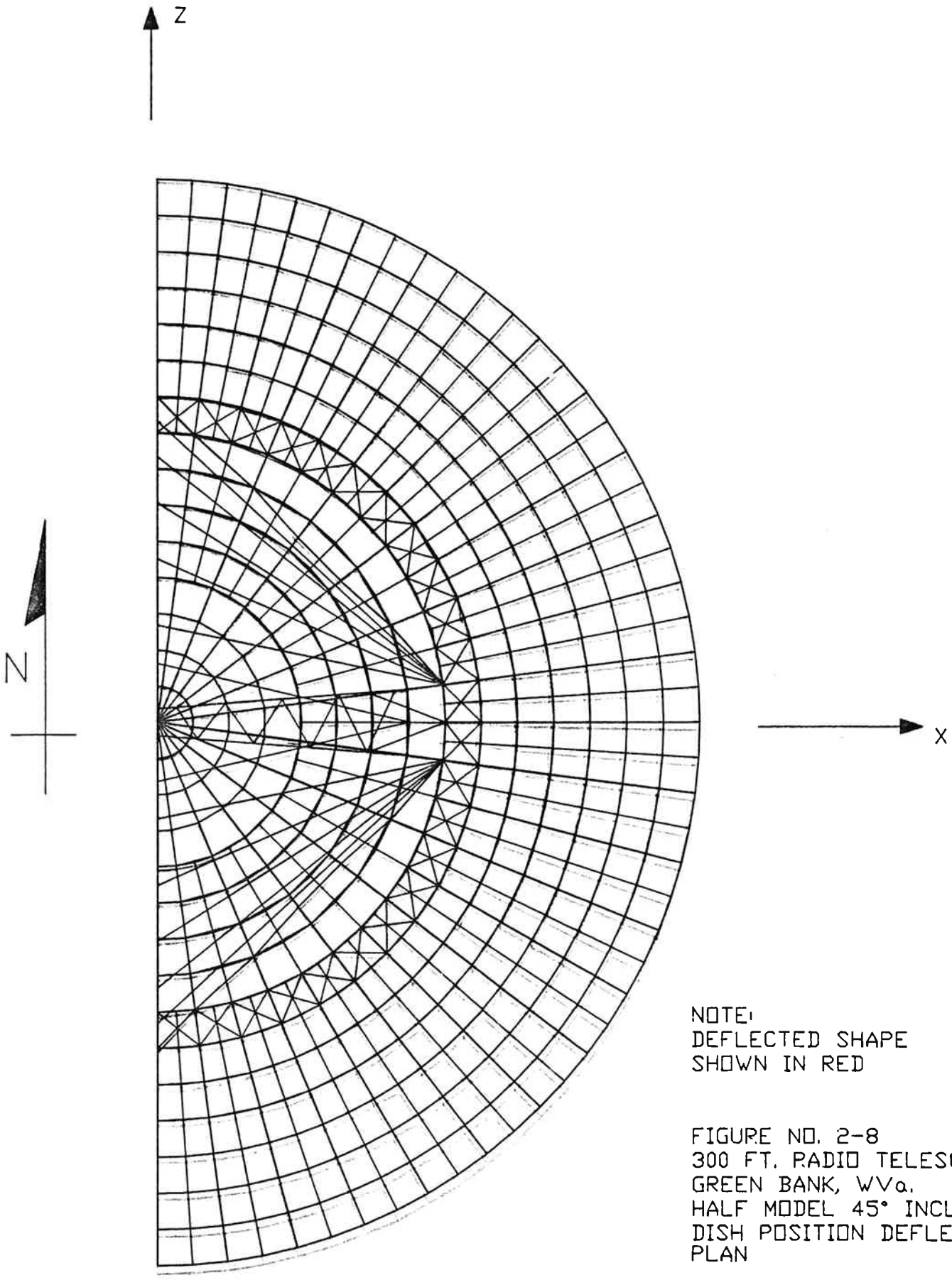

NOTE:
DEFLECTED SHAPE
SHOWN IN RED

FIGURE NO. 2-8
300 FT. RADIO TELESCOPE
GREEN BANK, WVa.
HALF MODEL 45° INCLINED
DISH POSITION DEFLECTION
PLAN

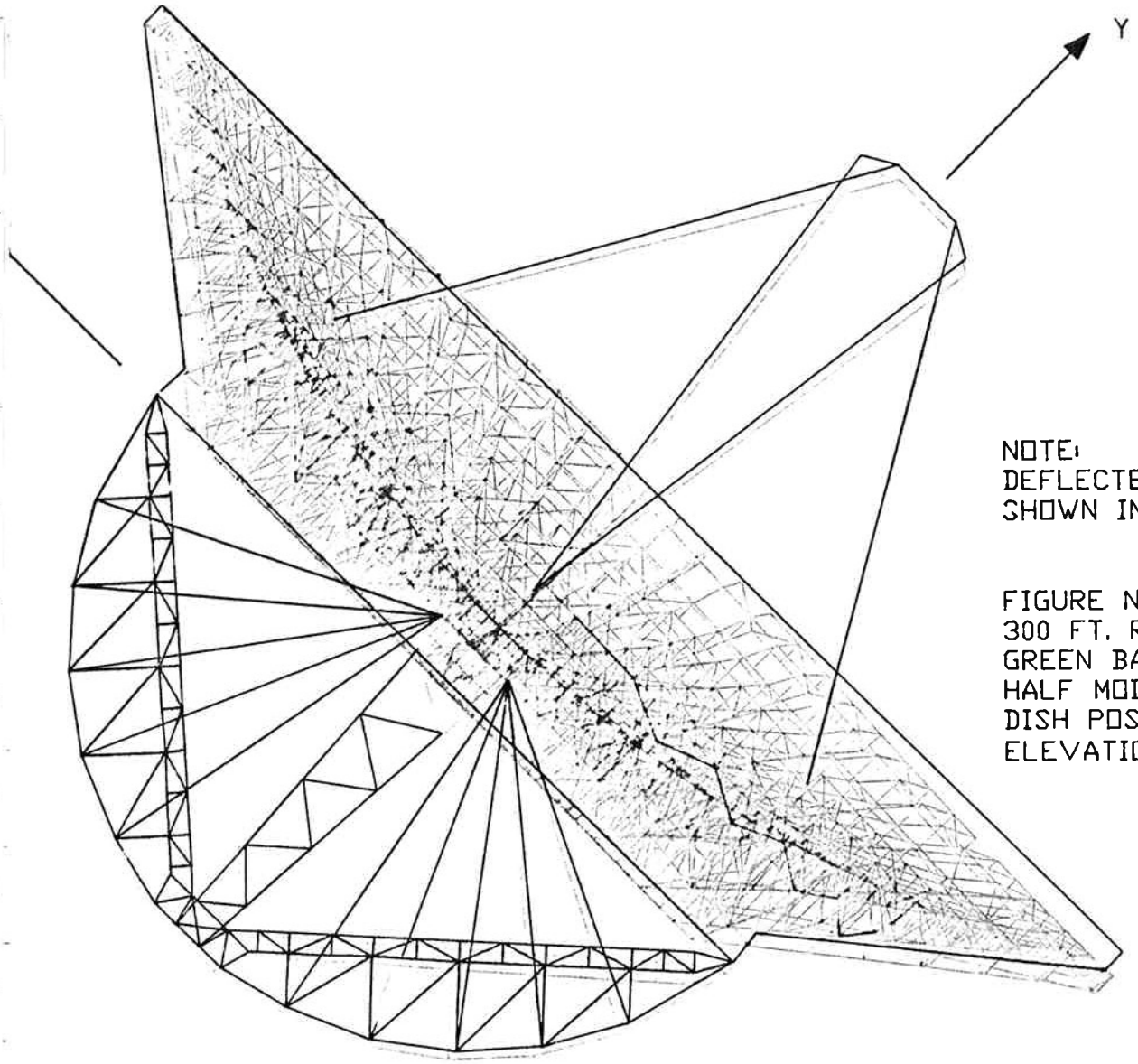

NOTE:
DEFLECTED SHAPE
SHOWN IN RED

FIGURE NO. 2-9
300 FT. RADIO TELESCOPE
GREEN BANK, WVa.
HALF MODEL 45° INCLINED
DISH POSITION DEFLECTION
ELEVATION LOOKING EAST

3.18"

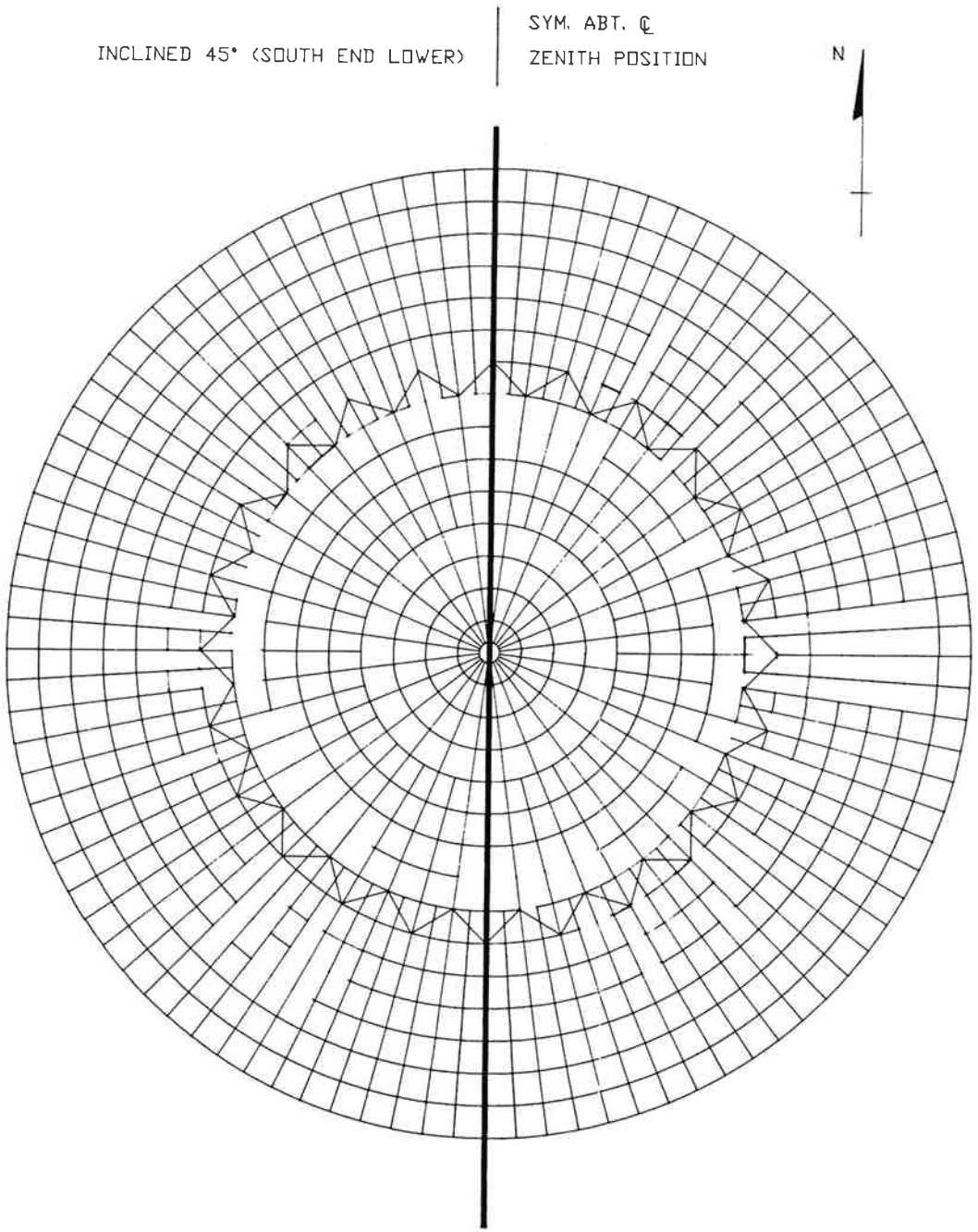

FIGURE NO. 2-10
300 FT. RADIO TELESCOPE
GREEN BANK, W.Va.
TOP SURFACE PROJECTION
MEMBER OVERSTRESSES,
ZENITH & 45° INCLINED DISH POSITIONS

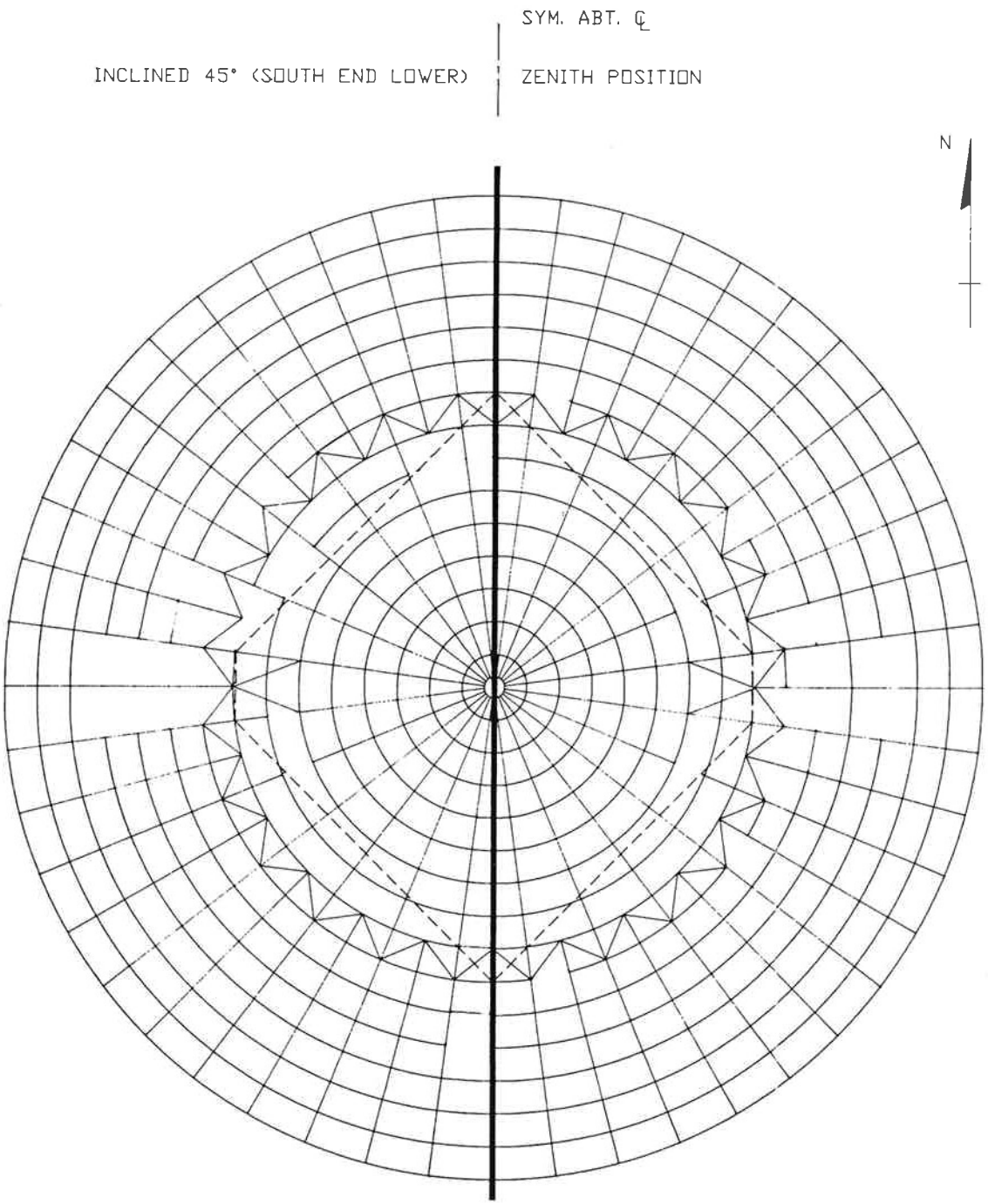

OVERSTRESSED MEMBERS
per AISC CODE EIGHTH
EDITION:

5% TO 45%
45% TO 100%
100% TO 200%
200% >

℄ TRUNNION
0°

FIGURE NO. 2-11
300 FT. RADIO TELESCOPE
GREENBANK, WVa.
BOTTOM SURFACE PROJECTION
MEMBER OVERSTRESSES,
SENITH & 45° INCLINED DISH POSITIONS

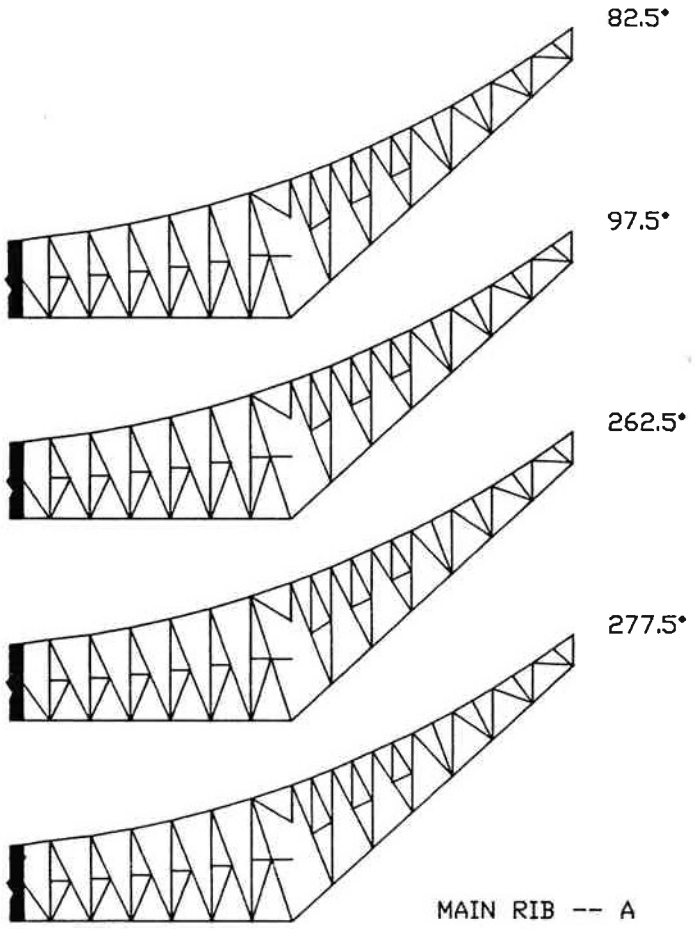

OVERSTRESSED MEMBERS
per AISC CODE EIGHTH
EDITION

5% TO 45%
45% TO 100%
100% TO 200%
200% >

FIGURE NO. 2-12
300 FT. RADIO TELESCOPE
GREEN BANK, WVa.
MAIN RIBS, A & D
MEMBER OVERSTRESSES,
ZENITH POSITION

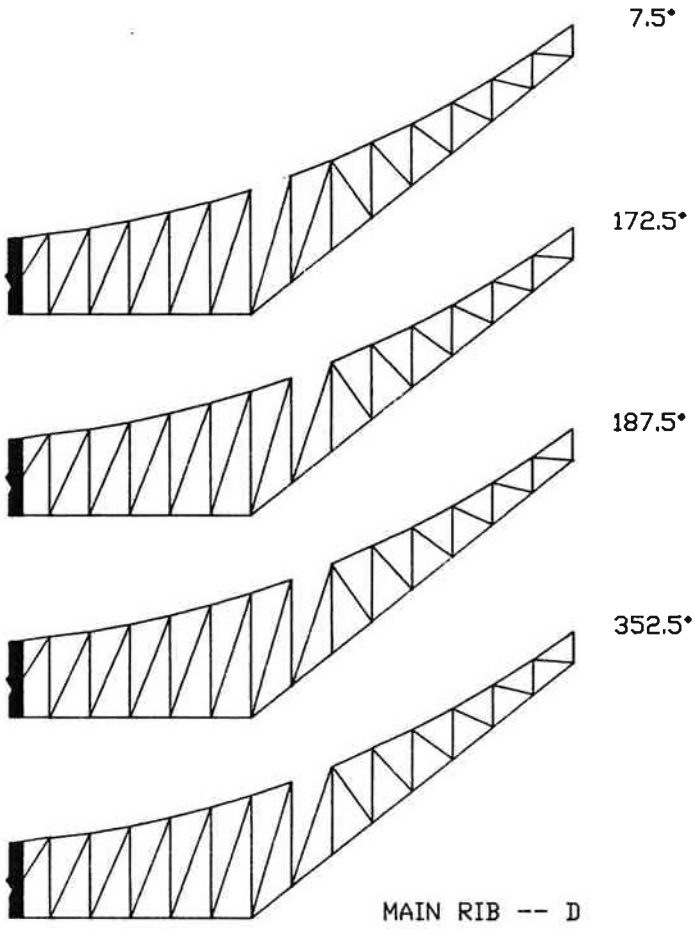

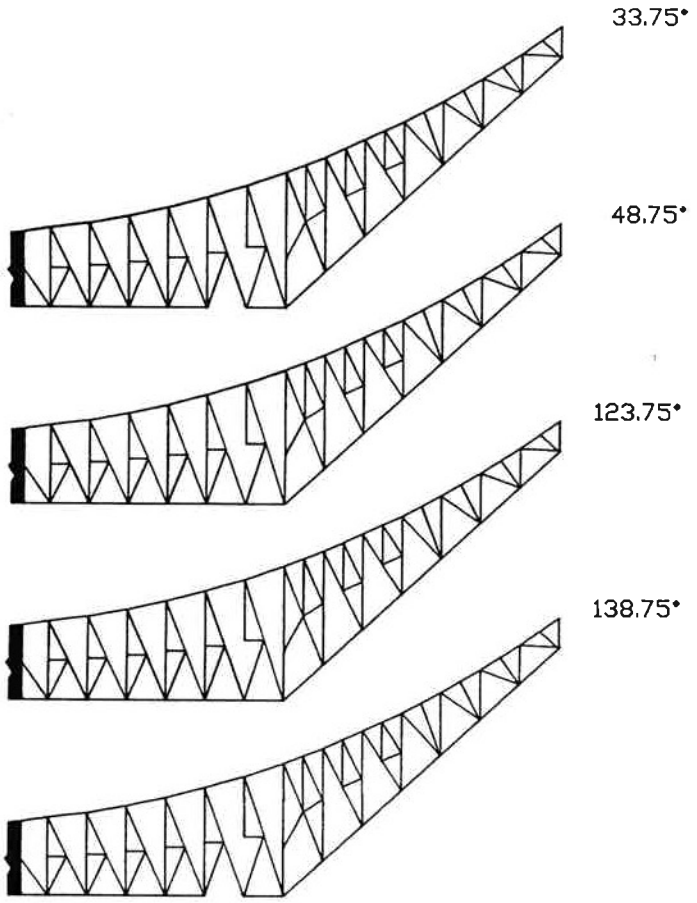

OVERSTRESSED MEMBERS
per AISC CODE EIGHTH
EDITION:

5% TO 45%
45% TO 100%
100% TO 200%
200% >

FIGURE NO. 2-13
300 FT. RADIO TELESCOPE
GREEN BANK, WVa.
MAIN RIBS, B
MEMBER OVERSTRESSES,
ZENITH POSITION

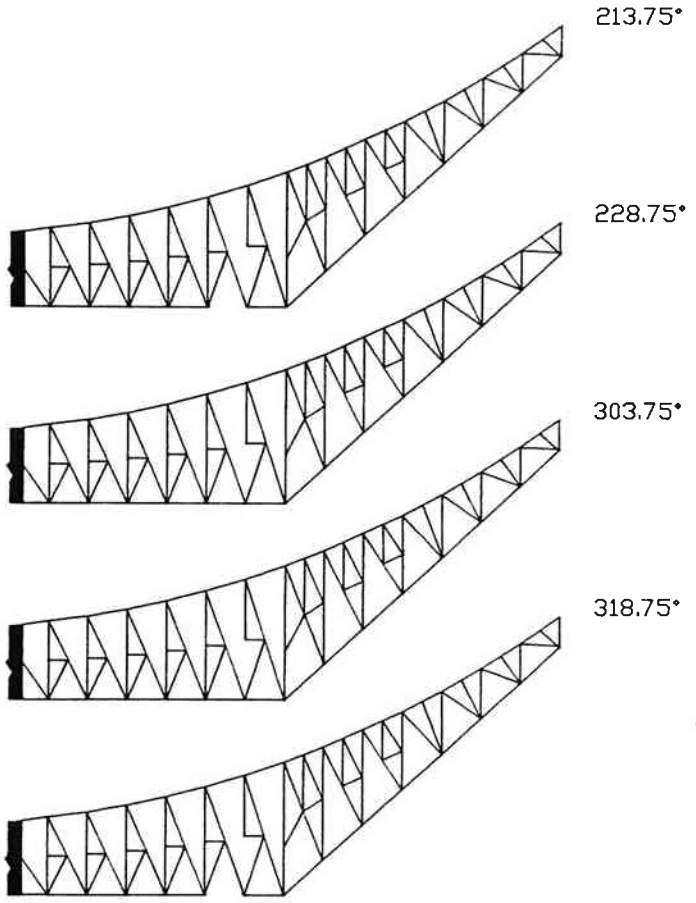

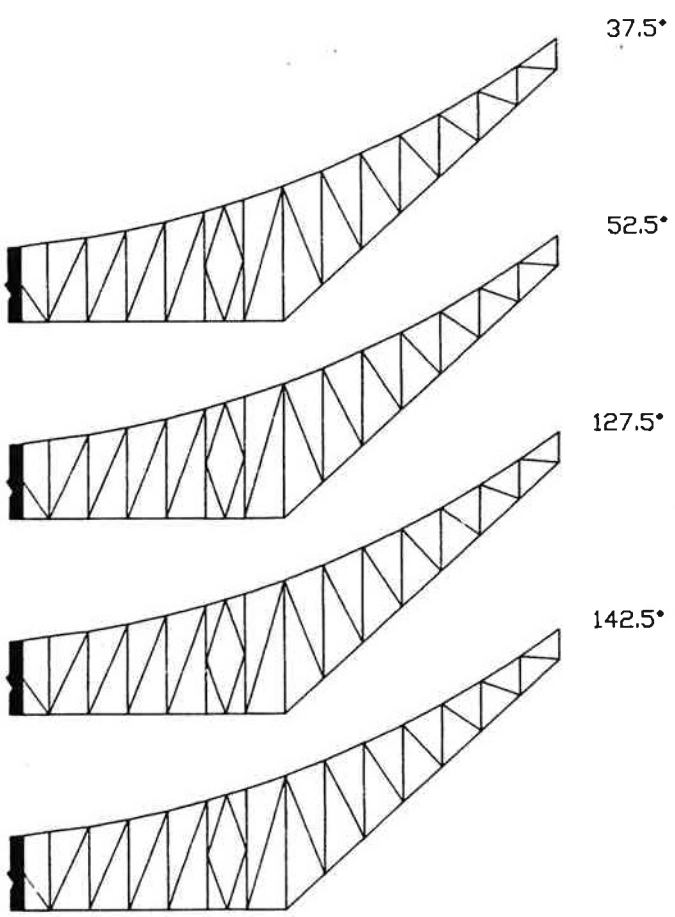

NOTE:
NO OVERSTRESSES
DETERMINED

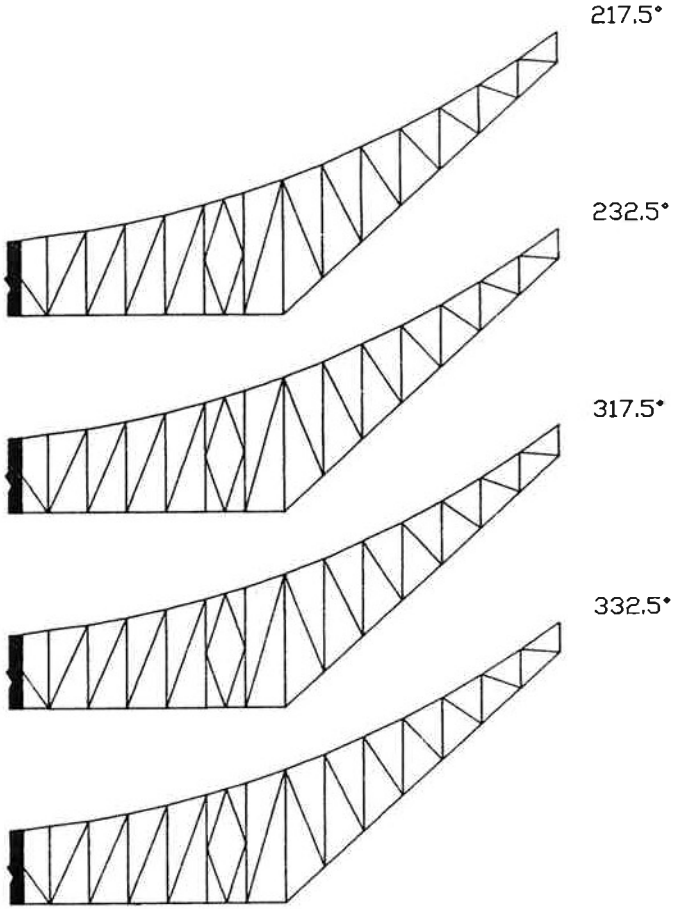

FIGURE NO. 2-14
300 FT. RADIO TELESCOPE
GREEN BANK, WVa.
MAIN RIBS C
MEMBER OVERSTRESSES,
ZENITH & 45° INCLINED
DISH POSITIONS

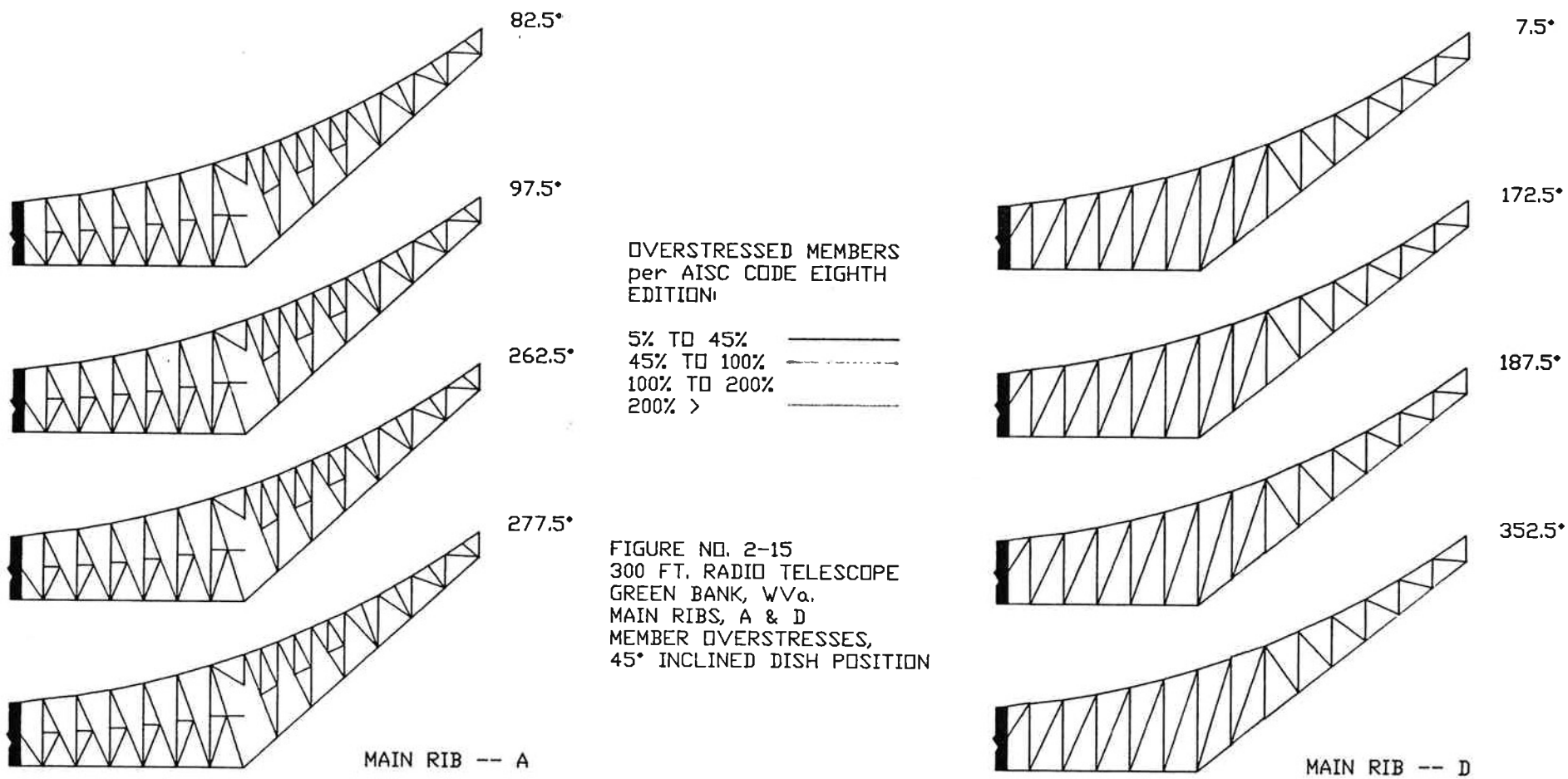

FIGURE NO. 2-15
300 FT. RADIO TELESCOPE
GREEN BANK, WVa.
MAIN RIBS, A & D
MEMBER OVERSTRESSES,
45° INCLINED DISH POSITION

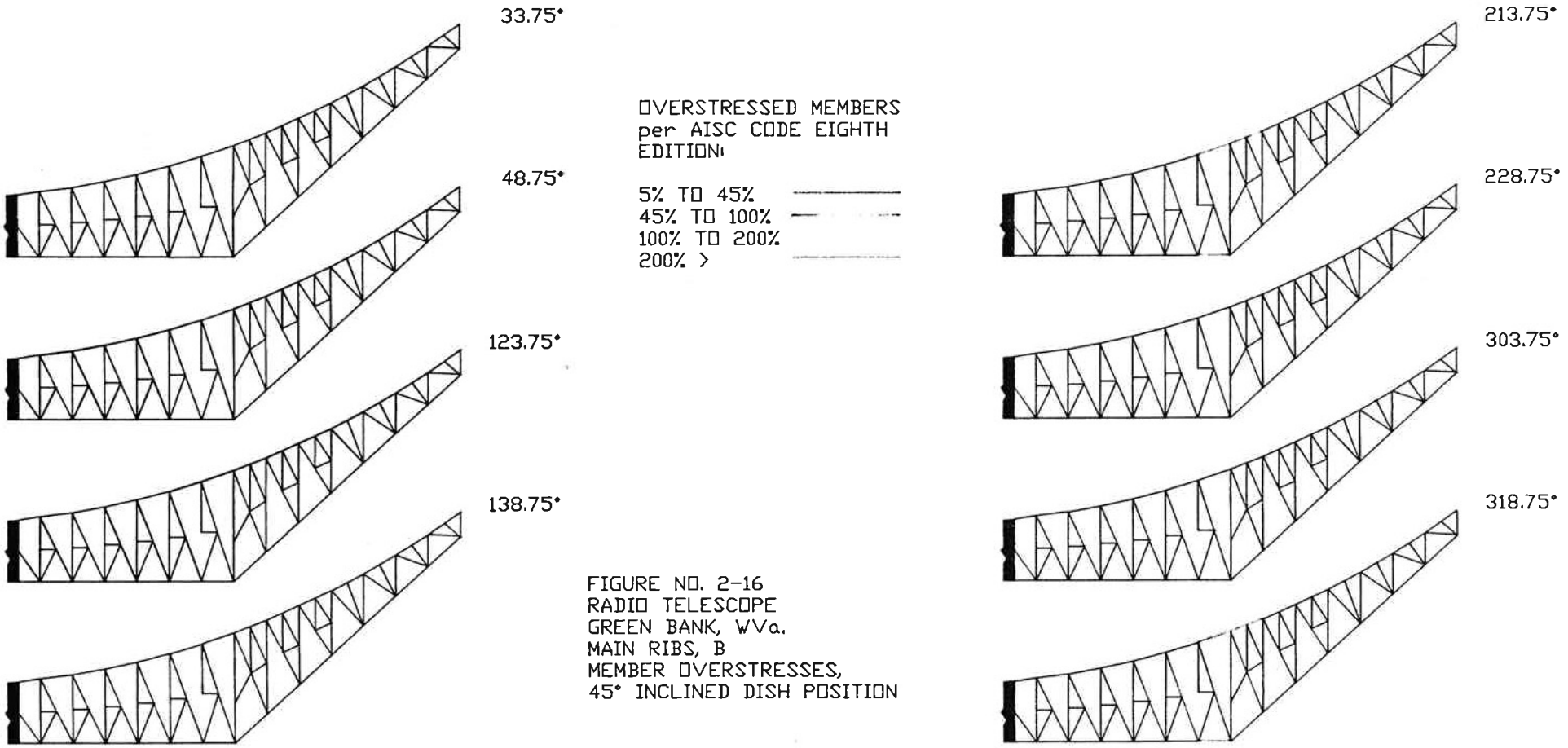

FIGURE NO. 2-16
RADIO TELESCOPE
GREEN BANK, WVa.
MAIN RIBS, B
MEMBER OVERSTRESSES,
45° INCLINED DISH POSITION

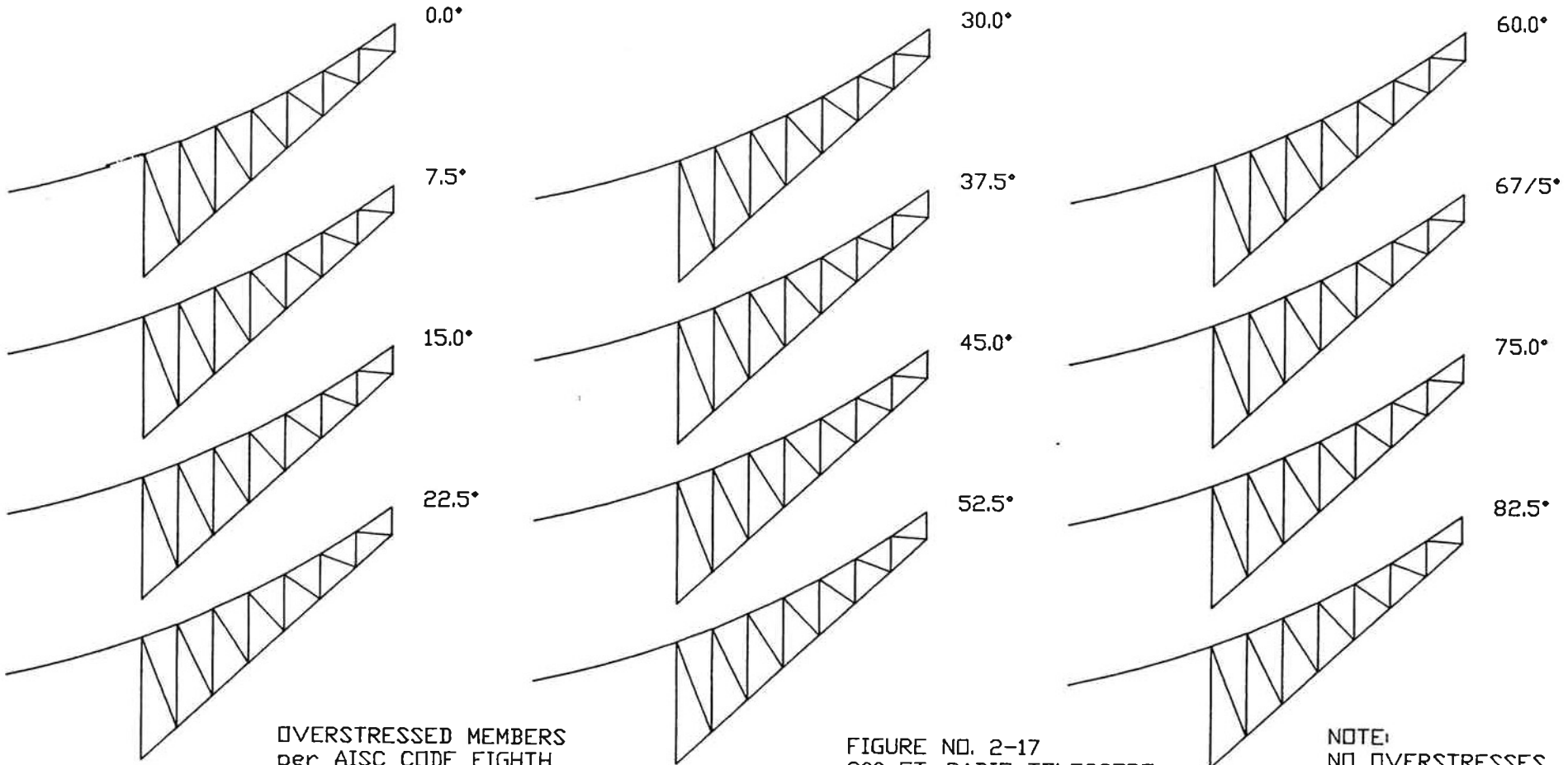

OVERSTRESSED MEMBERS
per AISC CODE EIGHTH EDITION:
5% TO 45% ——————
45% TO 100% —·—·—·—
100% TO 200%
200% > ——————

FIGURE NO. 2-17
300 FT. RADIO TELESCOPE
GREEN BANK, WVa.
AUXILIARY RIBS
MEMBER OVERSTRESSES,
ZENITH & 45° INCLINED
DISH POSITIONS

NOTE:
NO OVERSTRESSES
DETERMINED IN 45°
INCLINED DISH
POSITION

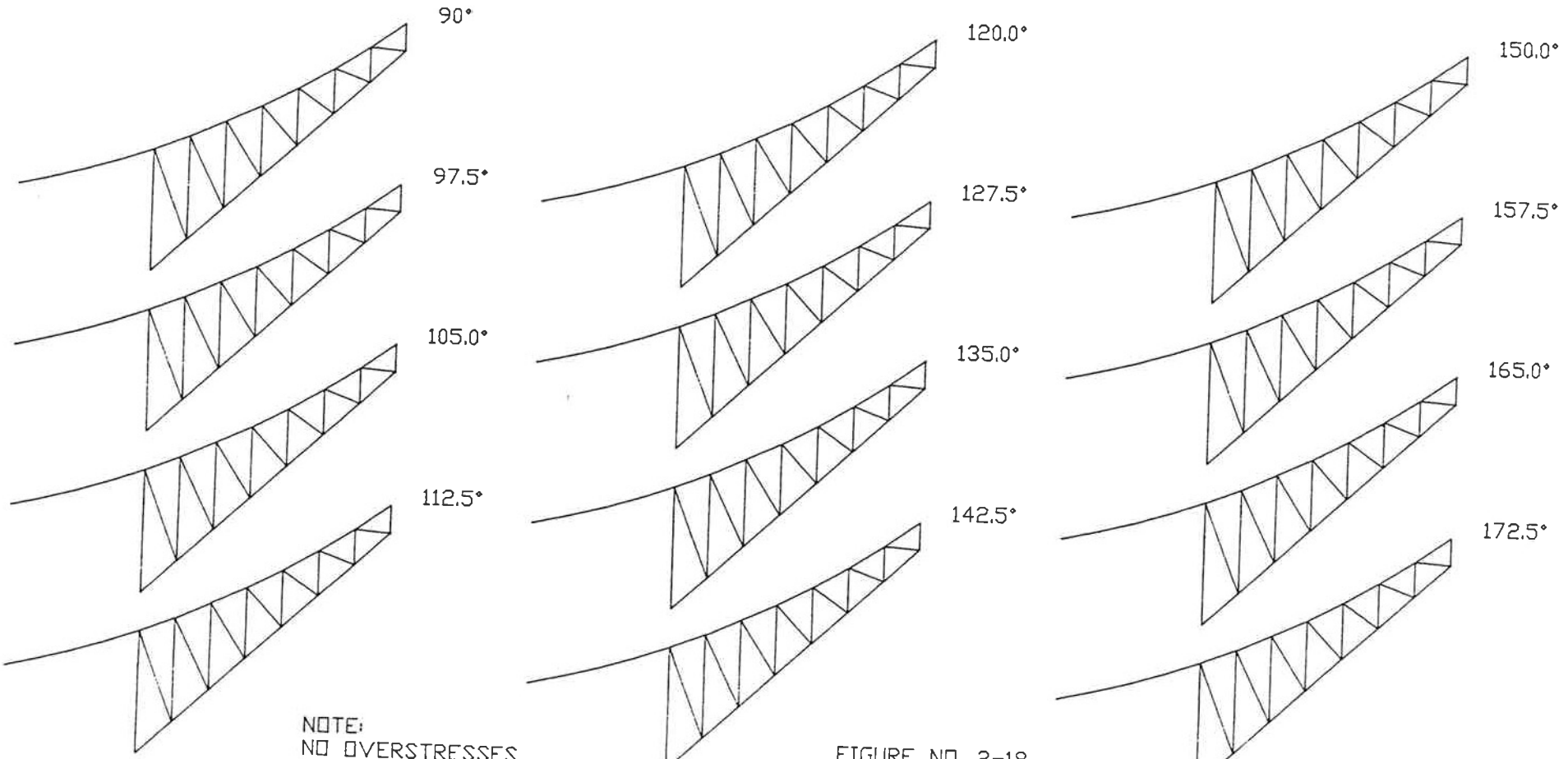

NOTE:
NO OVERSTRESSES
DETERMINED

FIGURE NO. 2-18
300 FT. RADIO TELESCOPE
GREEN BANK, WVa.
AUXILIARY RIBS
MEMBER OVERSTRESSES,
ZENITH & 45° INCLINED
DISH POSITIONS

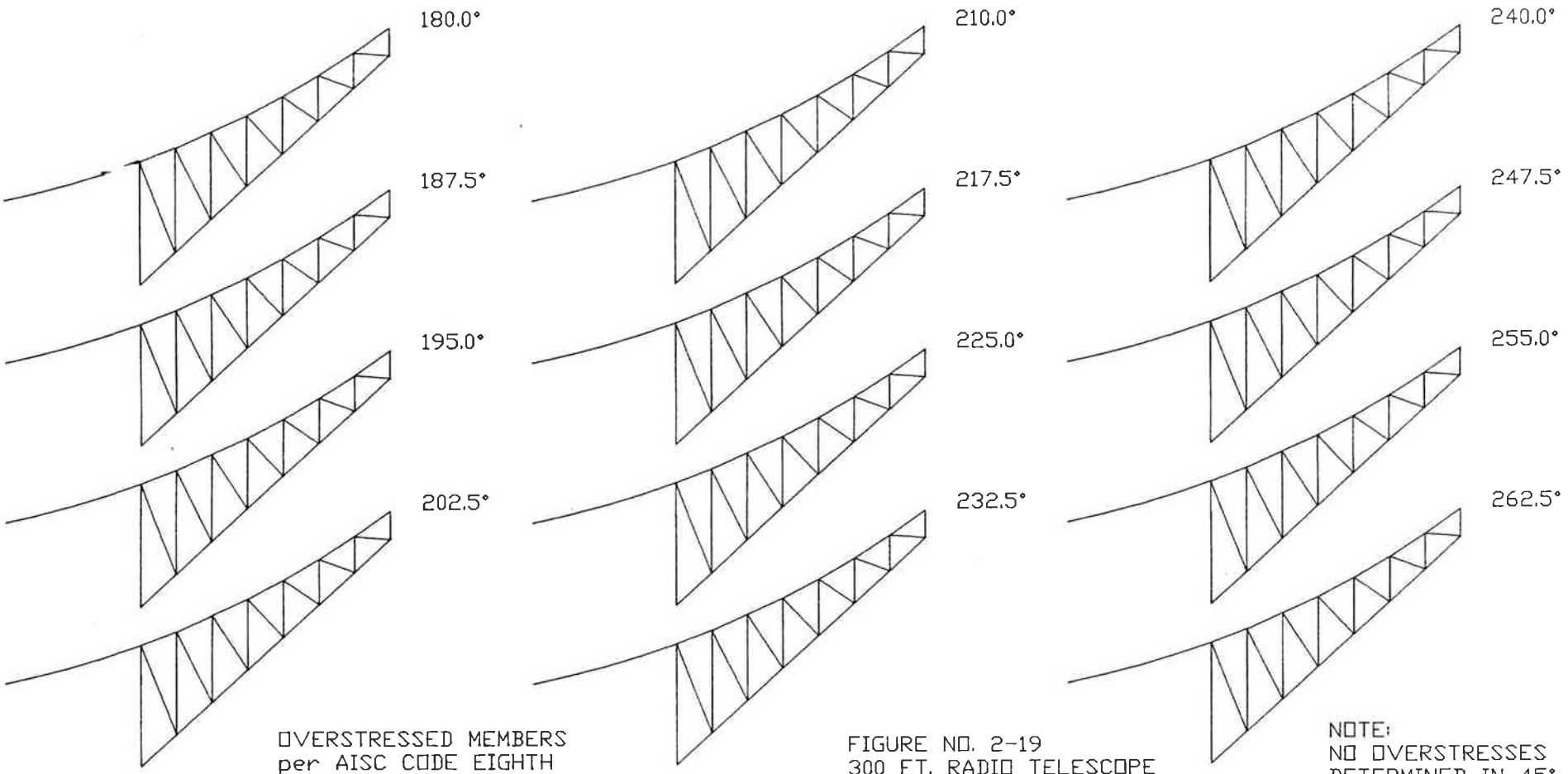

FIGURE NO. 2-19
300 FT. RADIO TELESCOPE
GREEN BANK, WVa.
AUXILIARY RIBS
MEMBER OVERSTRESSES,
ZENITH & 45° INCLINED
DISH POSITIONS

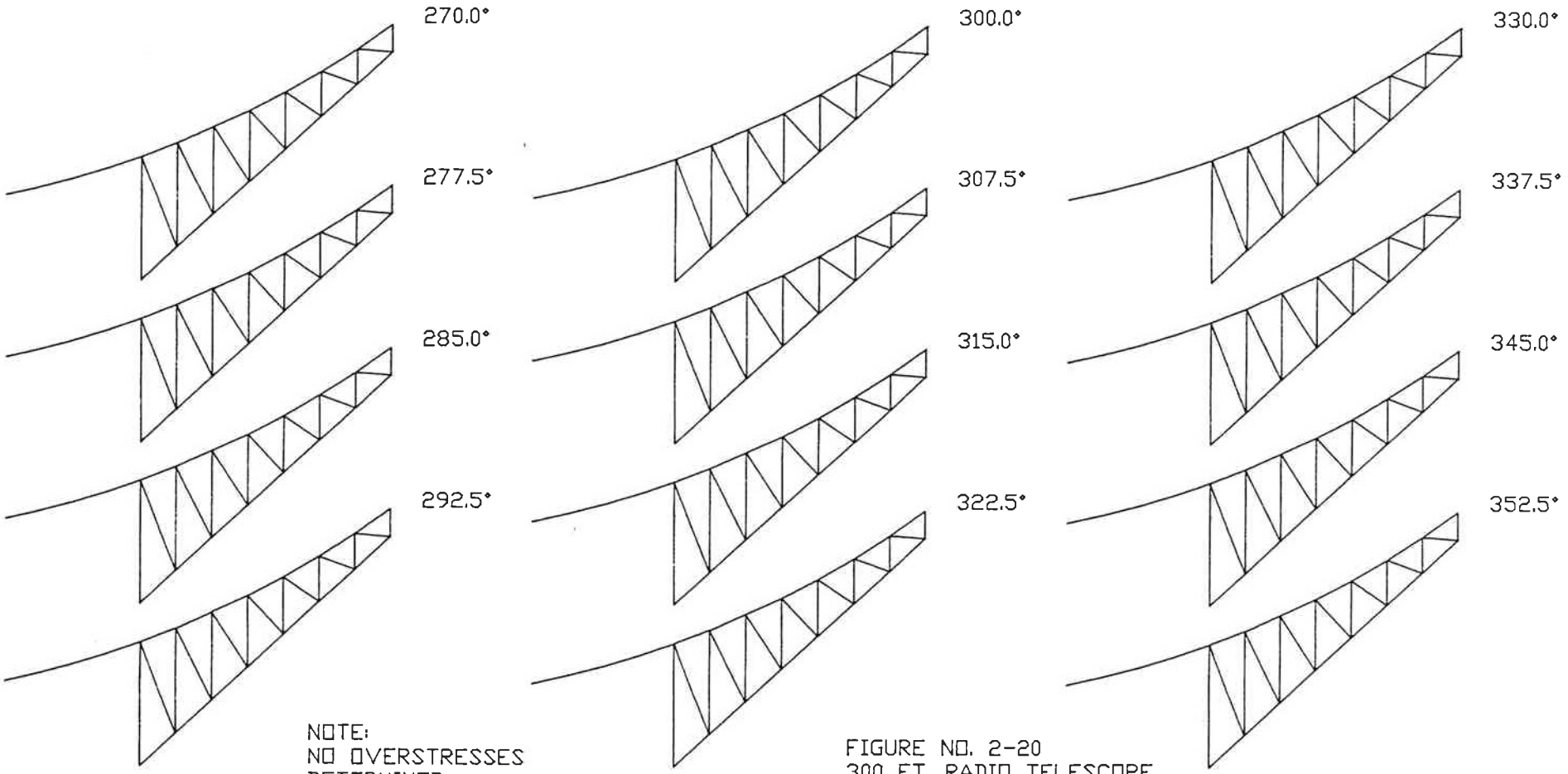

NOTE:
NO OVERSTRESSES
DETERMINED

FIGURE NO. 2-20
300 FT. RADIO TELESCOPE
GREEN BANK, WVa.
AUXILIARY RIBS
MEMBER OVERSTRESSES,
ZENITH & 45° INCLINED
DISH POSITIONS

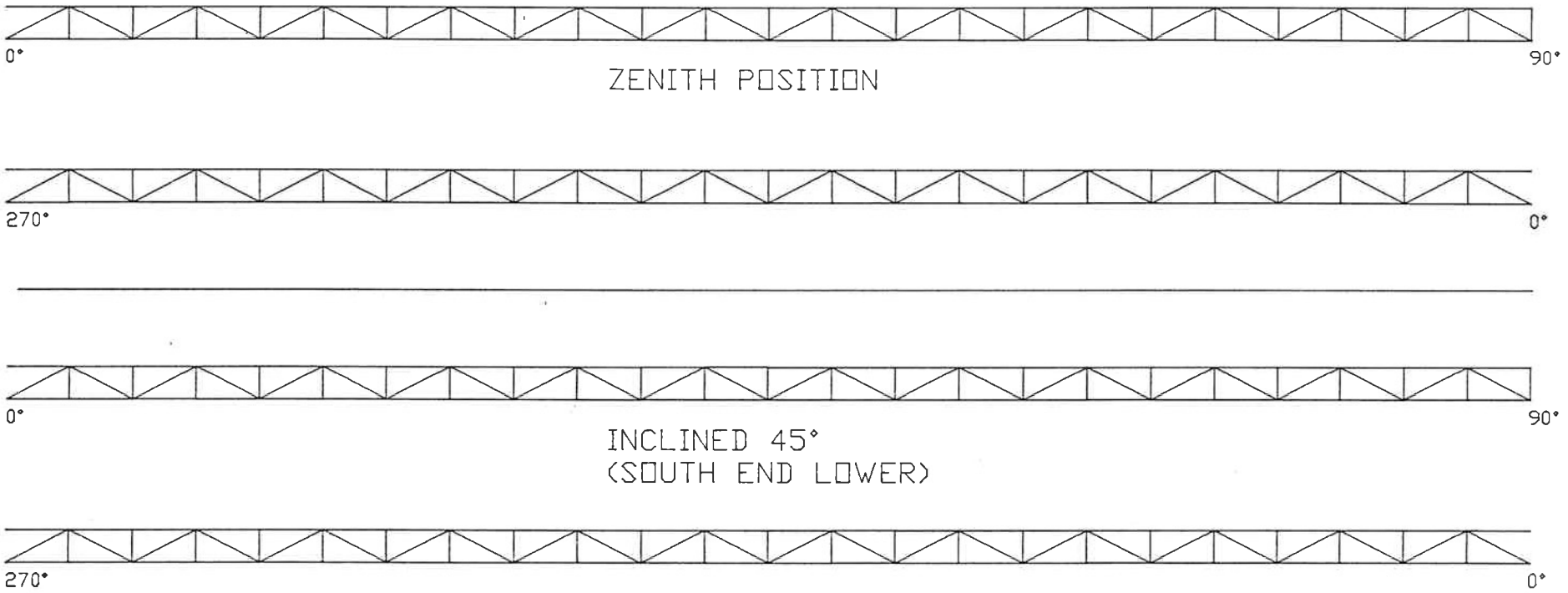

NOTE:
NO OVERSTRESSES
DETERMINED

FIGURE 2-21
300 FT. RADIO TELESCOPE
GREEN BANK, WVa.
CIRCUMFERENCE 1
MEMBER OVERSTRESSES,
ZENITH & 45° INCLINED
DISH POSITIONS

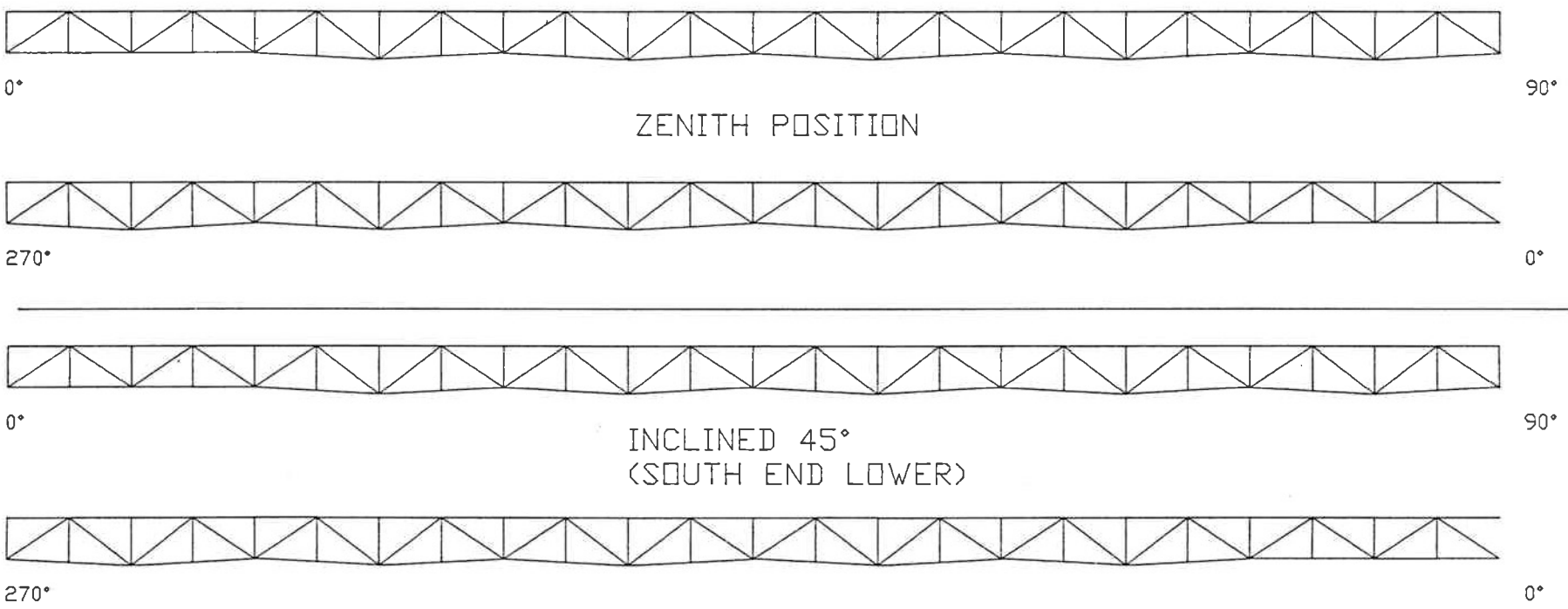

NOTE:
NO OVERSTRESSES
DETERMINED

FIGURE NO. 2-22
300 FT. RADIO TELESCOPE
GREEN BANK, WVa.
CIRCUMFERENCE 2
MEMBER OVERSTRESSES,
ZENITH & 45° INCLINED
DISH POSITIONS

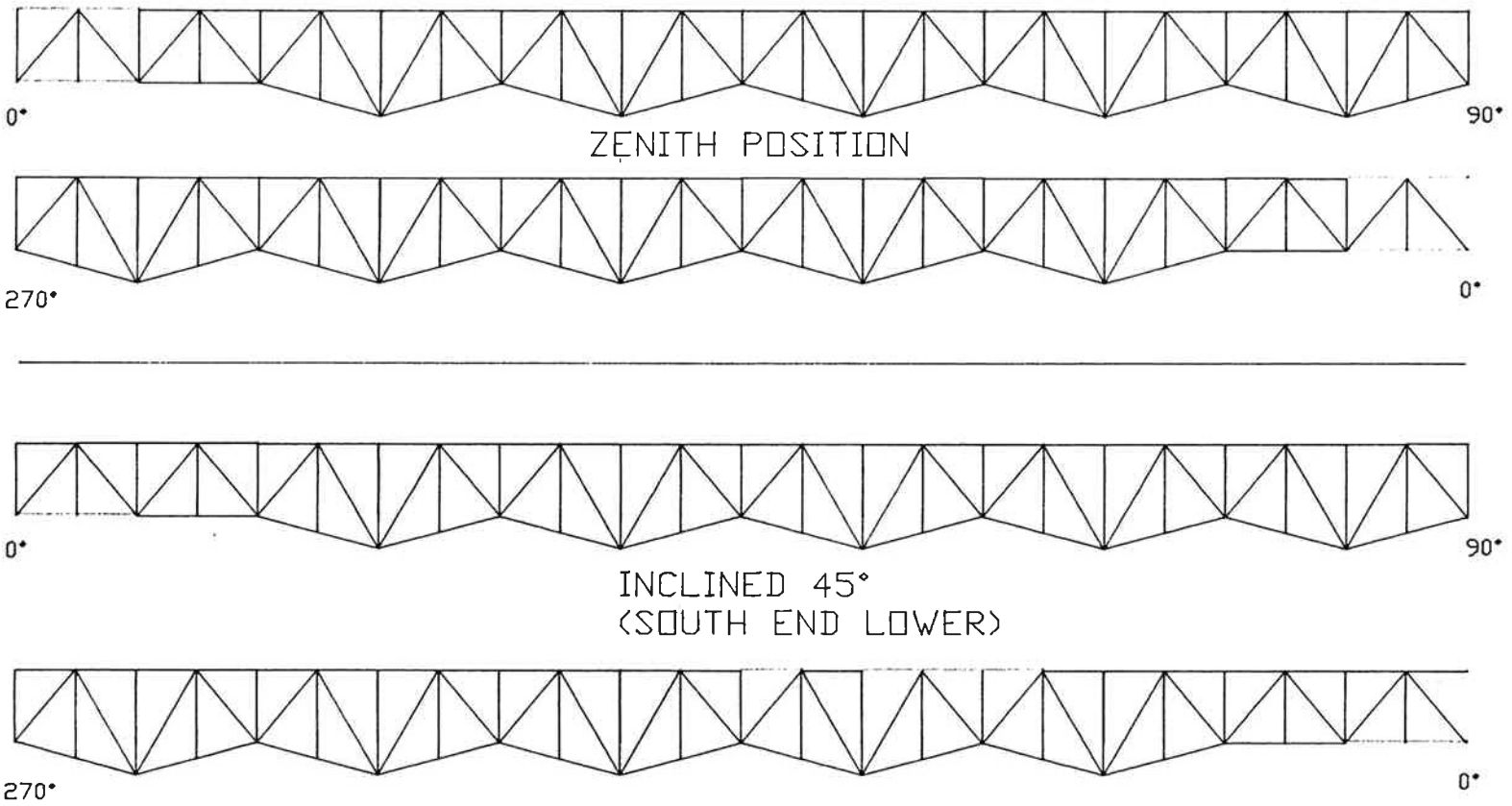

OVERSTRESSED MEMBERS
per AISC CODE EIGHTH
EDITION:

5% TO 45%
45% TO 100%
100% TO 200%
200% >

FIGURE NO. 2-24
300 FT. RADIO TELESCOPE
GREEN BANK, WVa.
CIRCUMFERENCE 4,
MEMBER OVERSTRESSES,
ZENITH & 45° INCLINED
DISH POSITIONS

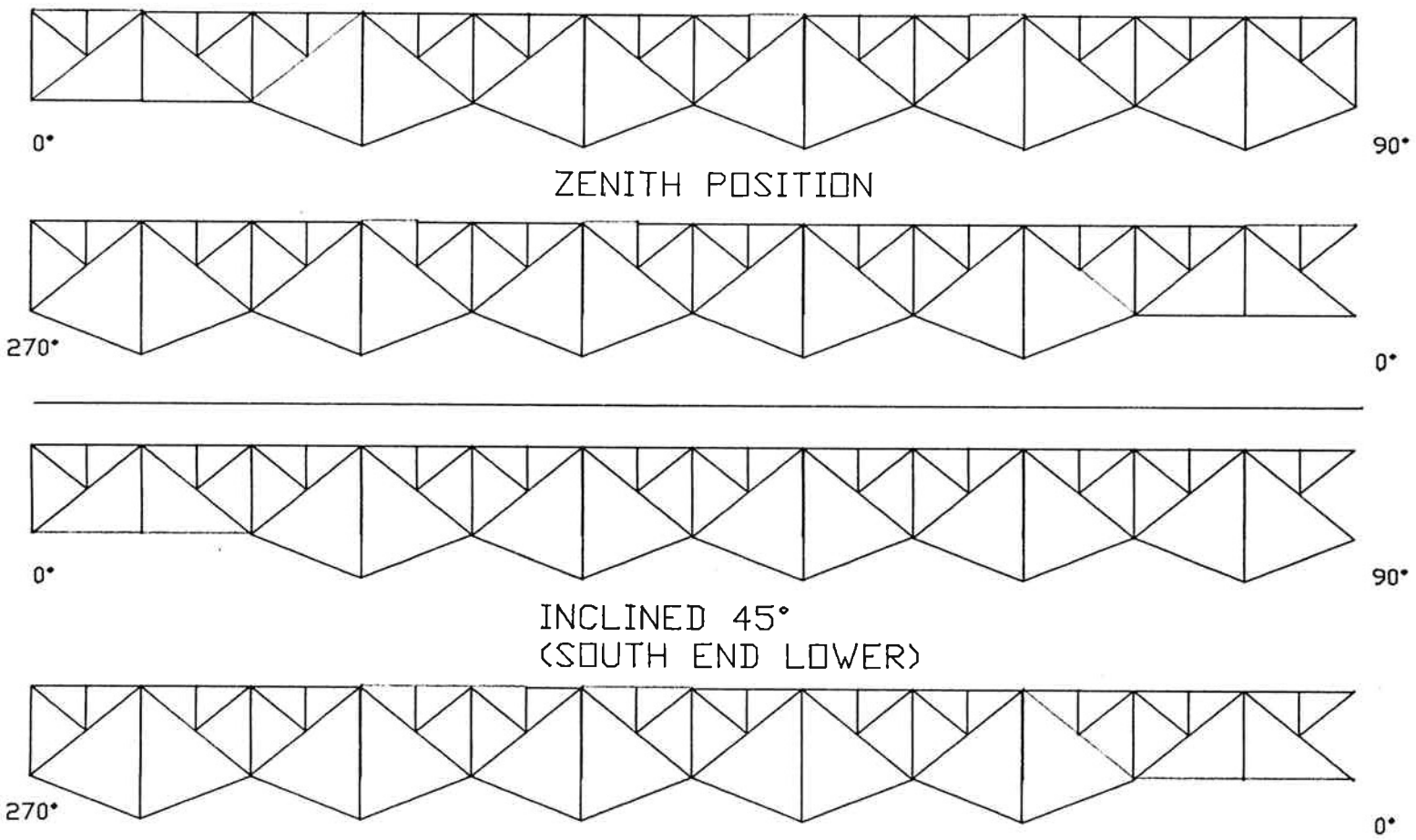

OVERSTRESSED MEMBERS
per AISC CODE EIGHTH
EDITION:

5% TO 45% _____
45% TO 100% _____
100% TO 200%
200% > _____

FIGURE NO. 2-25
300 FT. RADIO TELESCOPE
GREEN BANK, WVa.
CIRCUMFERENCE 5,
MEMBER OVERSTRESSES
ZENITH & 45° INCLINED
DISH POSITIONS

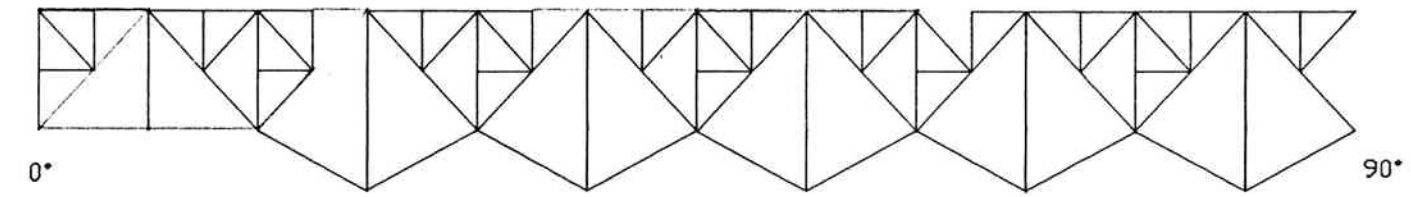

ZENITH POSITION

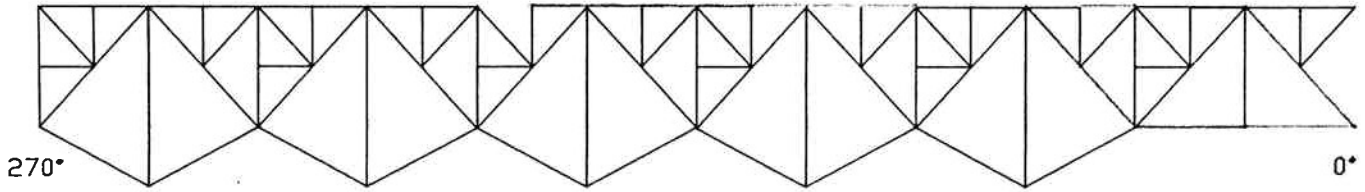

OVERSTRESSED MEMBERS per AISC CODE EIGHTH EDITION:

5% TO 45% ——————

45% TO 100% ——————

100% TO 200%

200% >

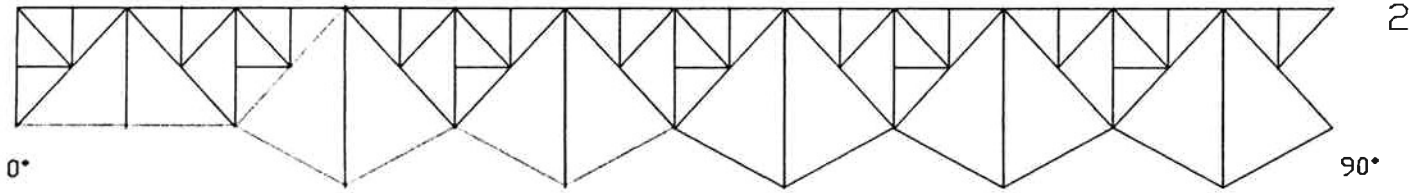

INCLINED 45°
(SOUTH END LOWER)

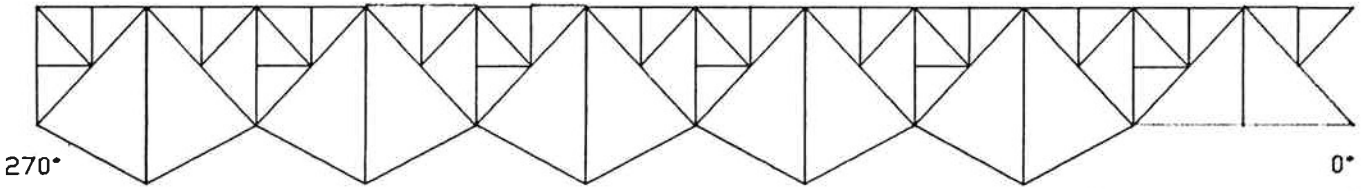

FIGURE NO. 2-26
300 FT. RADIO TELESCOPE
GREEN BANK, WVa.
CIRCUMFERENCE 6,
MEMBER OVERSTRESSES,
ZENITH & 45° INCLINED
DISH POSITIONS

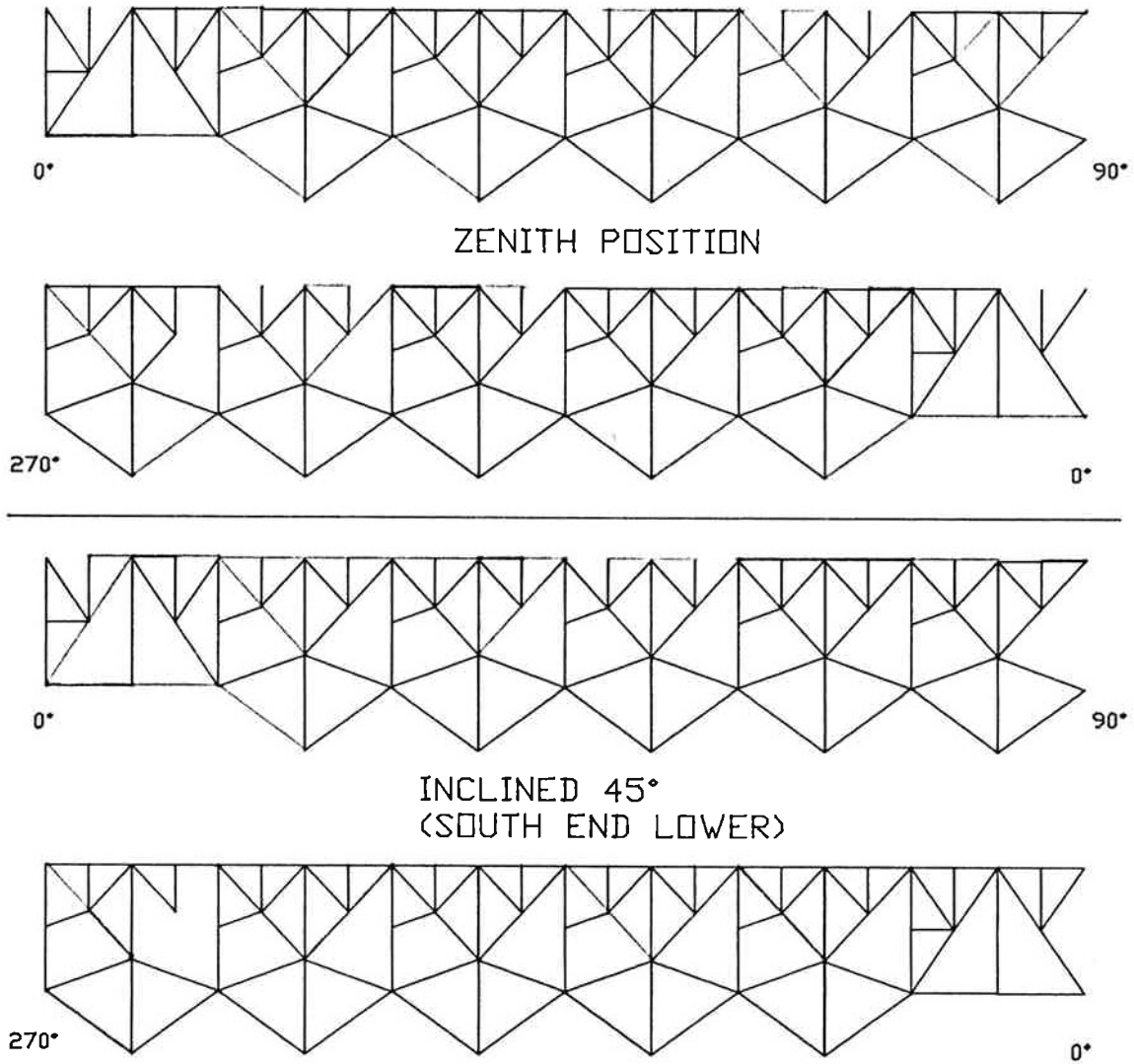

OVERSTRESSED MEMBERS
per AISC CODE EIGHTH
EDITION:

5% TO 45% ——————
45% TO 100% ——————
100% TO 200% -
200% > ——————

FIGURE NO. 2-27
300 FT. RADIO TELESCOPE
GREEN BANK, WVa.
CIRCUMFERENCE 7,
MEMBER OVERSTRESSES
ZENITH & 45° INCLINED
DISH POSITION

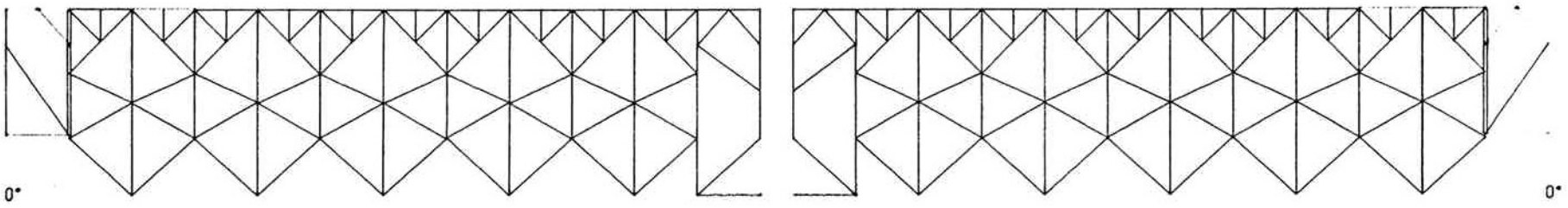

ZENITH POSITION

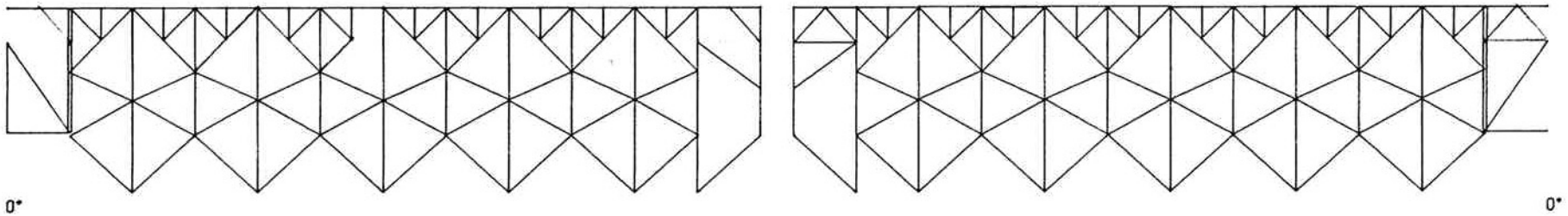

INCLINED 45°
(SOUTH END LOWER)

OVERSTRESSED MEMBERS
per AISC CODE EIGHTH
EDITION:

5% TO 45%
45% TO 100%
100% TO 200%
200% >

FIGURE 2-28
300 FT. RADIO TELESCOPE
GREEN BANK WVa.
CIRCUMFERENCE 8,
MEMBER OVERSTRESSES
ZENITH & 45° INCLINED DISH POSITIONS

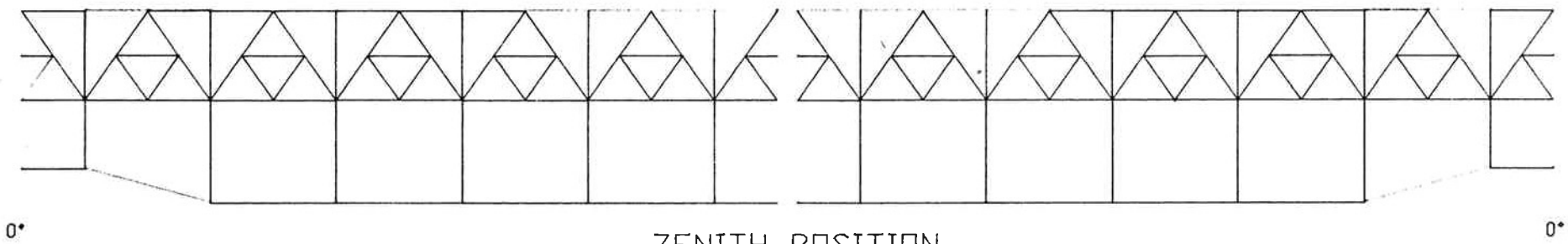

ZENITH POSITION

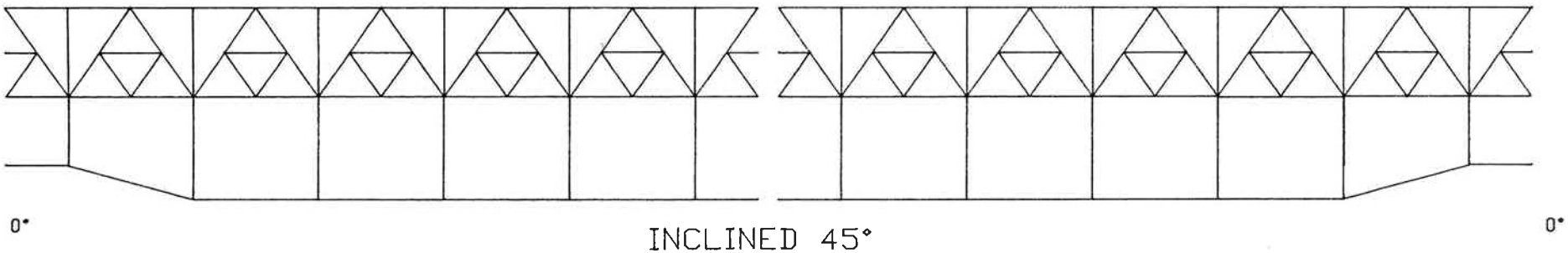

INCLINED 45°
(SOUTH END LOWER)

OVERSTRESSED MEMBERS
per AISC CODE EIGHTH
EDITION:

5% TO 45%
45% TO 100%
100% TO 200%
200% >

FIGURE NO. 2-29
300 FT. RADIO TELESCOPE
GREEN BANK, WVa.
CIRCUMFERENCE 9,
MEMBER OVERSTRESSES,
ZENITH & 45° INCLINED DISH POSITIONS

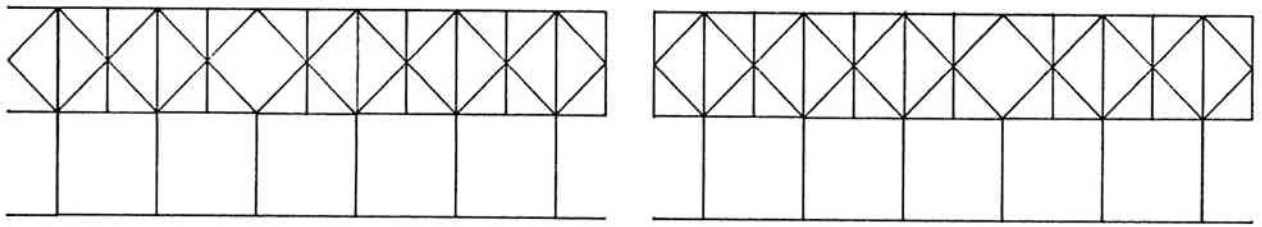

0° ZENITH POSITION 0°

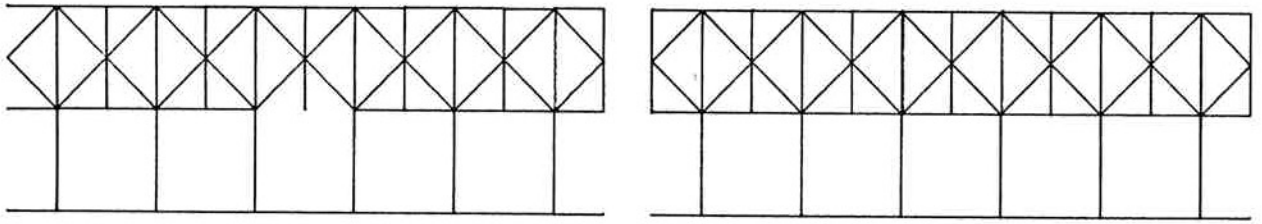

0° INCLINED 45°
(SOUTH END LOWER) 0°

OVERSTRESSED MEMBERS
per AISC CODE EIGHTH
EDITION:

5% TO 45% ————————
45% TO 100% ————————
100% TO 200%
200% > ————————

FIGURE NO. 2-30
300 FT. RADIO TELESCOPE
GREEN BANK WVa.
CIRCUMFERENCE 10
MEMBER OVERSTRESSES,
ZENITH & 45° INCLINED

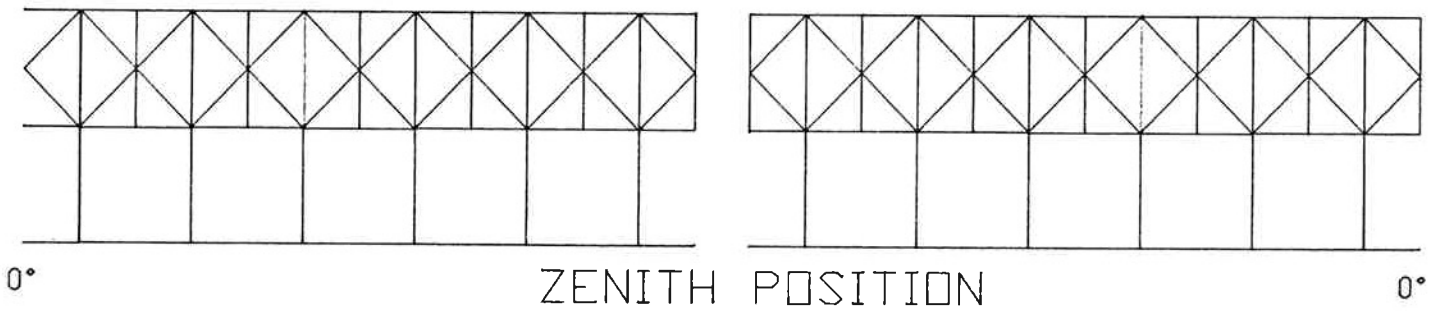

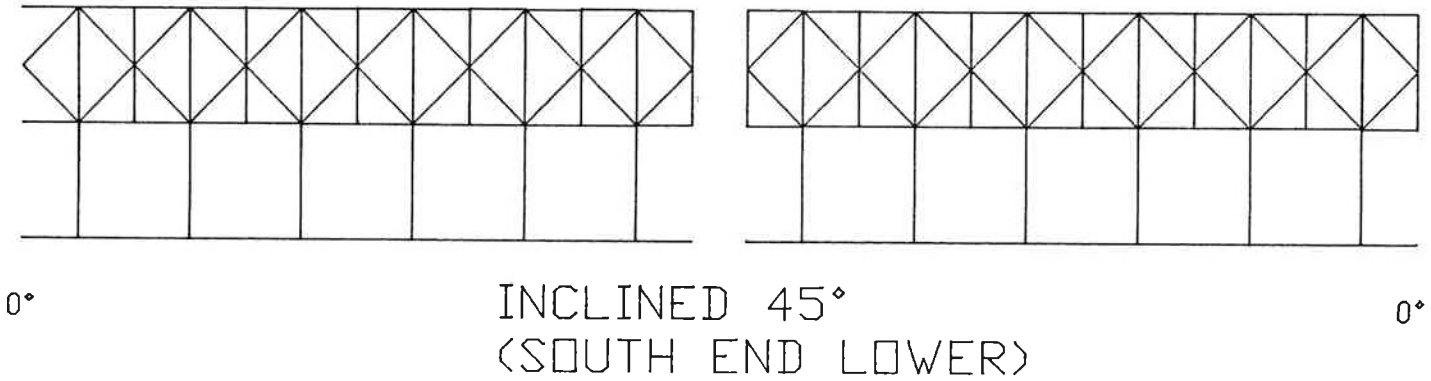

OVERSTRESSED MEMBERS
per AISC CODE EIGHTH
EDITION:

5% TO 45% ----------
45% TO 100% ——————
100% TO 200%
200% >

FIGURE 2-31
300 FT. RADIO TELESCOPE
GREEN BANK WVa.
CIRCUMFERENCE 11
MEMBER OVERSTRESSES,
ZENITH & 45° INCLINED

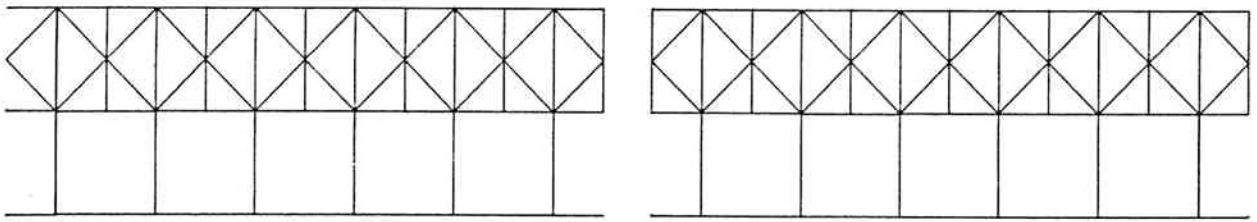

0° ZENITH POSITION 0°

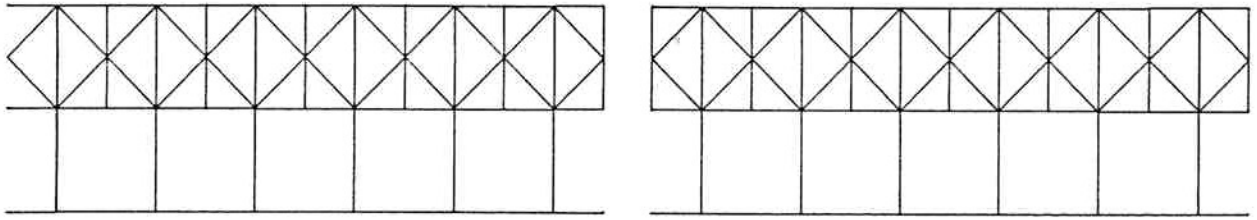

0° INCLINED 45°
(SOUTH END LOWER) 0°

NOTE:
NO OVERSTRESSES
DETERMINED

FIGURE NO. 2-32
300 FT. RADIO TELESCOPE
GREEN BANK WVa.
CIRCUMFERENCE 12
MEMBER OVERSTRESSES,
ZENITH & 45° INCLINED

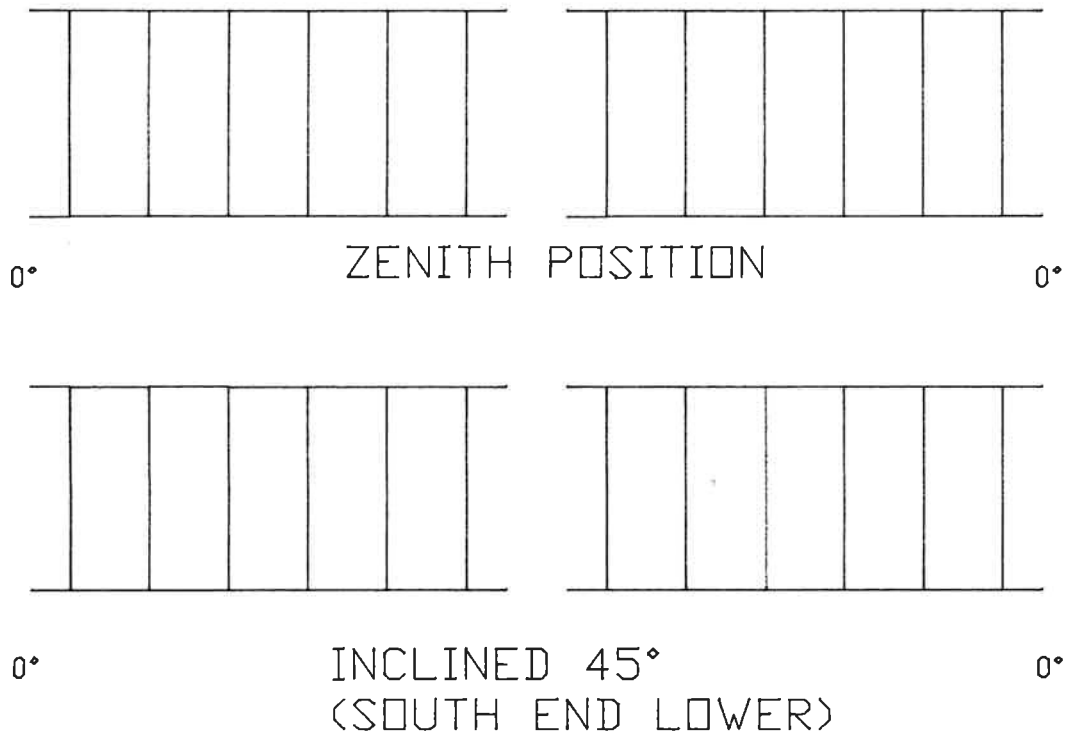

OVERSTRESSED MEMBERS
per AISC CODE EIGHTH
EDITION:

5% TO 45% ·····
45% TO 100% ——
100% TO 200%
200% > ·····

FIGURE 2-33
300 FT. RADIO TELESCOPE
GREEN BANK, WVa.
CIRCUMFERENCE 13,
MEMBER OVERSTRESSES,
ZENITH & 45° INCLINED POSITION

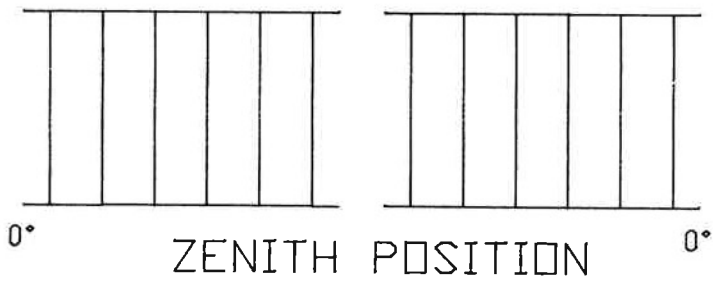

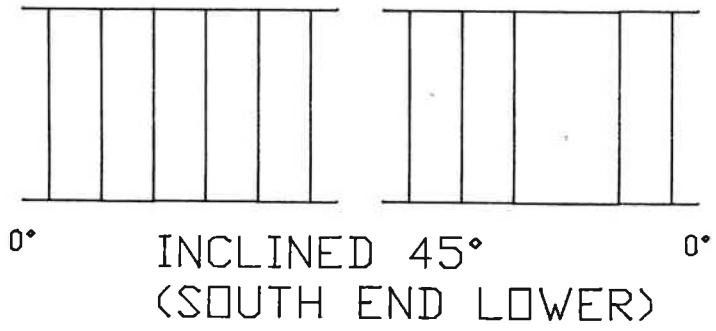

OVERSTRESSED MEMBERS
per AISC CODE EIGHTH
EDITION:

5% TO 45% ————————
45% TO 100% ————————
100% TO 200%
200% > ————————

FIGURE 2-34
300 FT. RADIO TELESCOPE
GREENBANK, WVa.
CIRCUMFERENCE 14,
MEMBER OVERSTRESSES
ZENITH & 45° INCLINED POSITION

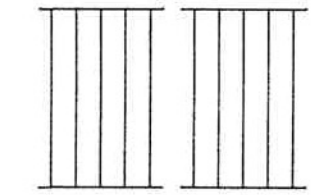

ZENITH POSITION

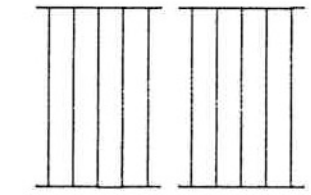

INCLINED 45°
(SOUTH END LOWER)

NOTE:
NO OVERSTRESSES
DETERMINED

FIGURE 2-35
300 FT. RADIO TELESCOPE
GREEN BANK, WVa.
CIRCUMFERENCE 15,
MEMBER OVERSTRESSES,
ZENITH & 45° INCLINED DISH POSITION

APPENDIX B

Metallurgical examination of the fractured gusset plate

TECHNICAL REPORT NO. 7878

300 FOOT RADIO TELESCOPE - FRACTURED MAIN BOX GIRDER PLATE

ASSOCIATED UNIVERSITIES, INC.

Lucius Pitkin
INCORPORATED
EST 1885
Metallurgical and Chemical Consultants
Testing Laboratories–Nondestructive Examination Services
50 HUDSON STREET, NEW YORK, N.Y. 10013 · (212) 233-2737
TELEX 12-6615 · CABLE NIKTIP (212) 233-2558

TECHNICAL REPORT

February 27, 1989

Report No. ME-1115

Technical Report No. 7878

Your P.O. No. 44521-130

Associated Universities, Inc.
Suite 603
1717 Massachusetts Avenue, N.W.
Washington, D.C. 20036

Attention: Mr. Thomas J. Davin, Jr.

Subject: 300 FOOT RADIO TELESCOPE -
FRACTURED MAIN BOX GIRDER PLATE

INTRODUCTION:

A failed plate from the main box girder of the 300 ft. radio telescope at Greenbank, West Virginia, was submitted to Lucius Pitkin, Inc. for metallurgical examination. We were advised that the telescope had been in-service approximately 26 years. In addition, we were advised that at the time of failure, temperatures were moderate and there were no severe winds or other inclement weather conditions.

OBJECT:

The purpose of this examination was to determine the nature and, if possible, the probable cause of failure of the submitted box girder plate.

PROCEDURE AND OBSERVATIONS:

A. Visual Examination

The submitted section of 1/2-in. thick fractured main box girder plate is shown in the as-received condition in Fig. 1. Examination of the subject plate revealed the fracture to be

This report is rendered upon the condition that it is not to be reproduced wholly or in part for advertising or other purposes over our signature or in connection with our name without special permission in writing.

approximately 37 inches long and passed through two bolt holes apparently used to fasten an adjacent gusset plate.

Visual examination revealed the majority of the fracture to be slanted and lightly oxidized (rusted), as is characteristic of a recent fast ductile fracture. Closer examination of the slanted fracture surfaces revealed faint chevron-like markings, the convergence of which indicated the bolt holes to be the fracture origins. The fracture surfaces adjacent to the bolt holes were relatively flat in appearance, exhibiting little or no plastic deformation, and were covered with a heavy black oxide. These heavily oxidized regions extended approximately 1-in.to 2-in. to each side of the bolt holes. The relatively flat and heavily oxidized appearance of the fracture surface adjacent to the bolt holes is characteristic of progressive long-term cracking in the nature of fatigue. Fig. 2 is a photograph showing the appearance of the plate fracture surfaces in the vicinity of the bolt holes.

In addition, approximately midway between the failed bolt holes and short edge of the plate, a 1/2-in. wide discontinuity intersected the fracture plane, as shown in Fig. 3. The appearance of this plate discontinuity was characteristic of weld metal deposit/splatter or an arc gouge. The fracture surface adjacent to this region was relatively flat and heavily oxidized indicating this damage may have been present for some time. It should be noted, however, that the fracture surface chevron-like ridges (which generally converge toward fracture origins) did not converge in the vicinity of the weld deposit/splatter and, as such, this discontinuity was not considered to be the primary fracture origin.

Close examination of the fracture surface adjacent to the bolt holes revealed the presence of ratchet marks at the bolt hole surfaces, as shown in Figs. 4 and 5, as is characteristic of fatigue crack initiation. In addition, as shown in Figs. 6 and 7, secondary cracks parallel to and below the primary fracture were also observed at the bolt holes. The presence of secondary cracks is also characteristic of fatigue crack growth and these cracks generally occur under moderate to high cyclic stresses.

B. Composition

Drillings from the failed plate were submitted for qualitative emission spectrographic analysis. The results of the

analysis indicated the box girder plate to be a plain carbon steel. Complete results of this analysis are given in Table I, appended.

C. Mechanical Properties

1. Hardness

A hardness survey was performed on a ground surface of the box girder plate material. Results of this survey indicated the plate material to have a relatively uniform hardness of Rockwell B 71.0. Based upon standard conversion charts for steel, this hardness corresponds to an ultimate tensile strength of approximately 62,000 psi

2. Tensile

One 1/2-in. wide flat tensile specimen was prepared from the plate material (perpendicular to the fracture plane) and tested at room temperature in accordance with ASTM: E8.

Results of the tensile test were as follows:

Yield strength, psi (0.2% offset)	46,300
Ultimate tensile strength, psi	62,400
Elongation, % (2-in. gage)	34.0

The tensile test results are typical of a plain carbon steel, i.e., ASTM: A36 structural steel.

D. Metallographic Examination

Longitudinal and transverse cross-section microspecimens were prepared so as to pass through the fatigue crack origins and fast ductile fracture regions. The specimens were mounted in Bakelite, carefully ground and polished for metallographic examination.

In the as-polished, unetched condition the plate material exhibited a normal quantity of non-metallic inclusions and no

laminations or seams at the fracture origin. The plate material was considered satisfactorily clean in this respect.

Etching the microspecimens revealed the general microstructure of the plate material to be comprised of fine grained ferrite (iron phase) and pearlite (iron iron-carbide phase), as is characteristic of a plain carbon structural steel. Fig. 8 is a photomicrograph showing the general microstructure of the plate material.

Examination of the fracture regions adjacent to the bolt holes revealed fracture profiles which were relatively flat and transgranular (propagating through the grains rather than along grain boundaries), as is typical of progressive or fatigue failure under cyclic loading. Fig. 9 is a photomicrograph showing the transgranular fracture profile adjacent to a bolt hole. Further, as shown in Fig. 10, small secondary transgranular cracks parallel to the primary fracture were also observed at the bolt hole surfaces. The presence of secondary cracks are characteristics of fatigue fracture at moderate to high cyclic stresses.

Remote from the fracture origin, the final fracture profile was slanted, transgranular and the grains adjacent to the surface were plastically deformed, as is characteristic of fast ductile fracture. Fig. 11 is a photomicrograph showing fracture profile through the final fracture region.

E. Scanning Electron Microscopy

The large secondary crack at one of the bolt holes was carefully back-cut and opened so as to expose the fracture surface for examination in a JEOL T330A scanning electron microscope. The fracture surface was heavily oxidized and therefore cleaned by immersion in Alconox and again in 3% EDTA prior to examination. However, these cleaning procedures removed very little of the oxide coating. The fracture surface was examined at an accelerating potential of 20 keV.

As shown in Fig. 12, the fracture surface was covered with an oxide scale and no significant fractographic information was obtained.

DISCUSSION AND CONCLUSIONS:

Results of our investigation revealed failure of the

submitted main box girder plate to have occurred as a result of progressive cracking in the nature of fatigue. Propagation of these fatigue cracks under cyclic loading from both bolt holes eventually resulted in a fast ductile fracture when the combination of cyclic stress range and crack size exceeded the fracture toughness of the plate material.

Further, the results of the fractographic examination revealed secondary fatigue cracks also had originated at the bolt hole surfaces. The presence of the secondary fatigue cracks at the bolt holes indicates the presence of intermediate to high cyclic stresses.

The bolt material was a plain carbon steel and exhibited yield and tensile strengths typical of ASTM: A36 structural steel. No metallurgical or fabrication defects were found in way of the bolt hole fracture origins.

Respectfully submitted,

LUCIUS PITKIN, INC.

Robert S. Vecchio, Ph.D.
Engineer

Approved:
A. J. Vecchio, P.E.
Vice President

RSV/pm/2

Lucius Pitkin
INCORPORATED

Metallurgical and Chemical Consultants

EST 1885

Testing Laboratories–Nondestructive Examination Services

50 HUDSON STREET, NEW YORK, N.Y. 10013 · (212) 233-2737
TELEX 12-6615 · CABLE NIKTIP (212) 233-2558

SPECTROGRAPHIC ESTIMATES

Report No. ME-1115 - T.R. 7878 Date February 27, 1989

The following is our analysis of 1 sample(s) of drillings from main box girder plate.

TABLE I

BY QUALITATIVE SPECTROGRAPHIC ANALYSIS

Iron	Major
Manganese	0.X
Silicon	0.X low
Aluminum	0.0X low
Vanadium	0.0X low
Molybdenum	0.0X low
Nickel	0.0X low
Chromium	0.0X low
Copper	0.00X
Magnesium	0.00X low

Elements checked for but not found: Titanium, Zinc, Zirconium, Bismuth, Lead, Tin, Antimony, Beryllium, Gallium, Germanium, Phosphorous, Boron, Cobalt, Columbium, Tungsten.

LUCIUS PITKIN, INC.

By

NOTE: Major = above 5% estimated. Minor = 1.5% estimated. .X, .OX, .OOX, etc. = concentration of the elements estimated to the nearest decimal place – e.g. .OX = .01-.09% estimated. *= less than. NF = not found.
The numbers in parenthesis indicate the estimated relative concentration of the element among the various samples. Detectability varies considerably among the elements and also depends upon the amount and nature of the sample, therefore, "Not Found" or NF means not detected in the particular sample by the technique employed.

A
LUCIUS PITKIN INC.

Lucius Pitkin
incorporated

Associated Universities, Inc.
Attention: Mr. Thomas J. Davin, Jr.

February 27, 1989
ME-1115 - T.R. 7878

Fig. 1 FAILED MAIN BOX GIRDER PLATE, AS-RECEIVED

Photograph showing the submitted 1/2-in. thick main box girder plate from the 300 ft. radio telescope at Greenbank, West Virginia, in the as-received condition. The plate fracture was approximately 37 in. long (arrows) and intersected two bolt holes.

LUCIUS PITKIN, INC.

Associated Universities, Inc.
Attention: Mr. Thomas J. Davin, Jr.

February 27, 1989
ME-1115 - T.R. 7878

Fig. 2 PLATE FRACTURE SURFACE

Photograph showing the flat and heavily oxidized appearance of the plate fracture surfaces adjacent to the bolt holes. This flat and heavily oxidized fracture appearance is characteristic of long-term progressive or fatigue cracking. The convergence of chevron-like marks indicates the bolt holes to be the fracture origins.

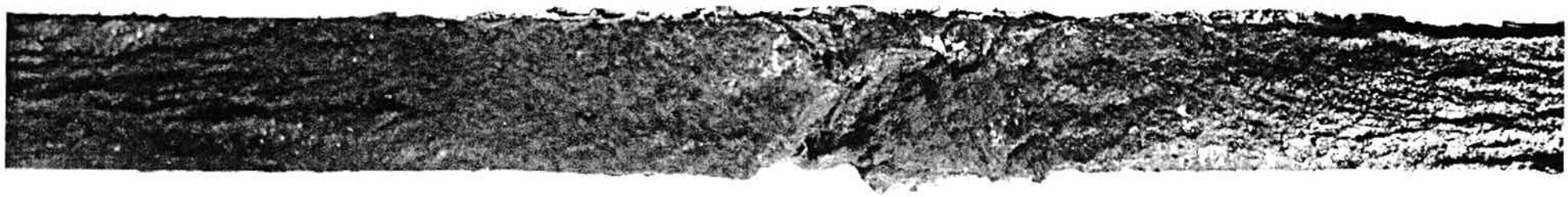

LUCIUS PITKIN, INC.

Associated Universities, Inc.
Attention: Mr. Thomas J. Davin, Jr.

February 27, 1989
ME-1115 - T.R. 7878

Fig. 3 PLATE FRACTURE SURFACE DISCONTINUITY

Photograph showing a weld deposit/splatter or arc gouge discontinuity in the fracture plane approximately midway between the bolt holes and the short edge of the plate. The lack of converging chevron-like marks near this discontinuity indicated it was not a primary fracture origin.

Associated Universities, Inc.
Attention: Mr. Thomas J. Davin, Jr.

February 27, 1989
ME-1115 - T.R. 7878

Fig. 4 FRACTURE ORIGIN

Close-up photograph showing the presence of fracture surface ratchet marks (arrows)at the bolt hole surfaces, as is characteristic of progressive crack initiation in the nature of fatigue.

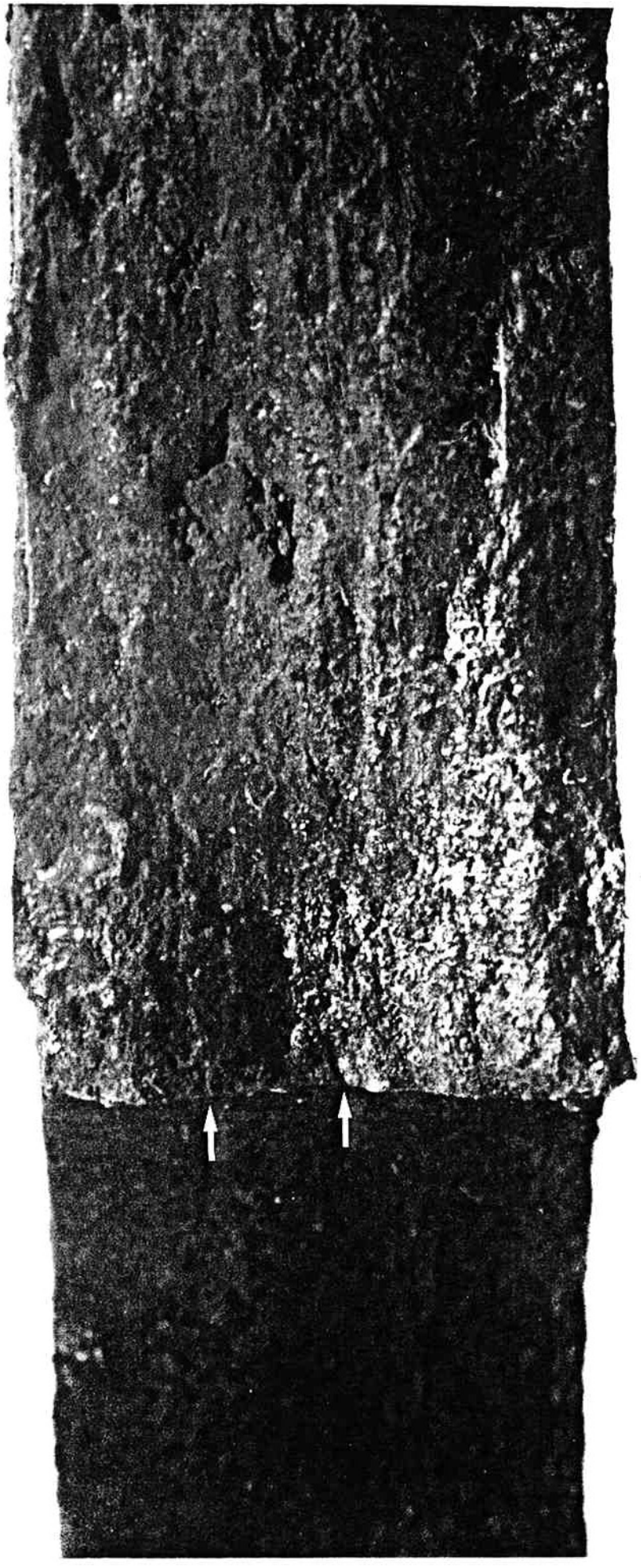

Associated Universities, Inc.
Attention: Mr. Thomas J. Davin, Jr.

February 27, 1989
ME-1115 - T.R. 7878

Fig. 5 FRACTURE ORIGIN

Close-up photograph showing the presence of fracture surface ratchet marks (arrows) at the bolt hole surfaces, as is characteristic of progressive crack initiation in the nature of fatigue.

1
2
3
4
8
12
16
20
24
28

Associated Universities, Inc.
Attention: Mr. Thomas J. Davin, Jr.

February 27, 1989
ME-1115 - T.R. 7878

Fig. 6 SECONDARY FATIGUE CRACK

Close-up photograph showing a secondary fatigue crack (arrow) parallel and adjacent to the primary fracture, as is characteristic of fatigue cracking under intermediate to high cyclic stresses.

32
8
12
16
20
24
28
1
4
8
12
16
20
24
28
2
4
8
12
16
20
24

Associated Universities, Inc.
Attention: Mr. Thomas J. Davin, Jr.

February 27, 1989
ME-1115 - T.R. 7878

Fig. 7 SECONDARY FATIGUE CRACK

Close-up photograph showing a secondary fatigue crack (arrow) parallel and adjacent to the primary fracture, as is characteristic of fatigue cracking under intermediate to high cyclic stresses.

Associated Universities, Inc.
Attention: Mr. Thomas J. Davin, Jr.

February 27, 1989
ME-1115 - T.R. 7878

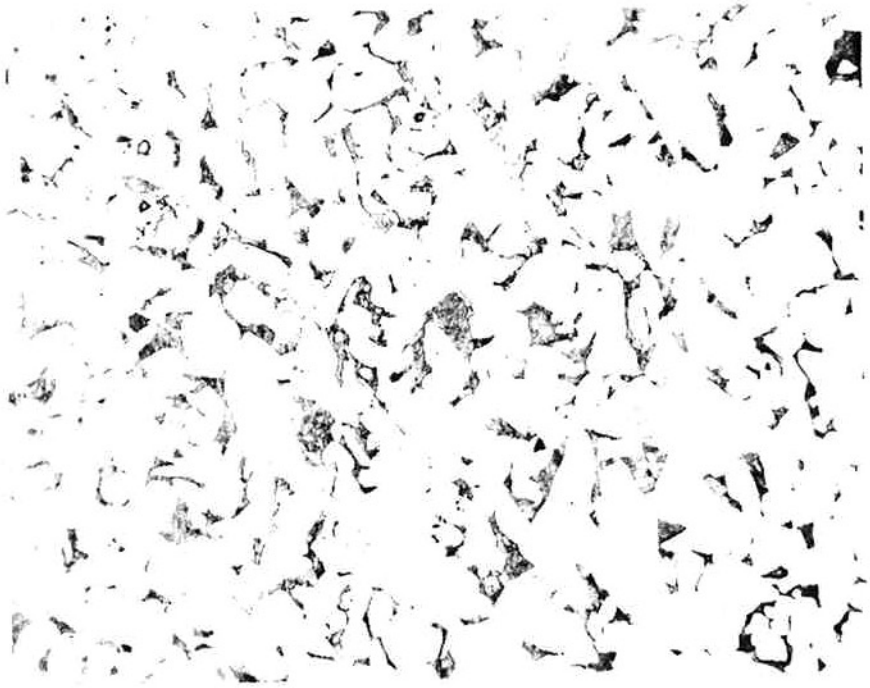

Fig. 8 GENERAL MICROSTRUCTURE 200 X

Photomicrograph showing the general microstructure of the main box girder plate material to be comprised of fine grained ferrite (iron phase) and pearlite (iron iron-carbide phase), as is typical of a plain carbon steel.

Associated Universities, Inc.
Attention: Mr. Thomas J. Davin, Jr.

February 27, 1989
ME-1115 - T.R. 7878

Fig. 9 FRACTURE PROFILE AT ORIGIN 200 X

Photomicrograph showing the box girder plate fracture profile (top) at the fracture origin (bolt hole surface - right side) to be relatively flat and transgranular, as is characteristic of progressive cracking in the nature of fatigue.

Associated Universities, Inc.
Attention: Mr. Thomas J. Davin, Jr.

February 27, 1989
ME-1115 - T.R. 7878

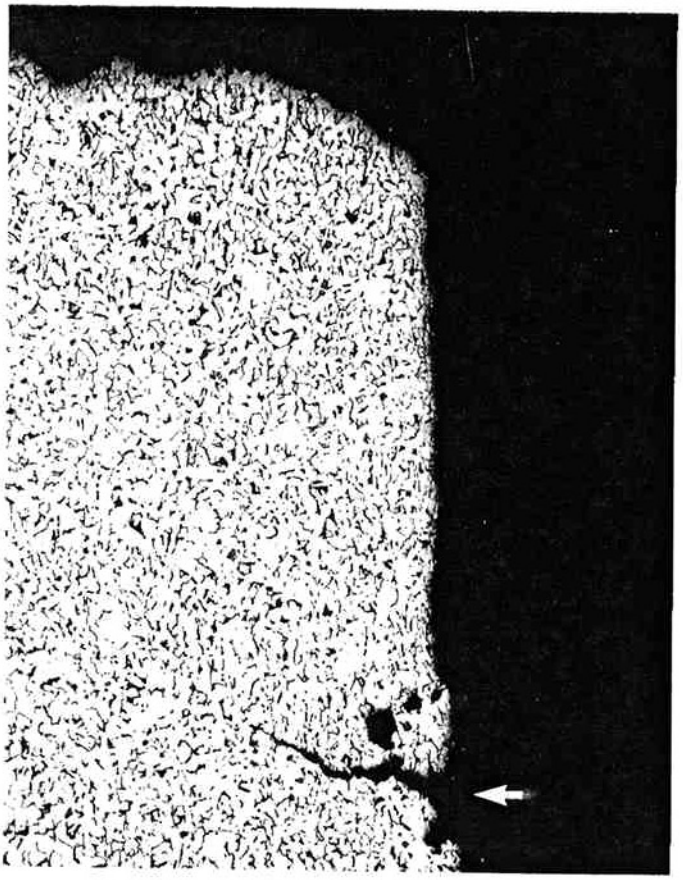

Fig. 10 SECONDARY FATIGUE CRACK 50 X

Photomicrograph showing a secondary fatigue crack (arrow) parallel to and just below the primary fracture (top) at the bolt hole surface (right side). The presence of secondary cracks is characteristic of fatigue fracture at moderate to high cyclic stresses.

Associated Universities, Inc.
Attention: Mr. Thomas J. Davin, Jr.

February 27, 1989
ME-1115 - T.R. 7878

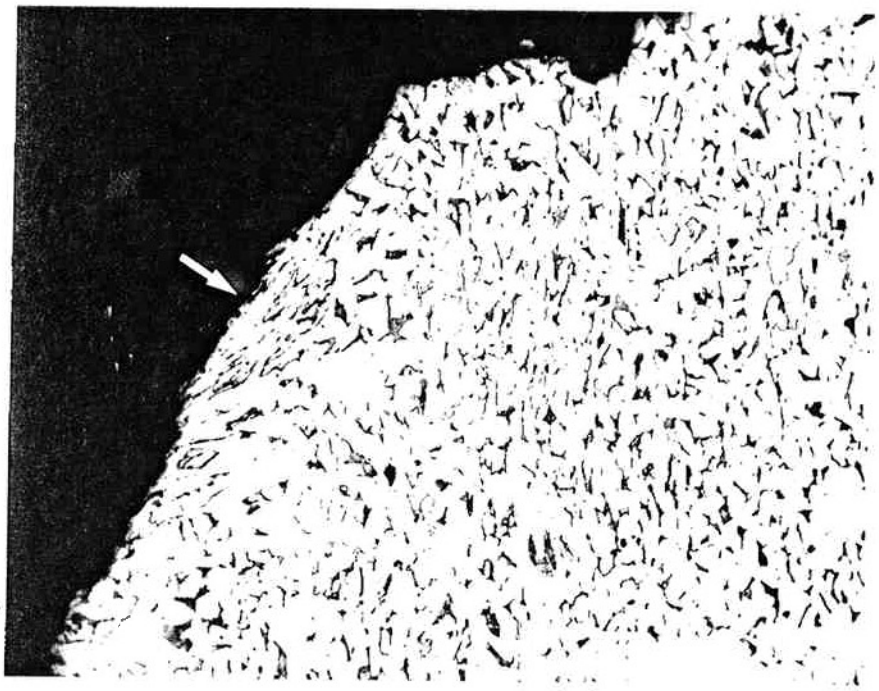

Fig. 11 FRACTURE PROFILE REMOTE FROM BOLT HOLE ORIGIN 100 X

Photomicrograph showing the slanted and transgranular fracture profile of the plate fracture remote from the bolt hole origin. In addition, the grains adjacent to the fracture surface (arrow) are plastically deformed, as is characteristic of fast ductile fracture.

Associated Universities, Inc.
Attention: Mr. Thomas J. Davin, Jr.

February 27, 1989
ME-1115 - T.R. 7878

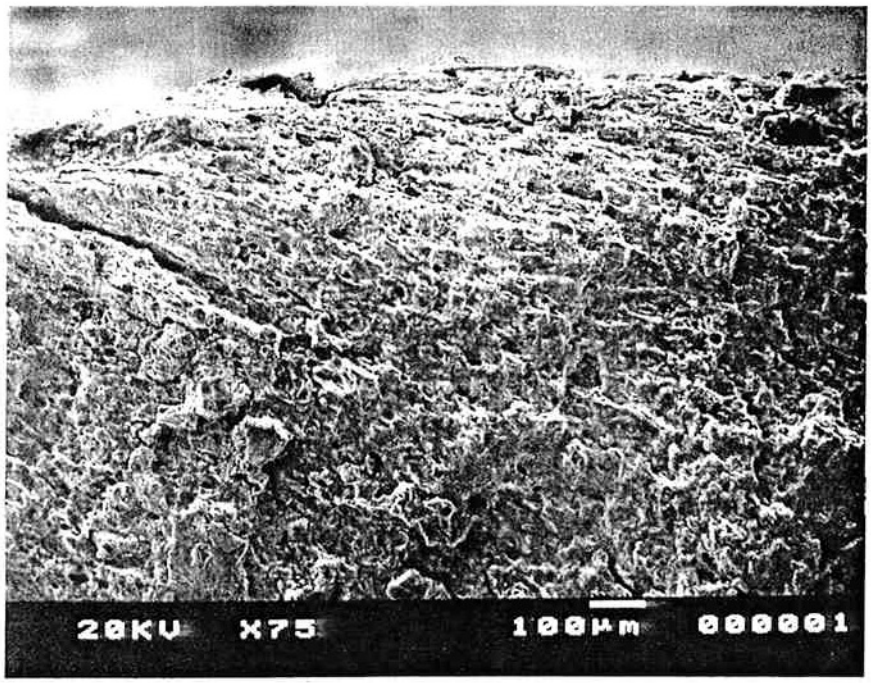

Fig. 12 FRACTURE ORIGIN AT ORIGIN 75 X

Scanning electron micrograph showing the box girder plate fracture surface at a bolt hole fracture origin. Even after extensive cleaning procedures the fracture surface exhibited a tenacious oxide, thus, no significant fractographic information was obtained.